



**POLITECNICO DI TORINO**

Master's Degree in Civil Engineering

MASTER'S DEGREE THESIS

**Optimization of Steel Exoskeletons for the  
Seismic Retrofit of Reinforced Concrete  
Structures via Genetic Programming**

Supervisor:

**Prof. Marco Domaneschi**

Co-supervisors:

**PhD. Eng. Raffaele Cucuzza**

Candidate:

**Jana Candelaria Olivo Garcia**

---

OCTOBER 2023 - A.Y. 2022/2023

*A mi familia,  
este logro es tan suyo  
como es mío*

## **Abstract**

In the last decade, the use of steel exoskeletons as an alternative for the seismic retrofit of existing structures received great attention due to their non-invasive and time-efficient nature. Furthermore, it represents the preferred solution in cases where the use of the existing building cannot be interrupted during the intervention, or when a limited level of knowledge of the existing building is available and high seismic activity is expected.

Nowadays, the proposed design approaches mainly rely on simplified models employing single or multi-degree-of-freedom systems with lumped masses to determine optimal overall values for exoskeletons' stiffness, mass, and damping. Even though the benefits derived by these methodologies were largely proven, further investigations are required to fully understand the influence of mechanical and geometrical properties on the outcomes. Moreover, once global optimal values of the system have been obtained, no consolidated procedures for the sizing process of the exoskeleton have been recognized in the literature.

Therefore, the primary objective of this research is to overcome the limitations associated with existing methodologies by evaluating the optimal quantity and spatial placement of the exoskeletons, as well as determining the optimal sizing of their constituent elements.

To accomplish this goal, a comprehensive optimization procedure, based on a modified Genetic Algorithm has been adopted. In the mathematical statement of the problem, the total weight of the exoskeletons has been assumed as the Objective Function (OF). Two critical constraints are considered: firstly, aiming to maintain the structural integrity of the building in the elastic range, a maximum allowable inter-storey drift has been imposed corresponding to the threshold beyond which damage occurs at the level of the structure's infills. Secondly, the stress requirements that the exoskeletons must satisfy have been considered.

To determine the fitness and assess the viability of each potential solution, modal analyses are conducted using SAP2000 OAPI, a software tool that facilitates the

generation of models with automatic routines and allows the implementation of optimization tools governed by MATLAB.

The results obtained from this research demonstrate that the proposed approach effectively controls damage in existing structures subjected to horizontal actions, ensuring compliance with safety requirements while offering slender and cost-effective designs. Additionally, the stiffness ratio between the exoskeletons and the base structure can be significantly reduced below the limit suggested by the NTC2018 Italian code. Comparative analyses of different exoskeleton configurations and base structures provide valuable insights into their performance, enabling a better understanding of their behavior and aiding in the selection of appropriate retrofitting strategies.

The thesis presents the following organization: in Chapter 1 the topic of the thesis is introduced together with the definition of the scope and main goals of the work, in Chapter 2 a well-comprehensive literature review is reported by summarizing the main results achieved by other authors. The definition of several case studies, the F.E. modeling, and the problem statement of the optimization are presented in Chapter 3. In Chapter 4 the results for each scenario are discussed while the final conclusions and the potential future developments of the work are explained in Chapters 5 and 6, respectively.

# Contents

<b>1</b>	<b>Introduction</b>	<b>4</b>
<b>2</b>	<b>Literature Review</b>	<b>7</b>
2.1	Seismic Retrofit . . . . .	8
2.2	Exoskeletons . . . . .	9
2.2.1	Usefulness . . . . .	9
2.3	Types of Exoskeletons . . . . .	10
2.3.1	Orientation . . . . .	11
2.3.2	Dissipation Capacity . . . . .	13
2.4	Design of Exoskeletons . . . . .	14
2.4.1	Considerations . . . . .	14
2.4.2	Proposed Design Procedures . . . . .	16
2.4.3	Main Outcomes . . . . .	17
<b>3</b>	<b>Revision of the NTC18 and Alternative Approach Proposal</b>	<b>18</b>
3.1	Review of the Regulation . . . . .	19
3.2	Issues Related to the Regulation . . . . .	21
3.3	Proposed Displacement-Based Approach . . . . .	22
<b>4</b>	<b>Problem Statement and Analysis Setting</b>	<b>24</b>
4.1	Definition of the Optimization via Genetic Programming . . . . .	25
4.1.1	Mathematical Formulation of the Objective Function . . . . .	26
4.1.2	Employed Algorithm . . . . .	30
4.2	FEM Analyses . . . . .	38
4.2.1	Linear Dynamic Analysis with Response Spectrum . . . . .	38

---

4.2.2	Non-Linear Static Analyses . . . . .	39
<b>5</b>	<b>Overview of the Case Studies</b>	<b>41</b>
5.1	Considered Existing Structures . . . . .	42
5.1.1	Structure 1 . . . . .	46
5.1.2	Structure 2 . . . . .	47
5.1.3	Structure 3 . . . . .	49
5.2	Exoskeleton Typologies . . . . .	51
5.2.1	Orthogonal Exoskeleton . . . . .	53
5.2.2	Parallel Exoskeleton . . . . .	54
<b>6</b>	<b>Results and Discussion</b>	<b>56</b>
6.1	Case Study 1 . . . . .	57
6.1.1	Results of the Optimization . . . . .	58
6.1.2	Structural Interpretation of the Results . . . . .	60
6.1.3	Results in Relation to the Stiffness Ratio . . . . .	63
6.2	Case Study 2 . . . . .	67
6.2.1	Results of the Optimization . . . . .	67
6.2.2	Structural Interpretation of the Results . . . . .	69
6.2.3	Results in Relation to the Stiffness . . . . .	72
6.3	Case Study 3 . . . . .	76
6.3.1	Results of the Optimization . . . . .	76
6.3.2	Structural Interpretation of the Results . . . . .	78
6.3.3	Results in Relation to the Stiffness . . . . .	83
6.4	Case Study 4 . . . . .	87
6.4.1	Results of the Optimization . . . . .	87
6.4.2	Structural Interpretation of the Results . . . . .	89
6.4.3	Results in Relation to the Stiffness . . . . .	93
6.5	Case Study 5 . . . . .	98
6.5.1	Results of the Optimization . . . . .	99
6.5.2	Structural Interpretation of the Results . . . . .	100
6.5.3	Results in Relation to the Stiffness . . . . .	105
6.6	Case Study 6 . . . . .	111
6.6.1	Results of the Optimization . . . . .	112

---

6.6.2	Structural Interpretation of the Results . . . . .	113
6.6.3	Results in Relation to the Stiffness . . . . .	118
<b>7</b>	<b>Conclusions and Future Developments</b>	<b>124</b>
<b>8</b>	<b>Bibliography</b>	<b>130</b>

# Chapter 1

## Introduction

In the past decades, seismic retrofitting of existing structures has emerged as a primordial concern, especially in regions where a substantial portion of the building stock predates current seismic codes. The situation in Italy, where over 60% of existing structures were constructed prior to the introduction of the first seismic regulations, highlights the immediate need for innovative retrofitting solutions. Furthermore, many of these buildings have exceeded their intended lifespan, posing significant durability and seismic safety challenges. Simultaneously, there is a growing imperative to enhance the energy performance and aesthetic appeal of the building stock.

Facing these challenges in a context where retrofitting interventions pose several complications, such as the elevated cost they represent, the requirement of interrupting the activities in the building, and the limitations of traditional retrofitting techniques, becomes difficult to achieve. The social, environmental, and economic impacts of the different routes that can be taken make retrofitting, rather than demolition and reconstruction, the preferred solution.

In response to these needs, steel exoskeletons have emerged as a promising retrofitting alternative. These structures are designed to enhance the seismic resistance of existing buildings without requiring internal interventions. They achieve this by augmenting the system's stiffness and significantly unloading the primary structure.

The advantages of this innovative solution are many. Among them, their time-efficient and non-invasive nature enables the overcoming of the most typical limitations when it comes to retrofitting interventions. Additionally, they represent a multifaceted option, making an integrated design possible, combining structural, energetic, and architectonic renovations. Steel exoskeletons are a prefabricated and dry solution, being a reversible and recyclable option, with easy maintenance, addressing the Life Cycle Thinking Principles.

The present work has two main aims, the first one is related to the design approaches proposed until nowadays. Most proposed procedures are based on the simplification of the building and the exoskeletons as two Single Degree of Freedom systems connected through a rigid link, to then determine the overall optimal values of mass and stiffness that the exoskeleton's system must have, as a whole. The gap in this approach is related to the design of the retrofitting system once the parameters have been obtained. Variables such as the position and amount of exoskeletons, the topology of such structures, and the sizing of the elements, have been proven to have a great impact on the structural behavior of the building-exoskeletons coupled system.

Aiming to provide a comprehensive solution, an optimization procedure is introduced, transforming the theoretical framework of exoskeleton design into practical design strategies. This approach seeks to determine the optimal quantity and spatial placement of exoskeletons, along with the sizing of their constituent elements.

The algorithm is based on Genetic Programming, and its goal is to minimize the weight of the retrofitting system while guaranteeing the satisfaction of certain constraints. The first constraint aims to prevent any damage to the building when facing the considered seismic action, encompassing the structural elements and non-structural infills. The second constraint is related to the structural verification of the exoskeletons to ensure the correct behavior in the seismic event. Finally, a third constraint is included to comply with architectonic barriers and keep the building accessible. In this way, the study endeavors to aid designers with a tool that provides a complete retrofitting solution, that optimizes cost-effectiveness while accomplishing the structural performance targets imposed.

The second aim guiding this work is related to the suggestions, given by the Italian regulation NTC2018, for the design of exoskeleton structures. Even though the code does not address specifically the exoskeletons, their design process is affected by the categorization of the elements as 'primary' or 'secondary'. Firstly, accurately determining the single element behavior represents a challenge, forcing the designer to consider the entire structure as 'primary' or 'secondary'. Considering the existing structure as primary is complicated due to the uncertainties given by the lack of knowledge about the building; on the other hand, considering it as secondary leads to oversized, heavy, and costly solutions.

To address these challenges, this thesis proposes a novel displacement-based approach, centered on inter-storey drift, as a viable alternative to the classification based on the stiffness contribution of the elements. The aim is to link the exoskeleton design to an elastic inter-storey drift threshold of the existing structure, ensuring that the structure as a whole complies with the structural verifications.

The main advantage of this proposal is the possibility to achieve the established targets with a lighter, less expensive, intervention. In this way, choosing exoskeletons for the seismic retrofitting intervention of existing buildings becomes a more feasible solution, overcoming the limitations and barriers that are nowadays faced by designers.

## Chapter 2

# Literature Review

In this chapter, the main aspects that arise from a well-comprehensive literature review performed, of over 50 papers, are summarized.

Firstly, in [2.1](#), an overview of the current situation of the building stock is done, encompassing structural, energetic, and aesthetic aspects, along with an interpretation of the barriers and limitations that arise when facing the need for a massive retrofitting intervention.

Secondly, in [2.2](#), the new retrofitting alternative center of this study is characterized and its intrinsic aspects and main advantages are presented. In [2.3](#), exoskeletons are classified according to their orientation with respect to the existing structure's façade, and to their dissipation capacity, reporting the characteristics of each typology.

Finally, in [2.4](#), a state-of-the-art on proposed design approaches is done, starting with the general considerations that should be done when facing a retrofit with exoskeletons. This is followed by a description of the most proposed design procedure nowadays, divided into four major steps. In the end of the chapter, the most important outcomes obtained are reported.

## 2.1 Seismic Retrofit

The census performed by the Italian National Institute of Statistics in 2011 [1] gives an interesting insight into the current situation of the Italian building stock, indicating that more than 60% of the structures' construction year is previous to the issue of the first specific Italian code for earthquake-resisting buildings (law 64/1974) [2]. Furthermore, more than half of the existing buildings have already exceeded the designed lifespan of 50 years [1].

This situation implies that structures are very vulnerable due to the lack of seismic provisions and durability issues, failing to ensure the basic safety of the citizens. Simultaneously, the energy performance of the building stock is very poor; as reported in the document for E2B European Initiative (2012), more than a third of total greenhouse gas emissions derive from constructions; given the context, an energetic renovation is urgent to reduce the energy consumption [3, 4]. Lastly, as remarked by [5], the lack of consideration for the aesthetic features in Italian territory is a situation that should be addressed together with the previously described issues.

It becomes evident that, to reach current standards in terms of structural safety, energetic performance and aesthetic value, a massive renovation of the existing building stock is imperative [6]. Even though demolition and reconstruction is an option, it has important disadvantages, as the amounts of waste produced and the production of new materials required, along with the need to relocate the inhabitants, that has social, environmental and economic impacts [7].

In consideration of these aspects, retrofitting is the preferable solution. Although, the renovation rate pairs the 1% per year [8], as consequence of several limitations. Examples of these are technical limits that emerge when none of the conventional solutions fits the specific requirements of the case, organizational limits caused by the interruption of the building's use, or economic limits [5].

## 2.2 Exoskeletons

Due to the current situation, explained above, the exploration for innovative retrofitting systems has risen. In this context, exoskeletons appear as a very promising solution for the retrofit of structures that do not have the required resistance or stiffness to resist lateral actions on their own [9, 10].

Exoskeletons are steel structures, with a two or three-dimensional frame arrangement of its conforming elements, inspired by nature on the basis of biomimicry [11, 12]. This system is applied from the outside to the existing structure, without the need of internal interventions [13, 14]. The principle of these structures is to absorb the seismic loads taken by the primary building, transferred from one to the other by a link that connects them, and unloading this forces in their own foundation system [15]; protecting or enhancing, in this way, the original structure [16].

### 2.2.1 Usefulness

For residential buildings, the relocation of the inhabitants to perform an intervention of this kind represents an organizational limit [5], since it would imply to proportion a temporary accommodation for the inhabitants and the furniture, until the end of the construction works. In the case of structures with different uses, the interruption of the activities can lead to important downtime losses or may just not be possible. The fact that exoskeletons are applied from the outside of the structure is one of the main advantages that they present, making them the only possible alternative for the described cases.[17, 18]

Additionally, this retrofitting system gives the possibility to create an integrated design system [19–24], combining a structural retrofit [25] with an improvement of the energetic efficiency [26] and an architectural makeover of the façade [27], by becoming the support for a double skin for the building. This holistic approach also makes the solution cost-efficient, especially in Italy, where an intervention of this nature is suitable to receive three different types of tax credits, which are ‘sismabonus’, ‘ecobonus’ and ‘facade bonus’ [13].

The selection of the material to be used does not represent a hard choice given that metallic materials, especially steel, present many advantages. This technological choice provides as result a structure with low weight and very resistant, easy to transport, and simple to install. The sustainability of the intervention and Life Cycle Thinking perspective are addressed by the possible prefabrication and dry assembly of metallic structures, which have a low environmental impact given by the significant reduction in the construction times, the reversible nature that characterizes them, and the use of recyclable materials; moreover, steel exoskeletons can be easily maintained or the singular elements can be replaced in case of damage or breakage. [5, 13, 28]

Nevertheless, there are some limitations to the use of exoskeletons; even though this system can still be effectively applied when facing architectonic constraints in some parts of the building perimeter [28], there is an inevitable requirement for free space around the building that may not have urban restrictions, for the installation of the new foundations, making it a possible solution only for isolated buildings[6]. Furthermore, exoskeletons are not an alternative when façade preservation is required [29], and sometimes local interventions must be done prior to the installation, such as strengthening of the floors or the column-beam joints [5]. Finally, given their costs and high performance, it would not be recommended to use exoskeletons in cases of minor strengthening, but only to use them if the goal is a complete retrofit or an important strengthening intervention [28].

## 2.3 Types of Exoskeletons

Exoskeletons are very adaptable structures, thus, according to the requirements of the specific case of application they can vary their shape, connection, or dissipation capacity, among others. As expected, these variables have a substantial impact on the behavior of the retrofitting system, which led several authors to study the different alternatives.

### 2.3.1 Orientation

Firstly, exoskeletons can be designed as bi-dimensional or three-dimensional structures, the latter generating a shell behavior where the different elements collaborate to distribute the moment and shear stresses along the entire perimeter of the building. The former, on the other hand, are suitable to many possible arrangements regarding their orientation with respect to the façade of the existing building, for example, parallel or perpendicular to the façade, or diagrids. [30]

#### Perpendicular Orientation

This configuration is particularly interesting for allowing the volume increase of the floor, creating additional housing space for new activities [28]. Nevertheless, there is a main matter to be considered when making such an addition, being that this new space must be provided with rigid floor diaphragms and withstand new loads; in a retrofitting system proposed to enhance the seismic behavior of the existing structure, the appearance of a non-negligible mass implies an increase in the seismic forces acting on the retrofitted system, which must be specially taken into account [31].

The connection between this kind of exoskeletons and the existing structure is characterized by being only axial and in correspondence with the beam-column joints of the building. This defines a primary in-plane behavior of the exoskeletons, making deep foundations essential to counteract the overturning moment and shear at the base. On the other hand, the out-of-plane behavior can be related to the arousal of a torsional flexural behavior of the entire truss wall, a problem that requires special attention in the case where the walls are not connected to each other. [28, 31]

Another consideration worth making is that this orientation implies the requirements for bigger free space in the surroundings of the building for the location of the exoskeletons and their respective foundations, thus being better suited for isolated buildings [28].

The two latter considerations, about the mechanisms of which these structures may be subject and the required free space, suggest that said configuration of the retrofitting system is admissible only for single-storey or low-storey buildings [13].

### Parallel Orientation

Regarding exoskeletons that are oriented parallel to the existing building façade, a crucial advantage of this typology is the decrease in the free space required for the installation of the retrofitting system, enabling its use also in more restrained situations. Another virtue, in this case, is that the shear nodal connection can be coupled with perimetral shear links to obtain a high degree of redundancy and exploit the beams all along the perimeter. [31]

Furthermore, avoiding the issue mentioned for exoskeletons positioned perpendicularly to the façade regarding torsional flexural mechanisms arousing, and, if proper shear transfer devices are provided, this configuration is suitable also for multi-storey buildings. [13]

### Diagrid

Diagrids are an inclined structural grid with no columns, usually applied for the construction of new tall buildings, which have the potential to withstand both horizontal and vertical loads [29, 32]. This structural typology gains attention as a possible exoskeleton configuration since it is characterized by a high structural efficiency, coupled with the wide range of shapes and configurations it can take according to the specific requirements of the case, and with the aesthetic appeal it has [33].

Some interesting advantages of the diagrids, even if these are shared with the previously described configurations of exoskeletons, are worth mentioning. The possible standardization and prefabrication of the components is an essential factor for the replicability of the solution as for the reduction of the construction time, reducing the costs [34]. Additionally, the possible volume increase of the floor plan pointed out by [28] for the perpendicular exoskeleton configuration, is also possible in this case, taking advantage of the diagrid structure to create new free space able to accommodate new activities [29].

### 2.3.2 Dissipation Capacity

Another distinction worth making is related to the energy dissipation of the exoskeletons. This intrinsic characteristic of the retrofitting system has a strong impact on the manner in which the seismic response of the existing structure is controlled, on the stresses' magnitude and distribution in the coupled system, on the technical feasibility of the solution, and on the final costs of the intervention. Given these differences between one system and the other, exoskeletons may be conceived as either dissipative or elastic high-strength systems [35].

#### High-Strength Exoskeletons

Elastic high-strength solutions control the seismic response by adding parallel lateral resistance to the original structure by the incorporation of very stiff external elements. This solution is characterized by having an elastic behavior until collapse, simplifying the design phase. Also, the exoskeletons are composed of bigger structural elements to provide enough strength to the building, increasing the cost of the intervention. [6]

The increase in the stiffness in the retrofitted structure directly results in stronger higher accelerations and substantially higher seismic actions. Consequently, the floor diaphragms that must withstand these forces may require a strengthening intervention. Additionally, special attention must be paid in the design phase since the collapse mechanism is not ductile and the foundation system is at risk of being over-stressed. [29, 34]

#### Dissipative Exoskeletons

Exoskeletons conceived in this way control the system's response by dissipating seismic energy through sacrificial devices or dampers, reducing the acceleration and inertia forces on the structure [36]. In this case, the cross-sectional area required for the elements is smaller, and the damage after the seismic episode is localized in the dissipation devices. The overall cost of the intervention is reduced by the decrease in the amount of material needed, but also increased by the elevated cost of the devices. [6]

There are several alternatives for the introduction of dissipation in the retrofitting system, for example, in [31], dampers are included in the bracings of the exoskeletons; in [37], the connection between the retrofitting system and the building is provided with self-centering and energy-dissipating mechanisms; in [34], dissipation is introduced by means of a responsive mechanism that changes the boundary conditions between the steel frame and the foundation according to the earthquake intensity; among many other possibilities.

Certain considerations must be made when incorporating dissipation into the retrofitting system, the main problem that can arise is that dissipative devices need a certain displacement or velocity for their activation, hence, larger ductility in the existing structure must be ensured [38], so additional preliminary weakening becomes a possibility to augment the deformation capacity. [13, 31]

Furthermore, the effectiveness of the dampers can be overestimated in some cases; this is a possibility when the level of knowledge of the original structure is not sufficient, or when the stiffness of the building is underestimated by neglecting the effect of stiff and brittle parts of the structure, as infills or staircases, during the modeling of the structure. These aspects are worth special attention to avoid designing a structure that fails to control the design parameters. [39–41]

## 2.4 Design of Exoskeletons

### 2.4.1 Considerations

As mentioned at the beginning of this literature review, a massive intervention is needed to update the existing building stock to current standards [5]. In this context, the sustainability and technical feasibility of the proposed intervention must be considered in the operative choices and in the definition of the performance objectives and related design targets [42].

Exoskeletons as a retrofitting alternative go along with sustainability goals, enabling a holistic intervention approach. Nevertheless, once these structures have been chosen, the consideration of the Life Cycle Thinking design approach for the reduction of environmental, social, and economic impacts can be very valuable [7, 43]. Taking

into account the entire life cycle of a structure means thinking about the ease of the repair and adaptation of the solution during the use phase, as about the potential reuse or recycling of the components at the end of life [44]. These objectives can be accomplished by the use of dry, prefabricated, and standardized solutions [45], for example, with the selection of metallic materials; additionally, the adoption of more restrictive design parameters to avoid the breakage of structural and non-structural elements of the existing structure may be considered [6].

Furthermore, when thinking about a global renovation of the building stock, a number of limitations arise. The high construction times and costs, along with the business disruption or need for relocation of the buildings' inhabitants, are inconveniences that lead to a low retrofitting rate [8, 46]. These aspects play a crucial role in the design of a retrofitting solution; prefabricated and standardized techniques must be prioritized, as well as solutions integrating structural, energetic, and architectural aspects, because of their effectiveness in reducing construction times and improving the return of the investment. Opting for techniques applied exclusively from the outside of the building, all three of the mentioned limitations are being addressed [47, 48]; to this end, preliminary interventions must be avoided whenever possible by finding the appropriate exoskeleton configuration. [6]

Apart from the above, there are other aspects to consider in the design phase. First, structures that increase the structural performance by providing additional stiffness to the system can play a crucial role in regularizing the floor plan, which reduces the participation of rotational modes during seismic events [49]. Secondly, neglecting the mass of the exoskeleton can lead to inaccurate assessments of the building's dynamic behavior, thus, this assumption must be made with caution [18]. Lastly, to enhance the load transfer between the structures, a rigid connection is preferable, and the diaphragmatic behavior of the existing floors must be secured [50].

The preferred control parameters for the design process are floor displacements, inter-storey drifts, shear forces, and floor accelerations [49]. According to the Performance Based Design principle, these parameters must be chosen to limit the damage of structural and non-structural elements at the Life Safety Limit State [13, 51]. Moreover, exoskeletons can be conceived as 'sacrificial appendages', that undergo damage to protect the existing structure during the seismic excitation [16].

### 2.4.2 Proposed Design Procedures

The procedures for the design of exoskeleton structures proposed by various authors [6, 16, 28, 29, 31, 49] share several of the main points. These approaches are mainly presented as a series of steps, that could be summarized in the following way:

**Step 1:** Definition of the design targets

The design targets are the parameters that represent the aimed performance, these will be controlled during the design process, and must comply with certain imposed limits. The preferred ones in literature are displacements relative to the ground, inter-storey drifts, seismic forces, stresses, and frequencies.

**Step 2:** Multi-Degree-of-Freedom to Single-Degree-of-Freedom (MDoF to SDoF)

This step is related to the simplification of the coupled system as two SDoF systems, coupled by means of a rigid link, or a Hook spring with a certain stiffness. The first oscillator is equivalent to the existing structures, with defined parameters, while the second oscillator is representative of the retrofitting system, and its characteristic parameters are to be determined in the next step.

**Step 3:** Evaluation of the design parameters

The design parameters are the characteristics that represent the second oscillator of the system, the SDoF model of the exoskeleton structure. In high-strength exoskeletons, these parameters are related to the overall mass and stiffness of the retrofitting system, considered as they are, as ratios with the corresponding values or adimensionalized, but representing the same characteristics. If dissipative devices are introduced in the intervention, an additional parameter is introduced to account for the damping of the device.

**Step 4:** Single-Degree-of-Freedom to Multiple-Degree-of-Freedom (SDoF to MDoF)

Once the overall values of mass and stiffness, have been obtained, these design parameters must be transformed into the properties of each element of the retrofitting system. The definition of the number and position of the exoskeletons, as well as the topology of the truss configuration and dimensioning of the elements, is predominantly based on previous experiences of designers in similar cases. Authors propose

different criteria to orientate these choices, based, for example, on geometrical relations, or on the simplification of the exoskeletons as a cantilever beam and obtaining its maximum top displacement with the Timoshenko theory.

As explained in [52], from which the bases of the procedure have been derived by the cited authors, this methodology based on a SDoF system must be complemented with an analysis of the proper stiffness and yield forces distributions in order to be suited for the application to MDoF systems. Specifying that the building response is very sensitive to these distributions.

### 2.4.3 Main Outcomes

The behavior of the coupled system after the application of the exoskeleton structures is strongly modified due to the significant increase of the stiffness. Several improvements are noted in the bibliography, mainly remarking the substantial reduction in displacement, inter-storey drifts, and deformations of the building [31]. Additionally, if the exoskeletons have been conceived in order to provide more regularity to the structure, as in [49], the rotational modes can be reduced up to the point of nearly disappearing.

Furthermore, and also due to the increase in the stiffness, higher frequencies are attained by the retrofitted structure, and consequently, an amplification of the acceleration should be expected [5], described by [18] as a trade-off for the deformation control given by the solution.

The seismic action to which the structure is subjected increases with the stiffness and mass of the system, causing an increase in base shear. Nevertheless, the new total base shear of the coupled system is taken both by the building and the exoskeletons, meaning that, if the mechanical properties of the latter are chosen appropriately, they can succeed in unloading the primary structure, leaving it with lower internal stresses and shear forces than before the retrofit. [18, 53]

If a dissipative behavior is introduced with the retrofitting structure, the acceleration response can be controlled by these devices [6]. Additionally, in this case, greater improvements in the behavior can be expected when facing stronger seismic actions [37], due to the more imminent activation of the dampers.

## Chapter 3

# Revision of the NTC18 and Alternative Approach Proposal

In this chapter, a detailed discussion of section 7.2.3 of the Italian regulation NTC 2018 is done. It highlights a crucial aspect related to the distinction between 'primary' and 'secondary' elements.

In the beginning, in [3.1](#), said section is reported and its meaning is analyzed, explaining its primary aim and reasoning that leads to these considerations, along with the practical implications it has on the design phase of a structure.

In [3.2](#), the concepts provided by the regulation are related to the design of exoskeleton systems. Additionally, several limitations that arise from these suggestions are remarked, enlightening barriers that are present in the practice when trying to comply with this approach.

In the end, in [3.3](#), a different approach is proposed, based on the control of the inter-storey drift as the main parameter, and its advantages and disadvantages are exposed.

## 3.1 Review of the Regulation

The Italian regulation NTC 2018, in the part 7.2.3, states:

*"7.2.3. CRITERI DI PROGETTAZIONE DI ELEMENTI STRUTTURALI  
SECONDARI ED ELEMENTI COSTRUTTIVI NON STRUTTURALI*

***ELEMENTI SECONDARI***

*Alcuni elementi strutturali possono essere considerati "secondari"; nell'analisi della risposta sismica, la rigidezza e la resistenza alle azioni orizzontali di tali elementi possono essere trascurate. Tali elementi sono progettati per resistere ai soli carichi verticali e per seguire gli spostamenti della struttura senza perdere capacità portante.*

*Gli elementi secondari e i loro collegamenti devono quindi essere progettati e dotati di dettagli costruttivi per sostenere i carichi gravitazionali, quando soggetti a spostamenti causati dalla più sfavorevole delle condizioni sismiche di progetto allo SLC, valutati, nel caso di analisi lineare, secondo il § 7.3.3.3, oppure, nel caso di analisi non lineare, secondo il § 7.3.4.*

*In nessun caso la scelta degli elementi da considerare secondari può determinare il passaggio da struttura "irregolare" a struttura "regolare" come definite al § 7.2.1, né il contributo totale alla rigidezza ed alla resistenza sotto azioni orizzontali degli elementi secondari può superare il 15% dell'analogo contributo degli elementi primari."*

The translation is:

*"7.2.3. DESIGN CRITERIA FOR SECONDARY STRUCTURAL ELEMENTS AND CONSTRUCTIVE NON-STRUCTURAL ELEMENTS*

***SECONDARY ELEMENTS***

*Some structural elements can be considered "secondary"; in the analysis of the seismic response, the stiffness and resistance to the horizontal actions of these elements can be neglected. These elements are designed to withstand only vertical loads and to follow the movements of the structure without losing bearing capacity.*

*The secondary elements and their connections must therefore be designed and equipped with constructive details to withstand the gravitational loads, when subjected to displacements caused by the most unfavorable of the design seismic conditions of the Collapse Limit State, evaluated, in the case of linear analysis, according to § 7.3.3.3, or, in the case of non-linear analysis, according to § 7.3.4.*

*In no case the choice of the elements to be considered secondary can determine the transition from "irregular" structure to "regular" structure as defined in § 7.2.1, nor the total contribution to stiffness and strength under horizontal actions of secondary elements can exceed the 15% of the analog contribution of the primary elements."*

This specification is done in chapter 7 of the NTC 2018, the chapter is about design for seismic action, the point is to suggest to the designer which elements to verify as primary and which to verify as secondary. This is due to the fact that the design of these elements are different in terms of verifications, level of detail and considerations at the time of making technical choices. The verifications of the secondary elements are done only in terms of ductility.

The regulation allow the designer to consider some elements as secondary, to profit from these 'simplifications', when the element meet certain requirements. It specifies that an element, considered as secondary, is designed to resist only vertical loads, and must have a limited participation in the structure's mechanism to face horizontal

loads. In the overall stiffness and strength of the structure to resist horizontal actions, the contribution given by the secondary elements cannot be more than 15% of the contribution given by the primary elements.

## 3.2 Issues Related to the Regulation

The reasoning that guided this suggestion of the regulation was not specifically thought for the addition of exoskeleton structures. Nevertheless, in the design process of exoskeletons, the distinction between primary and secondary elements plays a fundamental role.

The reason is that, if exoskeletons are designed entirely with primary elements, as a 'primary structure', while the existing structure is considered as a 'secondary structure', the aim of the exoskeletons is to unload almost completely the existing structure. In this case, the stiffness of the retrofitted system must be at least 7 times the stiffness of the existing structure, leading to an oversized and expensive solution.

In many cases, practitioners and designers prefer to consider the existing structure as secondary due to the lack of knowledge of how the stresses spread in the structure when consolidation is performed through exoskeletons. In this way, the safe solution is obtained by almost completely unloading the building becoming a secondary structure.

As explained, the differentiation between primary and secondary elements is done based on the contribution of the element to the overall stiffness and strength of the structure under horizontal actions. However, in the majority of the cases, assessing the real level of stress in each structural element could be impossible to obtain or could lead to hard work. To obtain this information, exhaustive surveys must be carried out on each element causing inconveniences and interruption of daily activities. Considering that one of the main advantages of exoskeletons is that it is a non-invasive methodology, it is a preferred option in cases where the interventions inside the structure should be avoided (e.g. strategic buildings like hospitals, airports, and military structures).

Furthermore, if the level of knowledge of the structure is low, the constituent materials are penalized by a factor that reduces its resistance, but this approach doesn't assure an accurate estimation of the distribution of stresses between the elements.

Additionally, even if an accurate level of knowledge of the structure is achieved, retrofitting solutions with exoskeletons contributes to a significant change in the stress distribution and load path inside the structure. Specifically, this change could be related to several geometric and technical parameters like the position and sizing of the exoskeletons and/or type of connections, among other factors.

In conclusion, identifying the contribution to the overall stiffness and strength of horizontal actions of the single element is difficult to accomplish, hence, the integrity of the existing structure must be considered 'secondary' when performing an intervention with exoskeletons, limiting its contribution to the stiffness facing horizontal actions to the 15%. Consequently:

$$\frac{K_{syst}}{K_{str}} = \frac{100\%}{15\%} = 6.67$$

### 3.3 Proposed Displacement-Based Approach

The proposed approach is based on inter-storey drift, instead of the stiffness contribution of the elements. The aim is to link the exoskeleton design to an elastic inter-storey drift threshold of the existing structure demonstrating that, in this way, the entire structure verifies.

The main advantage of this procedure is that the displacement is an easily measurable parameter such that there is no intention of making a distinction between primary and secondary elements. In this way, the horizontal action is taken by both the exoskeletons and the existing structure in the right measure that allow to guarantee the overall structural safety of the system and, especially, of the existing building.

The disadvantage is that determining the limit inter-storey drift, for which the structure will be safe and verified, depends on the particularities of each case. Further investigations are required to determine the limit value of this parameter in each

case. However, it is reasonable to think that when a generic structure lives in an elastic field or when the ductility capacity of the structure is not exploited, critical configurations of failure should be prevented.

One of the aims of this thesis is especially related to the verification of this assumption obtained as a result of the optimal design of the exoskeletons among all the investigated scenarios. When the optimal configuration and sizing of the exoskeletons, for each scenario, will be obtained, the structural safety will be assessed.

Moreover, a critical discussion of the stiffness approach proposed by the Standard regulation is necessary. With specific regard to old existing buildings, though many structures exhibit significant inner stiffness due to the traditional massive design approach, a deficient seismic behavior is usually recognized. In other words, information related to the overall stiffness of the structure not only is often difficult to obtain, because of the natural uncertainty of several unknown structural parameters, but could lead to significant oversize of the retrofitting structure and important economic losses, which do not encourage this retrofitting technique.

In conclusion, the ultimate goal is not to propose an alternative methodology with respect to the one proposed by the Italian regulation, but to propose a paradigm shift where the level of knowledge of the structure and the experience of the designer still have a crucial role. As demonstrated by the investigation conducted on generic target structures, the feasibility of the displacement approach will be demonstrated as well as the inappropriateness of the suggested stiffness ratio between primary and secondary structure proposed by the NTC18.

## Chapter 4

# Problem Statement and Analysis Setting

In this chapter, the methodology conducted in this study is detailed, based on an optimization algorithm that performs Finite Element Analyses to determine the parameters that constitute the Objective Function.

In the first section, [4.1](#), the focus is put on the optimization. Firstly, the mathematical formulation of the objective function is presented, talking about the constraints and the penalty system implemented, the design variables, and the motivations that determined the choices in their definition.

Then, the outline of the employed algorithm, based on Genetic Programming, is summarized in a flow-chart and each step of the process is thoroughly described.

On the other hand, the second section, [4.2](#), is dedicated to the Finite Element Analyses conducted using SAP2000, where the specifics of both the linear dynamic analyses and the non-linear static analyses performed are mentioned.

## 4.1 Definition of the Optimization via Genetic Programming

Genetic Programming (GP) is a type of Evolutionary Algorithm that belongs to the Metaheuristic Algorithms. According to [54]: *"A metaheuristic is a high-level problem-independent algorithmic framework that provides a set of guidelines or strategies to develop heuristic optimization algorithms. The term is also used to refer to a problem specific implementation of a heuristic optimization algorithm according to the guidelines expressed in such a framework."*

These algorithms offer a high-level, problem-independent framework, which means they are not tied to a specific type of problem or mathematical model. Instead, they offer a set of general strategies and guidelines for creating heuristic optimization algorithms. The core idea behind metaheuristics is to find solutions that meets practical criteria and constraints while being computationally efficient.

These algorithms can be classified as evolutionary, physics-based, swarm-based, bio-inspired, and nature-inspired algorithms. In this work, the focus is put in the first ones. Evolutionary Algorithms take inspiration on the natural evolution of a population of individuals, according to the Darwinian Theory of Evolution and natural selection, to adapt to the environment.

The main differences between metaheuristic algorithms and the classical optimization approaches are that the former are problem-independent and versatile, making them suitable for a wide range of problems. Also, metaheuristics aim to find satisfactory or near-optimal solutions within a reasonable time frame. These combine local and global search strategies, introduce randomness in the process, and they are generally more robust in handling ill-defined problems.

In this work, an optimization algorithm based on Genetic Programming strategies is implemented. Some modifications were made to the classical Genetic Algorithm to adjust better to the particularities of this specific study, nevertheless, maintaining all the core ideas of the methodology.

### 4.1.1 Mathematical Formulation of the Objective Function

The optimization, is focused on weight minimization. To properly formulate the problem, three primary components of the optimization, namely the objective function (OF), applied constraints (C), and design variables (DV), must be defined. The optimization formulation is expressed as follows:

$$\min F(\mathbf{x}) = \left[ N_{Ex} \cdot \rho \sum_{i=1}^{N_{el}} A_i \cdot l_i \right] \cdot \phi_1(D_i) \cdot \phi_2(S_i) + \phi_3(N_{Ex})$$

$$\mathbf{x} = \left[ \overbrace{x_1, \dots, x_i, \dots, x_n}^{\text{Topology DV}}, \overbrace{x_{n+1}, \dots, x_{n+j}, \dots, x_{n+m}}^{\text{Size DV}} \right]$$

subjected to :

$$x_i = \begin{cases} 0 \\ 1 \end{cases} \quad ; \quad x_{n+j}^{lower} < x_{n+j} < x_{n+j}^{upper}$$

$$D_i = \frac{\delta_i}{\delta_{allowable}} < 1 \quad \forall i = 1, \dots, N_{nodes} \quad ; \quad \delta_{allowable} = \frac{H_{storey}}{\beta}$$

$$S_{i,1} = \frac{N_{Ed}}{N_{Rd}} + \sqrt{\left(\frac{M_y^{Ed}}{M_y^{Rd}}\right)^2 + \left(\frac{M_z^{Ed}}{M_z^{Rd}}\right)^2} < 1$$

$$S_{i,2} = \frac{N_{Ed}}{\frac{\chi_z \cdot N_{Rk}}{\gamma_{M1}}} + \sqrt{\left(k_{zy} \cdot \frac{M_y^{Ed} + N_{Ed} \cdot e N_y}{\frac{\chi_{LT} \cdot M_y^{Rk}}{\gamma_{M1}}}\right)^2 + \left(k_{zz} \cdot \frac{M_z^{Ed} + N_{Ed} \cdot e N_z}{\frac{M_z^{Rk}}{\gamma_{M1}}}\right)^2} < 1$$

Where  $N_{Ex}$  is the total number of exoskeletons,  $N_{El}$  is the number of elements of a single exoskeleton,  $A_i$  and  $l_i$  are the cross-sectional area and length of the single element  $i$ , respectively.

Two critical constraints are considered: firstly, a maximum allowable inter-storey drift is imposed aiming to maintain the structural integrity of the building in the elastic range. To achieve this, a threshold beyond which damage occurs at the level of the structure's infills must be fixed. This limit is  $\delta_{allowable}$ , and consists of the storey height divided by a factor  $\beta$ , determined for each specific case study, from a minimum of 500 to a maximum of 750. This constraint is defined as  $D_i < 1$ .

Secondly, the stress requirements that the exoskeletons must satisfy, according to the NTC 2018 regulation, are considered as  $S_i < 1$ .  $S_{i,1}$  corresponds to the combined bending and axial force verification for class 1, 2, 3, or 4 pipe sections (EC3 6.2.1.(7)), while  $S_{i,2}$  corresponds to the buckling verification for class 4 pipe sections under flexure and axial compression (NTC Eq. C4.2.38).

A penalty system is employed to include the constraints in the OF.

$$\begin{aligned}\phi_1 &= \sum_{i=1}^{N_{nodes}} D_i^{unf} \\ \phi_2 &= \sum_{j=1}^{N_{Ex}} \sum_{i=1}^{N_{el}} S_{i,j}^{unf} \\ \phi_3 &= \alpha \cdot N_{Ex}\end{aligned}$$

To obtain the first penalty ( $\phi_1$ ), the inter-storey drift that the building experiences at each node ( $\delta_i$ ), when subjected to the seismic load combination defined in the regulation, is computed. Then, the ratios between each one of these values and the allowable inter-storey drift ( $\delta_{allowable}$ ) imposed following the first constraint, are obtained ( $D_i$ ). Then,  $\phi_1$  is the sum of the ratios with values bigger than 1, meaning, the ones corresponding to nodes with  $\delta_i > \delta_{allowable}$ , called  $D_i^{unf}$ . In this way, both the number and severity of the violations are being considered.

Following the same reasoning, the second penalty ( $\phi_2$ ) is determined by computing the ratios between the stresses of each element of the retrofitting system and the

allowable stresses, as  $S_{i,1}$  or  $S_{i,2}$ ; and summing all the ratios that exceed the value of 1, meaning, the ratios that correspond to the element in violation of the stress requirements, called  $S_i^{unf}$ .

Finally, the third penalty ( $\phi_3$ ) is related to the amount of exoskeletons being incorporated in the considered configuration ( $N_{Ex}$ ). The motivation for this penalty is that, in most cases, the free space around the building is in use for specific activities and enhances the accessibility to the structure, and by occupying this space with exoskeletons, the use of the building must be partially reorganized. Moreover, each exoskeleton to be used implies a certain organization for the transportation of the materials, construction time, and risk of mistakes during the assembly and erection, among other issues. Both these aspects make a configuration with fewer exoskeletons preferable, for this reason,  $\phi_3$ , obtained as the number of exoskeletons by a scaling factor  $\alpha$ , is summed to the objective function already multiplied by the two previous penalties.

### Design Variables

$$\mathbf{x} = \left[ \overbrace{[x_1, \dots, x_i, \dots, x_n]}^{\text{Topology DV}}, \overbrace{[x_{n+1}, \dots, x_{n+j}, \dots, x_{n+m}]}^{\text{Size DV}} \right]$$

In the present work, topology and size optimizations have been performed, which is reflected in the design variables. The variables from  $x_1$  to  $x_n$  are related to the topology of the solution, representing the positions and amount of exoskeletons of the considered configuration;  $n$  is the number of potential positions where the exoskeletons can be located.  $x_i$  are binary variables, if  $x_i = 1$ , an exoskeleton is put in the  $i^{th}$  position, instead, if  $x_i = 0$ , said position is left free. In this way,  $\sum_{i=1}^n x_i = N_{Ex}$ .

Meanwhile, the variables from  $x_{n+1}$  to  $x_{n+m}$  correspond to the sizing of the exoskeletons. These variables are discrete, and their value represents the position of the chosen cross-section in a table of steel profiles. The table is sorted according to the cross-sectional area of the profiles, and the value that  $x_{n+j}$  can take is limited between a lower and upper bound,  $x_{n+j}^{lower}$  and  $x_{n+j}^{upper}$ , respectively. For this work,  $m = 4$ , representing the sections assigned to the columns, beams, and bracings of

#### 4.1. DEFINITION OF THE OPTIMIZATION VIA GENETIC PROGRAMMING

the exoskeletons, and to the links between the exoskeleton and the existing structure, respectively; all the exoskeletons are designed with the same profiles.

### 4.1.2 Employed Algorithm

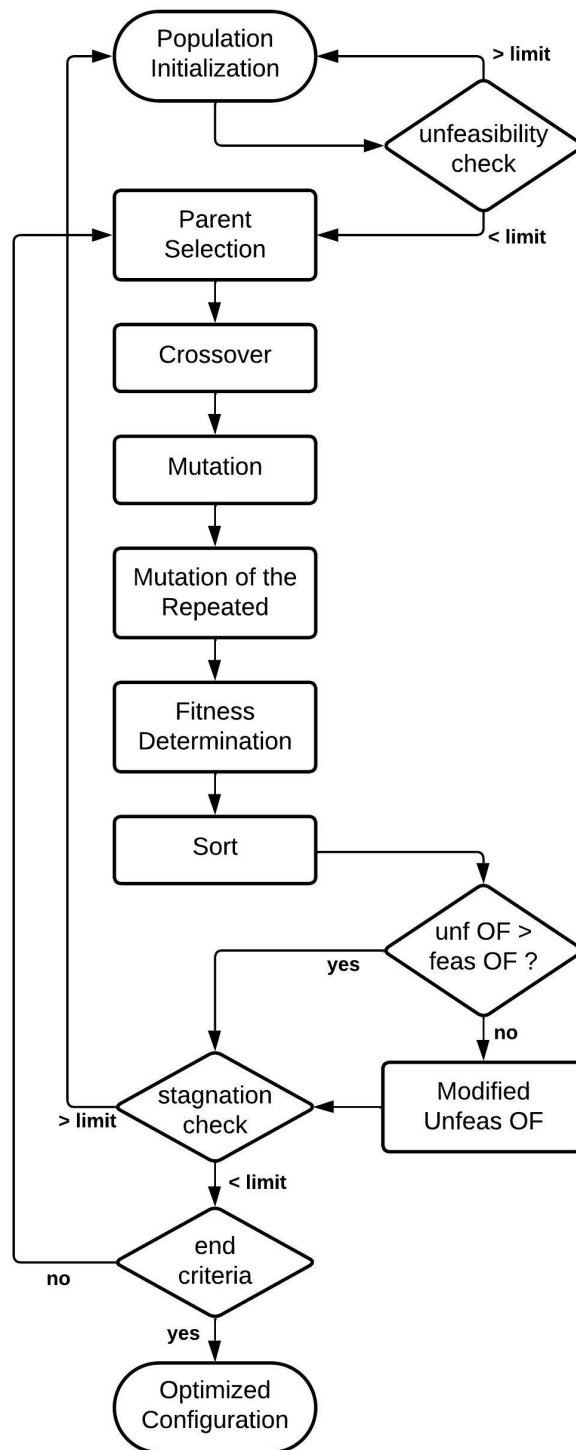


Figure 4.1: Flow-chart of the modified Genetic Algorithm employed for the Optimization Process

### **Population Initialization**

The starting point is the creation of the population composed of a chosen number of members (*popsize*), each population member represents a potential solution to the problem. The vector of design variables of each individual of the population is called 'chromosome'; to define a population member, the values of the variables are assigned. In this case, the definition of the initial population is done in a random way; the topology DVs are generated, with the only restriction that at least two exoskeletons must be included in the retrofitted configuration. The size DVs are chosen from a table of selected profiles, in a provided range.

Once the initial population has been defined, the value of the OF must be computed for each population member. In this case, a model is generated in SAP2000 for each configuration in consideration, and the results required to determine the OF are obtained from the analysis performed in said software.

### **Unfeasibility Check**

When a potential solution does not satisfy one of the constraints, namely the maximum allowable inter-drift of the original building or the structural verifications of the exoskeleton's members, the population member of said solution is called 'unfeasible'. The unfeasibility is the ratio between the number of unfeasible members in a population and the population size.

To have at least one feasible member in a population is useful to guide the algorithm in the way of the solutions that can satisfy the constraints imposed. In consequence, after the definition of each population member's fitness, the unfeasibility is computed and if there are no feasible elements, the initial population is regenerated.

### **Parent Selection**

The iterative process begins with the selection of the best potential solutions of the population, from now on called 'parents'. These members are selected through a Roulette Wheel, which assigns a probability to be chosen to each population member, based on their fitness, the members with lower cost will have a higher probability of being chosen.

### Crossover

From the parents, new individuals are derived, called 'children'. These are a combination of the parents' chromosomes, conforming a new, evolved, population. An internal iteration is performed including the parent selection and crossover steps. At each iteration, two parents are chosen from which a certain number of children is generated ( $\frac{numch}{2}$ ), as a combination of their variable's vector, in this case,  $numch = popsize$ .

There are several ways to perform the crossover, in this case, a Double-Point Crossover is employed. For this procedure, as illustrated below, two points of the chromosome are picked randomly ( $r_1$  and  $r_2$ ), excluding the beginning and the end of the vector, at which the chromosome vectors of both parents will be trimmed. The first child of these parents is composed of the first and last part of the first parent, and the middle part of the second parent; while the second child is the exact opposite. The iterations are repeated until  $numch = popsize$ .

$$\begin{aligned}
 parent_1 &= [ x_1^1, x_2^1, x_3^1 \mid x_4^1, x_5^1, x_6^1, x_7^1, x_8^1 \mid x_9^1, x_{10}^1 ] \\
 &\quad \quad \quad r_1 \quad r_2 \\
 parent_2 &= [ x_1^2, x_2^2, x_3^2 \mid x_4^2, x_5^2, x_6^2, x_7^2, x_8^2 \mid x_9^2, x_{10}^2 ] \\
 &\quad \quad \quad r_1 \quad r_2 \\
 children_1 &= [ \overbrace{x_1^1, x_2^1, x_3^1}^{\text{parent 1}}, \overbrace{x_4^2, x_5^2, x_6^2, x_7^2, x_8^2}^{\text{parent 2}}, \overbrace{x_9^1, x_{10}^1}^{\text{parent 1}} ] \\
 children_2 &= [ \overbrace{x_1^2, x_2^2, x_3^2}^{\text{parent 2}}, \overbrace{x_4^1, x_5^1, x_6^1, x_7^1, x_8^1}^{\text{parent 1}}, \overbrace{x_9^2, x_{10}^2}^{\text{parent 2}} ]
 \end{aligned}$$

The creation of children enables the exploration of new potential solutions for the problem, close to the best solutions obtained previously; by keeping the values of the variables that gave better results, but combined in a different way among them.

### Mutation

After a certain amount of iterations, the potential solutions may become more similar

among them; this happens because, as explained, the new populations are generated as combinations of the best individuals of the previous generations, guiding the algorithm to convergence; this situation will be called, from now on, 'repetition'. Nevertheless, it is possible that this solution, other than being the best possible one, has a very different configuration; but by outstanding from other solutions that share some aspects of the configuration, it was chosen. In this situation, such a solution is called 'local optima'.

When facing repetition, a good solution is to explore the solutions far from the preferred ones. A useful approach is to randomly regenerate one or more variables of the chromosome of a certain population member. Whether or not to pick a variable to be mutated is decided in a random way with a probability of occurrence defined at the beginning. If the variable chosen to be mutated is binary, the value is changed for the opposite; instead, if the variable is one of the cross-sections, another section is chosen in the determined range from the table of profiles.

In this algorithm, each variable of the chromosome of each population member is a possible subject to mutation, according to the predefined probability. In this way, one population member can have more than one variable mutated, while another one can keep all the same variables it had.

### **Mutation of the Repeated**

As described before, with the passing of the iterations, the population members begin to be more alike between them, generating repetition. It is possible that, in this case, two population members have the same chromosome, meaning, represent the same solution. The repetition of a given chromosome in the population indicates its potential, but having two or more times the same solution reduces the number of different solutions being analyzed at each iteration, and, consequently, the exploration of the algorithm is lower.

In the previously described mutation, the objective was to find configurations with significant differences from the present ones. Instead, in this case, a new strategy is implemented with the aim of exploring solutions very close to the preferred ones; it is a refinement of the configuration. This modified mutation is directed to the

population members that share the same chromosome, for which, one of them is kept as it is while the others are slightly modified.

$$individual_i = [ \overbrace{x_1^i, x_2^i, \dots, x_n^i}^1, \overbrace{x_{n+1}^i}^2, \overbrace{x_{n+2}^i}^3, \overbrace{x_{n+3}^i}^4, \overbrace{x_{n+4}^i}^5 ]$$

The modifications are performed in exactly one of five parts of the chromosome of each 'repeated' individual, excluding only one of the individuals for each repeated OF, to keep the original population member. The part to be mutated is selected through probabilities assigned to each part. If the mutation is applied in the part 1, the binary part of the vector is regenerated in order to obtain a configuration in which the positions of the exoskeletons change but the amount remains the same. Instead, if it is applied on either part 2, 3, 4, or 5, another section is chosen from the profile table, within a proximity to the current section, defined by a range.

### **Fitness Determination**

The fitness of each child is computed, as explained before, through a Finite Element Analysis (FEA) performed in SAP2000. Additionally, the component values of weight, inter-storey drift ratio, and stress ratio, are saved for each configuration. With this information, a population of twice the size of the original one is created, by combining the parents and the children.

An insight into this step, along with the details of the performed analyses, are given in the next section, [4.2](#).

### **Sort**

To sort the population, two divisions are made. The first one is between feasible and unfeasible members, and the second one is between members with a unique OF value and those with repeated values. The second division gains interest when considering that, if the mutation of the repeated members is applied on the part 1 of the chromosome, the weight of the retrofitting system is maintained, thus, if we have two members that experienced this kind of mutation, both being feasible, they will have the same objective function, because the penalties for which the weight

would be multiplied are equal to 1.

Among individuals with the same objective function, the sort is made according to the sum of  $\max D_i$  and  $\max S_i$ . Being feasible solutions, these values must be lower than 1. Only one solution for each OF value is chosen to be kept for the next population, this is the one that has the lower sum of ratios. The justification of this choice comes with the fact that, at equality of weights, the chosen solution managed to achieve a greater displacement control and/or the exoskeleton elements are less stressed, having a bigger improvement potential than the other one.

### **Assembly of the New Population**

For the creation of the new population, the first individuals to be introduced are the feasible ones with unique OF, chosen as explained in the previous paragraph. Nevertheless, a predefined percentage of the population is purposely conformed by unfeasible members, also with unique OF.

This is the ideal configuration of the population to be obtained, but, if in the population of a certain iteration the preferred category does not have enough individuals to complete the required quantity, the population is completed with the individuals of the other category. Furthermore, if there is a large amount of individuals with repeated OFs, there may not be enough individuals with unique OF neither if considering both feasible and unfeasible members, to complete the population; in this case, the missing individuals are completed with repeated OF members.

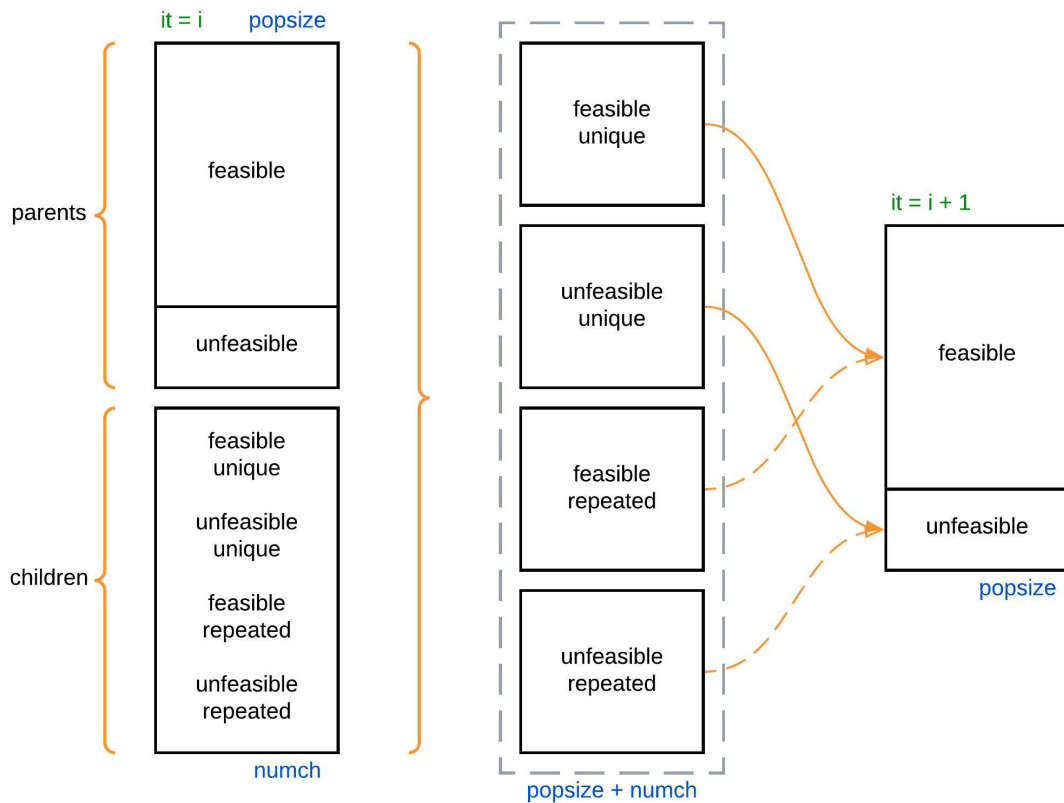


Figure 4.2: Strategy for the assembly of the population for the next iteration

### Modified Objective Functions of the Unfeasible Individuals

At this point, the population size returns to the original number. Nevertheless, before restarting the iteration loop with the new population, one final aspect must be considered. After the final procedure explained for the assembly of the population, the order of the individuals determines its fitness, but, for the parent selection, the probability of being chosen to generate children is given by the OF of the individual, and not by its position in the list. With this in consideration, it is possible to have an unfeasible member with a lower OF than a feasible member, for example, if the weight of a configuration is very low, the penalties employed might not be able to make the OF become bigger than a heavier, but feasible, configuration.

As a solution to the presented problem, when the OF of the last feasible population

member is bigger than the corresponding one of the first unfeasible individual, the latter, along with all the unfeasible population members, is multiplied by a factor. This factor is defined as the first entire number that, if multiplied by the OF of the first unfeasible individual of the population, the result is greater than the OF of the last feasible member.

### **Stagnation**

A local optimal solution is a configuration that gives better results than other configurations that are similar to it. This one may or may not be the global optimal solution, meaning, the configuration that provides better outcomes than any other possible solution.

When the algorithm finds a local optimal, the population starts to converge in the way of this solution. The more iterations that pass, the more population members become similar to this local optimal, and the more difficult it is for the algorithm to explore solutions that are significantly different from it. This situation is called 'stagnation'.

Such cases can be identified because, for a defined number of iterations, the preferred solution maintains the same, from which it can be assumed that the majority of the population is exploring a small area of the field of potential solutions. A solution in this case is to re-initialize the population, keeping only a small number of the best population members. In this way, the exploration of the algorithm is enhanced and the possibility of finding the global optimal is augmented. Nevertheless, if the configuration that has been preferred for several iterations is, actually, the global optimal, it should not be affected by this strategy.

### **Finalization**

After the assembly of the new population, a new iteration starts from the Parent Selection phase, this time selecting the parents from the new population created. This process is repeated until a certain criteria is met for the finalization of the optimization. These criteria can be related to finding an individual with an OF lower than a certain imposed value, or one that complies with all the constraints, among

others. In this case, the optimization is finalized when the number of iterations is equal to a predefined maximum amount.

## 4.2 FEM Analyses

### 4.2.1 Linear Dynamic Analysis with Response Spectrum

To perform these analyses, SAP2000 OAPI was employed. The OAPI enables the control of the FEM software through automatic routines defined in MatLab. This means that the models were created and then modified at each iteration directly by the algorithm, which additionally sets the analysis to run and retrieve the results as variables for the optimization process.

Using linear dynamic analysis for the prediction of displacements and member stresses presents many advantages. The method involves the calculation of only the maximum values of displacements and stresses for each mode. It assumes that the behavior of the structure remains within the linear elastic range, which is an assumption that suits in a satisfactory way the case studies. The computational effort is a crucial factor in this work, given the number of analyses that have to be performed for each case study; hence, the reduction of these times with respect to non-linear methodologies is one of the main highlights.

Eigen vectors were chosen to perform the analysis for their accuracy and completeness in describing the system's behavior. To combine the modal responses and determine the overall seismic response of the structure, the Complete Quadratic Combination method, CQC, has been employed, given that it accounts for the interaction of modes that are close to each other, adjusting better to the case.

The number of modes selected for the analysis is determined to reach 90% of the participation mass in 'x' and 'y' directions, and rotation around 'z'. This amount varies depending on the particularities of the case study, going from 120 to 220 modes. The more exoskeletons are included, and the lighter the sections, the higher the number of local modes with low contributions to the participation mass.

Through these analyses, the structural verifications of the exoskeletons along with the displacement of each node of the existing structure are obtained. With these

parameters and the weight of the exoskeletons, the objective function of the optimization is calculated.

### 4.2.2 Non-Linear Static Analyses

The pushover analysis is characterized by assessing the seismic performance of the structure by gradually applying static equivalent loads, that represent the distribution of forces given by the earthquake excitation, until the structure reaches a specified limit state. In this kind of analysis, the evolution of the deformation and redistribution of stresses can be assessed.

To determine the static equivalent loads to replicate the earthquake nature, two distributions of forces must be considered according to the standard regulation. The distribution of group 1 is given by  $F_i = F_h z_i \frac{W_i}{\sum z_j W_j}$ , where  $F_h = S_d(T_1) W \lambda/g$ ,  $W$  are the weights of the corresponding masses and  $z$ , the heights of the corresponding floors respect to the ground. On the other hand, the forces of group 2 are proportional to the masses of the floors, with the aim of generating a uniform distribution of the accelerations along the height of the building.

Once these distributions are determined, they are applied to the structure, each one in both the 'x' and 'y' directions. Then, the plastic hinges are assigned to the top and bottom of each column of the existing structure and exoskeletons, and the analyses are performed.

The aim is to obtain the structure's stiffness without simplifying the model to a SDoF system. Then, the stiffness of each case study, before and after the retrofit, and in 'x' and 'y' directions, is evaluated with the capacity curves, the procedure is detailed below.

- Firstly, the displacements of interest are determined. These are the top displacements of each configuration that correspond to a maximum inter-storey drift equal to the imposed one.

In the case of the existing structure, the seismic action is scaled to obtain such drift and compute the top displacement, instead, for the retrofitted configuration, as the maximum drift was a constraint of the optimization, this condition

is reached for the total seismic action. The top displacements are obtained in the 'x' and 'y' directions separately, but the maximum inter-storey drift is the total one.

- With these top displacements, the corresponding force can be determined from the capacity curves, interrogating the capacity curve in one direction with the displacement in that same direction.

The force that will be considered for the following steps is the average between the one obtained from the capacity curve that corresponds to the equivalent static forces of 'group 1' and the analog one using 'group 2'.

- The stiffnesses of the existing building and of the retrofitted system, in the 'x' and 'y' directions, are computed as  $K = F/d$ . This represents the slope of a secant that passes through the origin and the point given by the determined displacement and the corresponding force.
- Finally, the ratio between the stiffness of the retrofitted system and the existing structure before the intervention, in the same direction, is computed.

## Chapter 5

# Overview of the Case Studies

Each case study is constituted by one of the existing structures proposed, being retrofitted by one of the possible exoskeleton typologies. All the possible combinations between these are analyzed, and the results are presented and discussed in the next chapter.

In this chapter, the three existing structures considered are illustrated in [5.1](#), being a squared regular building, an L-shaped building, and a U-shaped building. The general aspects concerning the design matters, location, materials, loads, and support and releases that characterize them are exposed. Then, the particularities of each case are shown graphically.

Afterward, in [5.2](#), the general aspects of the retrofitting system, such as the steel sections employed, the support and release conditions, and some particular modeling considerations, are explained. Finally, the details of the two typologies of exoskeletons are analyzed, orthogonal and parallel to the building's façade, are provided.

## 5.1 Considered Existing Structures

For this work, three different existing structures are considered. All of them are projected in reinforced concrete, and their constituent elements are designed in order to comply with the verifications of the Ultimate Limit State (ULS) related to vertical actions, but to be in failure, globally, when facing the seismic excitation related to the Life Safety limit state.

The structures are composed by regular modules arranged in different ways to obtain variations in the structural behavior of the structures. The base module, that then is replicated to obtain the final configurations, is a 3 bay by 3 bay structure, each bay is 5 meters long, making the square module of 15 meters by 15 meters; it has 3 storeys of 4 meters each, thus, the total height of the module is of 12 meters. The module is perfectly regular in plant and in height.

All the columns of one existing structure have the same section and reinforcement, for the beams, the same thing happens, but beams in one direction are considered principal because the vertical loads are applied on them, while the ones in the other direction, even though they have the same configuration, are secondary. The details of the columns and beams of each existing structure considered are depicted in their corresponding subsections.

### Materials

<b>C35/45</b>	
modulus of elasticity 'E'	34.077 GPa
poisson 'U'	0.2
shear modulus 'G'	14.20 GPa
weight per unit volume	24.99 kN/m <sup>3</sup>
<b>A615Gr60</b>	
modulus of elasticity 'E'	199.90 GPa
poisson 'U'	0.3
weight per unit volume	76.97 kN/m <sup>3</sup>

Table 5.1: Properties of the materials of the existing structures

All columns and beams in reinforced concrete are designed employing concrete C35/45, with reinforcement bars in A615Gr60. The material's properties are specified in the previous table.

### Loads

It has been determined that, for these specific structures, the most determinant action is related to the seismic combination, being this the focus of the studies.

#### Vertical Loads

The vertical loads applied to the structure are reported in the following table.

$G_1$	8 kN/m <sup>2</sup>
$G_2$ , <i>slab</i>	3.6 kN/m <sup>2</sup>
$G_2$ , <i>fa</i>	10 kN/m
$Q$	4 kN/m <sup>2</sup>

Table 5.2: Values of the vertical loads applied on existing structures

$G_1$ ,  $G_2$  , *slab*, and  $Q$  are applied only in the principal beams, which are the ones in 'x' direction.  $G_2$  , *fa* is applied on all the beams on the perimeter of the structure.

#### Seismic Loads and Location of the Structure

All the structures are considered to be located in Foggia, Italy. The analyses are performed with the elastic response spectrum obtained with the following parameters:

- Limit State: Life Safety (SLV)
- Usage Class: II (normal occupancy, no public or social specific functions)
- Nominal Life: 50 years
- Soil Type: B
- Topography: T1

For these characteristics, the parameters for the definition of the spectrum, obtained according to the procedure specified in NTC2018, are:

- Peak Ground Acceleration ( $ag/g$ ): 0.1337
- Magnification Factor ( $F_0$ ): 2.6168
- Reference Period ( $T_c^*$ ): 0.4407

The elastic response spectrum employed, obtained as explained, is the following one.

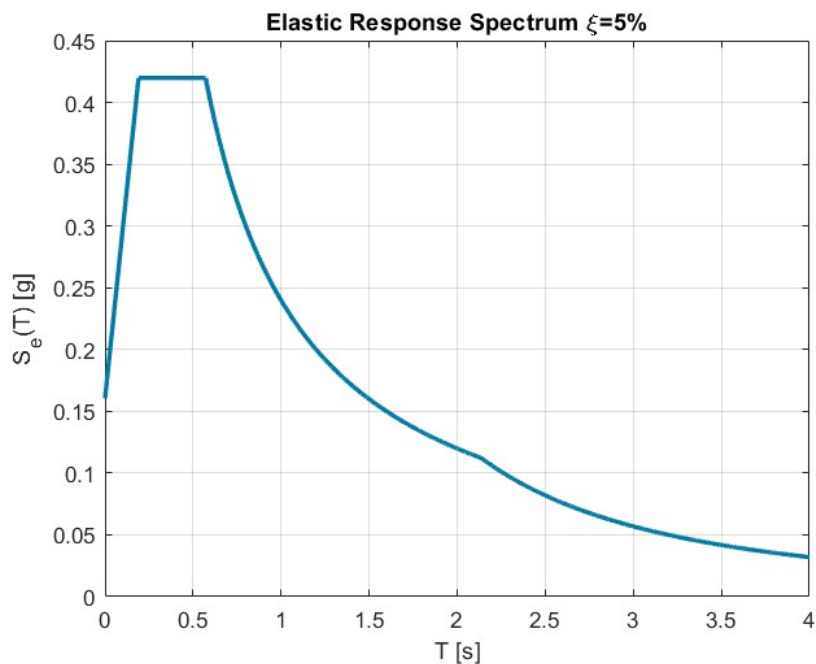


Figure 5.1: Elastic Response Spectrum of Foggia, Italy

The fundamental modes of all three existing structures proposed, which are the ones that have a bigger mass participation in both principal directions of the structure, and the torsional one, have periods that correspond to the peak acceleration of the response spectrum.

Eight load cases are considered for the application of the seismic action, considering 100% applied in one direction and 30% in the other one, and considering the positive and negative direction of the force, as shown in the following equations. Then, the envelope of the load cases' results is performed, to obtain the final value to use in

the load combination, 'E'.

$$\begin{array}{ll}
 E_1 = + 1 U_1 + 0.3 U_2 & E_5 = + 0.3 U_1 + 1 U_2 \\
 E_2 = + 1 U_1 - 0.3 U_2 & E_6 = + 0.3 U_1 - 1 U_2 \\
 E_3 = - 1 U_1 + 0.3 U_2 & E_7 = - 0.3 U_1 + 1 U_2 \\
 E_4 = - 1 U_1 - 0.3 U_2 & E_8 = - 0.3 U_1 - 1 U_2
 \end{array}$$

### Load Combination

The fundamental combination was employed in the Ultimate Limit State verifications, the design of the existing structures is done in order that they could resist this load condition. Additionally, the retrofitted system must also be verified when facing this combination.

$$1.3 G_1 + 1.5 G_2 + 1.5 Q$$

The seismic combination is the one employed for the structural verification within the optimization procedure, the values of displacement and stress ratio considered for the formulation of the Objective Function correspond to this load state.

$$E + G_1 + G_2 + 0.3 Q$$

### **Supports and Releases**

All the columns of the existing structure are clamped at the base, representing the foundations of the building. The beams are continuous, and the nodes between them and the columns aren't released.

The presence of the concrete slab generates a diaphragmatic behavior of each floor, since the slab wasn't modeled, its effect is considered by imposing this behavior to the points of the corresponding floor.

### 5.1.1 Structure 1

The first structure analyzed is composed by the single module described. This structure is regular in plant and in elevation, it provides a first approach for understanding the behavior of exoskeletons. This is used as the base for the other two considered structures.

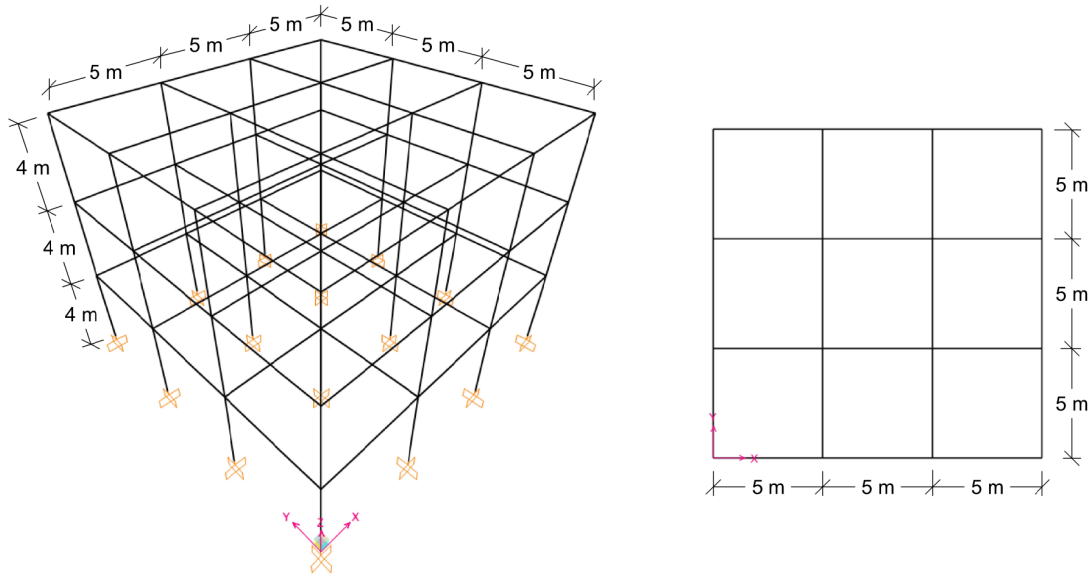


Figure 5.2: Axonometric and top view of the Existing Structure 1

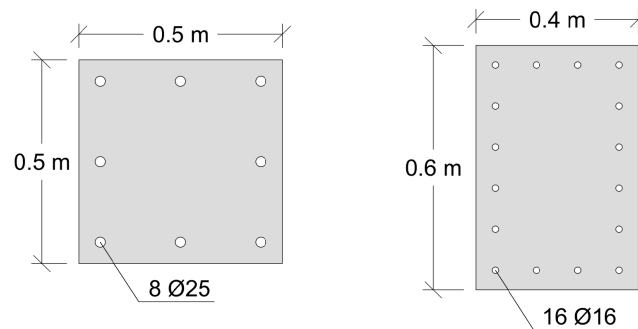


Figure 5.3: Column and beams section and reinforcement details for the Existing Structure 1

### 5.1.2 Structure 2

The second structure analyzed is obtained by replicating the single module forming an L-shaped building.

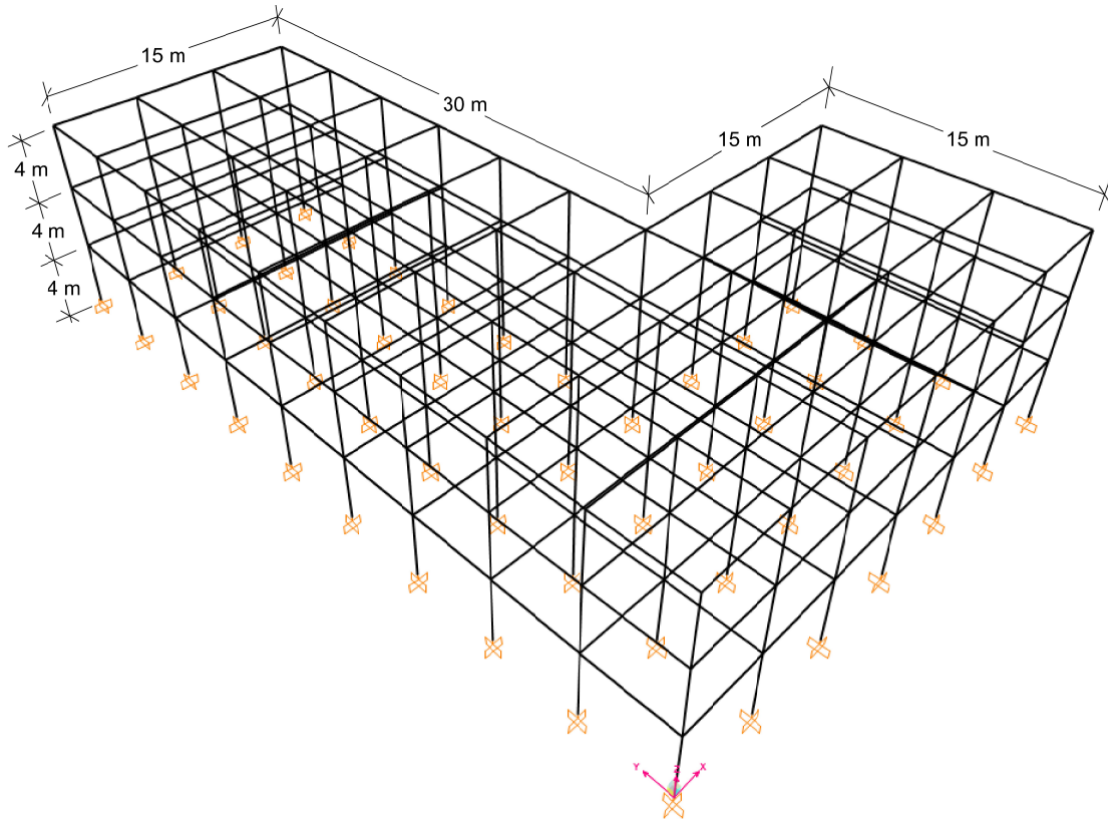


Figure 5.4: Axonometric view of the Existing Structure 2

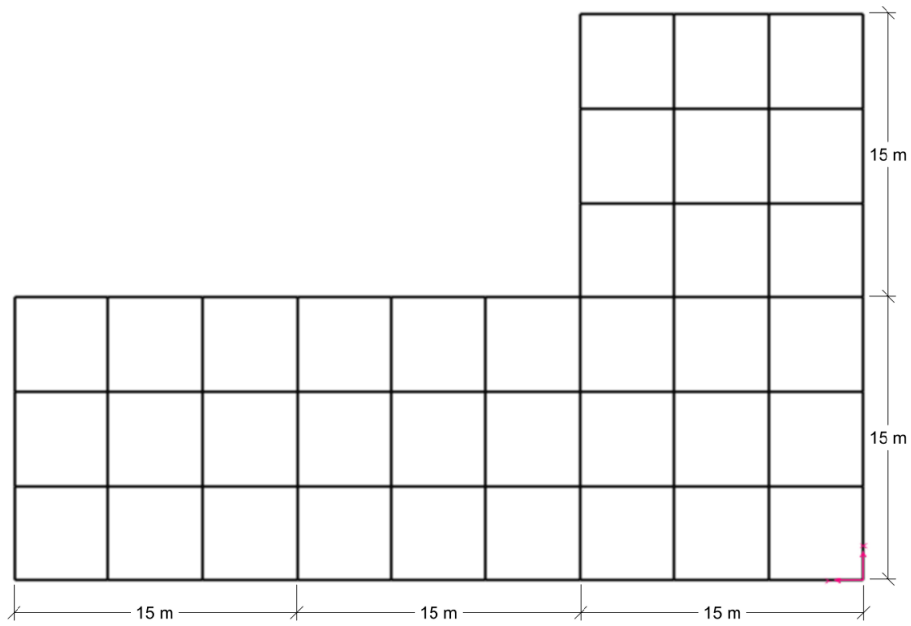


Figure 5.5: Top view of the Existing Structure 2

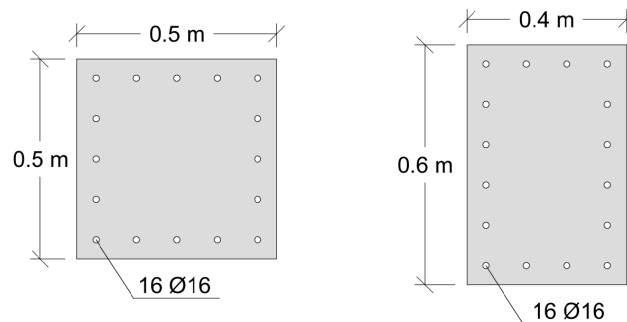


Figure 5.6: Column and beams section and reinforcement details for the Existing Structure 2

### 5.1.3 Structure 3

The third structure analyzed is obtained by replicating the single module forming an U-shaped building.

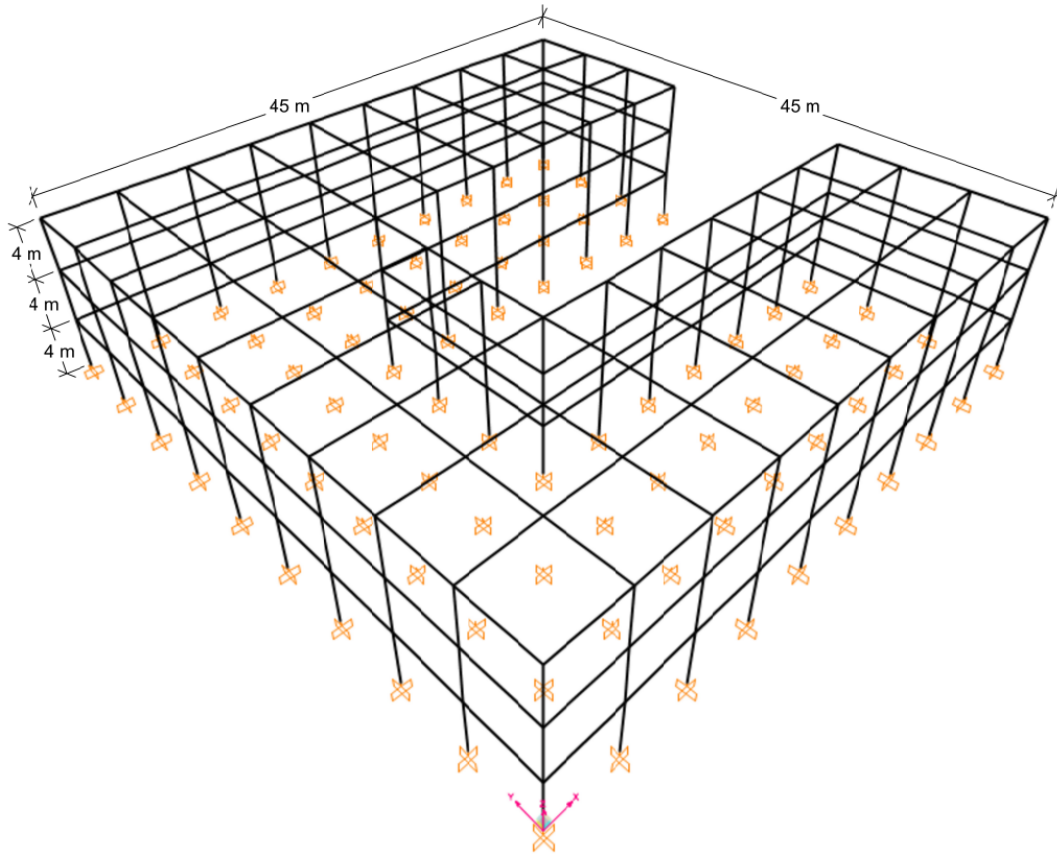


Figure 5.7: Axonometric view of the Existing Structure 3

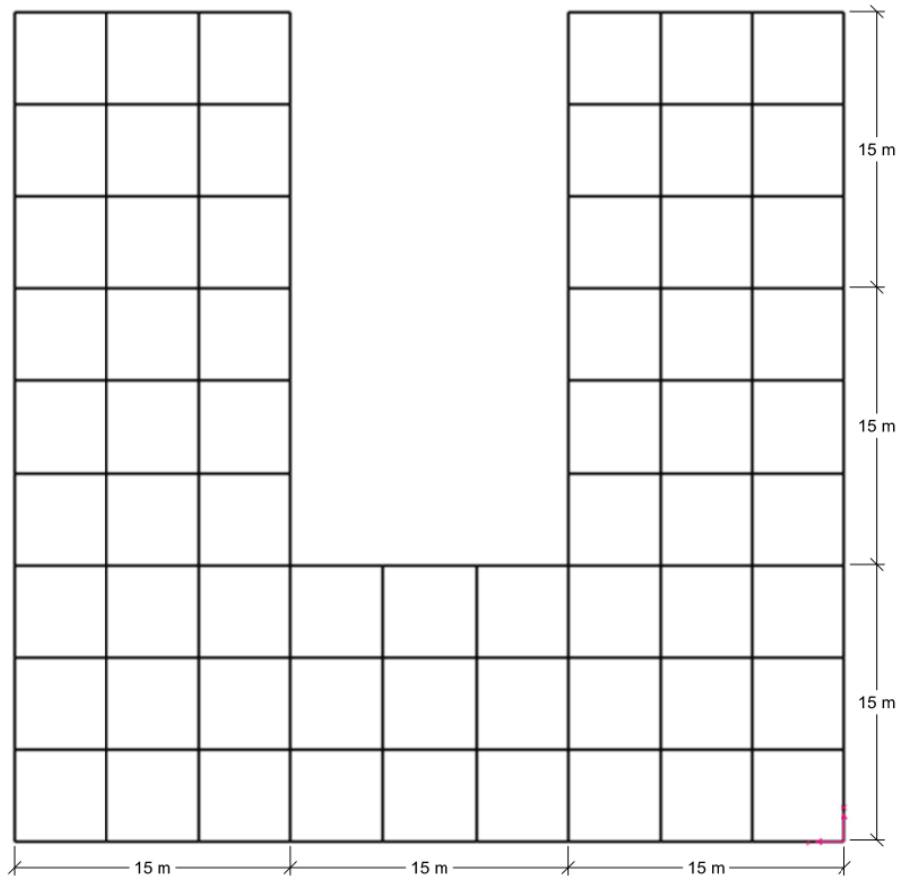


Figure 5.8: Top view of the Existing Structure 3

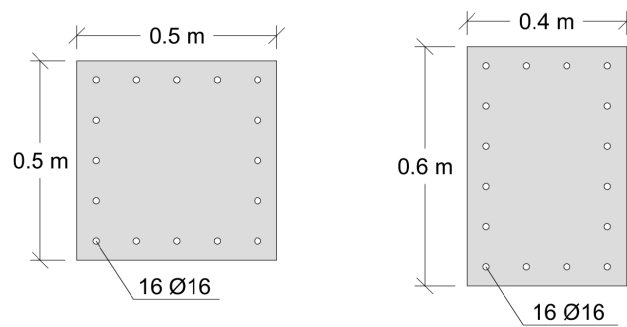


Figure 5.9: Column and beams section and reinforcement details for the Existing Structure 3

## 5.2 Exoskeleton Typologies

Two types of exoskeletons are considered, with different orientations with respect to the existing building's façade. Both typologies being non-dissipative, enhancing the performance of the structure by increasing the stiffness of the system.

### Materials

The exoskeletons are entirely composed of Circular Hollow Sections, all the sections belong to 'EN 1993-1-1'. All the exoskeletons of a final configuration are equal, and the steel profiles used for the columns, beams, bracings and connections are obtained as result of the optimization. The material employed is steel S355.

The selection of the section type is given by the equality of the second moment of inertia in both principal directions, for circular sections. This is an important point in this cases because, even through the exoskeleton has to resist stronger forces in its in-plane direction, receiving part of the loads of the existing structure, it is also subjected to the seismic action in the out-of-plane direction, generated by its own, non-negligible, mass. As the out-of-plane resistance of the exoskeletons is significantly lower than the in-plane one, given by the geometric characteristics of the structure, the shape of the elements plays a crucial role in the stability of the retrofitting structures. This situation gains interest specially in the case of orthogonal exoskeletons where the outer extreme of the exoskeleton is not connected to the building, making this part of the structure very susceptible to warping effects.

Additionally, as commercial steel profiles are being selected for the optimization, an important advantage of Circular Hollow Sections is the variety of sections to be chosen, along with the fact that this kind of profiles reach cross-sectional areas bigger than in other options, like HEA or IPE, with outer dimensions in a close order of magnitude.

### Supports and Releases

The exoskeletons are clamped at the base, representing the foundation system. The beams and bracings are designed to be hinged at both ends, having both flexural moments released at both ends, and torsional moment released in one end, so they

take only axial forces. The columns are continuous, clamped at the bottom and free at the top.

### **Bracings**

The particularity of these elements is that, as the seismic excitation acts in both directions, positive and negative, the element can be compressed or tensed depending on the action. The typical behavior of these kind of elements is to buckle when they are subjected to compression, losing their bearing capacity; consequently, for each direction of the horizontal force, the tensed bracing resists the force and the compressed one buckles.

As the analyses performed in the optimization are linear, this behavior could not be accounted for traditionally; the modelling strategy employed to replicate it is to model only one of the two diagonals, and neglect the buckling when the element is compressed. In this way, the verifications for tension and compression are equal for this element, and we can consider that its behavior is similar enough to the real one.

The final size of the bracing is the one determined for such stress, since during the exercise phase of the structure, the hole force will be taken by one or the other bracing, and for the determination of the weight of the retrofitting system, the two bracings with the final sizing must be considered, even if one of them is not modeled.

### 5.2.1 Orthogonal Exoskeleton

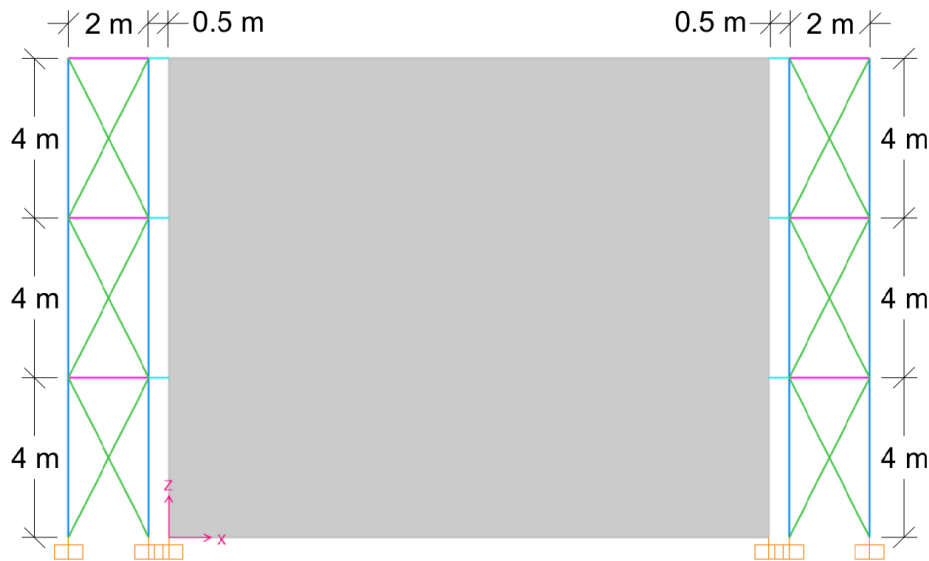


Figure 5.10: Orthogonal Exoskeletons' view and distinction of the elements for grouping: columns (blue), beams (pink), bracings (green), connections (light blue)

Orthogonal exoskeletons are constituted by two continuous columns, the first one is distant 0.5m from the building's façade, while the second one is at 2m from this one. The beams and links are positioned in concordance with the building's beam-column nodes, the beams can take only axial stresses. Three sets of X-bracings are included in each exoskeleton, which are designed to take the integrity of the tension loads, assuming that the compressed diagonal would buckle immediately. This consideration had to be made to be made because of the type of analysis performed, and it maintains the solution on the side of safety.

The connection between orthogonal exoskeletons and the existing structure is done in coincidence with the external beam-column nodes of the building. These connections are purely axial, since the exoskeleton is designed to resist the in-plane actions, while the forces in the other direction should be resisted by other exoskeletons, applied in the perpendicular facade.

The main problem related to this typology is given by the warping effect that affects the external column of the exoskeleton, driven by out-of-plane forces. This effect can be prevented by connecting the exoskeletons through their outer points.

### 5.2.2 Parallel Exoskeleton

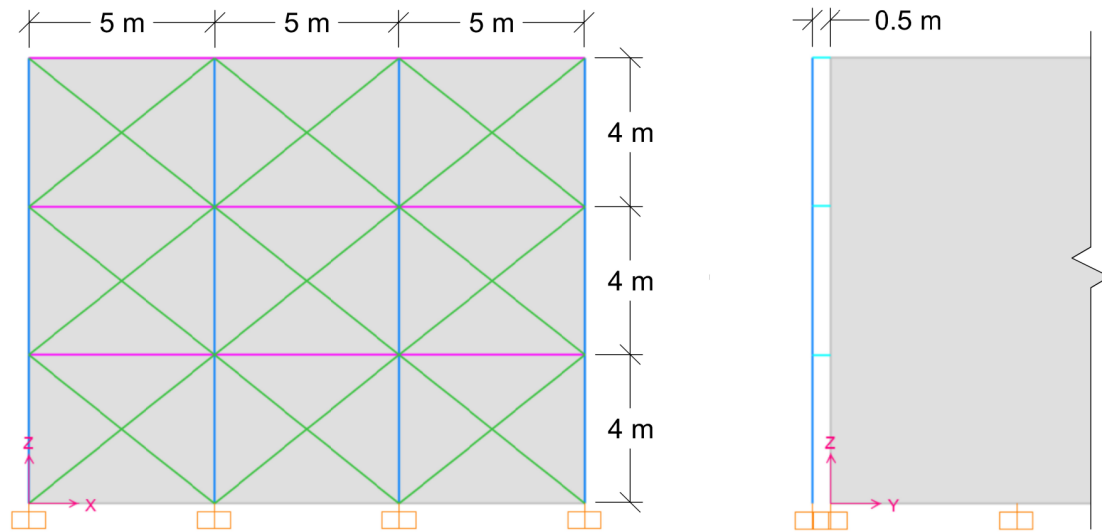


Figure 5.11: Parallel Exoskeletons' views and distinction of the elements for grouping: columns (blue), beams (pink), bracings (green), connections (light blue)

Parallel exoskeletons are constituted by two continuous columns, both located at 0.5m of the building's façade, in coincidence with the existing columns. The beams of the exoskeletons are 5m in length, as the bays of the structure. As in the orthogonal exoskeletons, three sets of X-bracings are placed in each exoskeleton, and their behavior, designed to resist tension loads, is the same as the previously described.

These exoskeletons don't present major instability issues as the previous ones, because, by being connected to the structure by both extremes, their deformation is more constrained, presenting a more efficient behavior.

Nevertheless, a necessary consideration is related to the architectonic barriers. Since these exoskeletons cover the integrity of the bay where they are located, they can generate a need for reorganization of activities carried out in the building. If this typology is to be implemented, an accurate bracing design should be chosen to maintain the windows and entrances operative.

Architectonic barriers can be introduced in the optimization process if necessary, to avoid the location of exoskeletons in zones that are critical for the normal function of the structure. This is the main disadvantage that parallel exoskeletons present

in comparison to orthogonal ones, since the latter only occupy the façade space of a column.

The connection between parallel exoskeletons and the existing structure is done in coincidence with the external beam-column nodes of the building. These connections have no releases, they can transfer axial stress, shear, and both flexural and torsional moments. They primarily work under shear, since, in the same way that orthogonal exoskeletons, they resist in-plane actions.

# Chapter 6

## Results and Discussion

This chapter is organized by case studies. For each case study, the meaning of the design variables is explained and the thresholds for the constraints are defined.

The presentation of all the results of each case study starts with the optimization outputs, containing the most important values and the plots that exhibit how the algorithm evolved over the iterations.

Then, the structural results are displayed, starting with the final design for the retrofitting intervention, followed by the main effects caused by it, in terms of inter-storey drift, base shear, and vibration modes, before and after the incorporation of the exoskeletons.

Finally, the structural verifications of each element of the existing structure are presented, followed by the explanation of the process to determine the stiffness of both the bare structure and the coupled system, along with the necessary data.

At the end of each case study's section, the stiffness ratio, between the value corresponding to the coupled system and to the building before the retrofit, in each direction, is computed to be compared with the one suggested by the regulation.

## 6.1 Case Study 1

The first case study is given by the 'Structure 1' retrofitted by Orthogonal Exoskeletons. In this case study, there are 16 positions where an exoskeleton can be placed, given by all the external beam-column nodes of the existing structure. Each one of these positions represents one of the binary design variables composing the chromosome. In the following image, a graphic representation of the exoskeleton to which each design variable corresponds is given, if the value of a certain binary variable is 1, an exoskeleton is placed in the corresponding position, instead, if the value is 0, the position is left free.

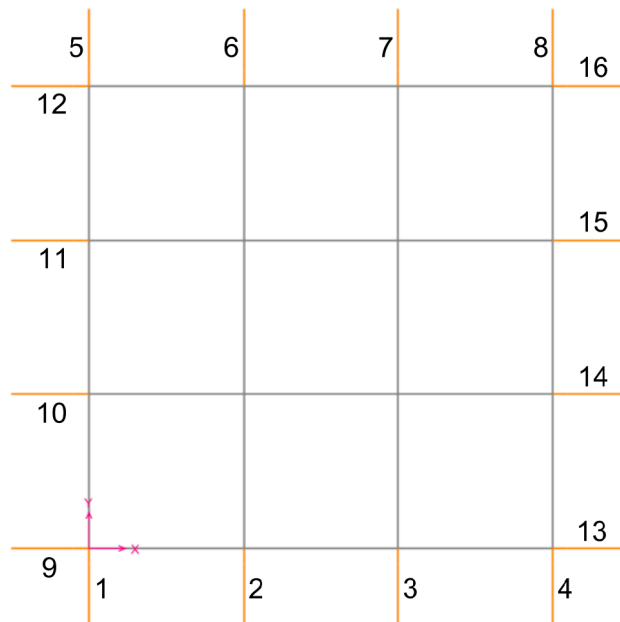


Figure 6.1: Definition of Topology DV as potential exoskeleton's positions

The maximum inter-storey drift imposed as constraint for this case is shown below,  $H$  being the storey height.

$$\frac{H}{600} = 6.67mm$$

### 6.1.1 Results of the Optimization

The main outputs of the algorithm are given by the chromosome, that provides the information of the disposition and amount of exoskeletons, as well as the steel profiles of their composing elements. The parameters that compose the objective function, hence, the weight, inter-storey drift ratio, and stress ratio of the exoskeletons, are shown, along with the chromosome, in the following table.

<b>OUTPUTS</b>	
chromosome	[ 1,0,0,1   1,0,0,1   1,0,0,1   1,0,0,1   30,17,25,12 ]
weight	1800 kN
inter-storey drift ratio	0.9978
stress ratio of the exosk.	0.1919
iteration of stagnation	46

Table 6.1: Summary of the main results of the optimization

To give an indication of how the algorithm worked and evolved towards the final configuration, the plots of the Objective Function, Stagnation, Inter-Storey Drift Ratio, and Stress Ratio of the Exoskeletons, against the iterations, are useful.

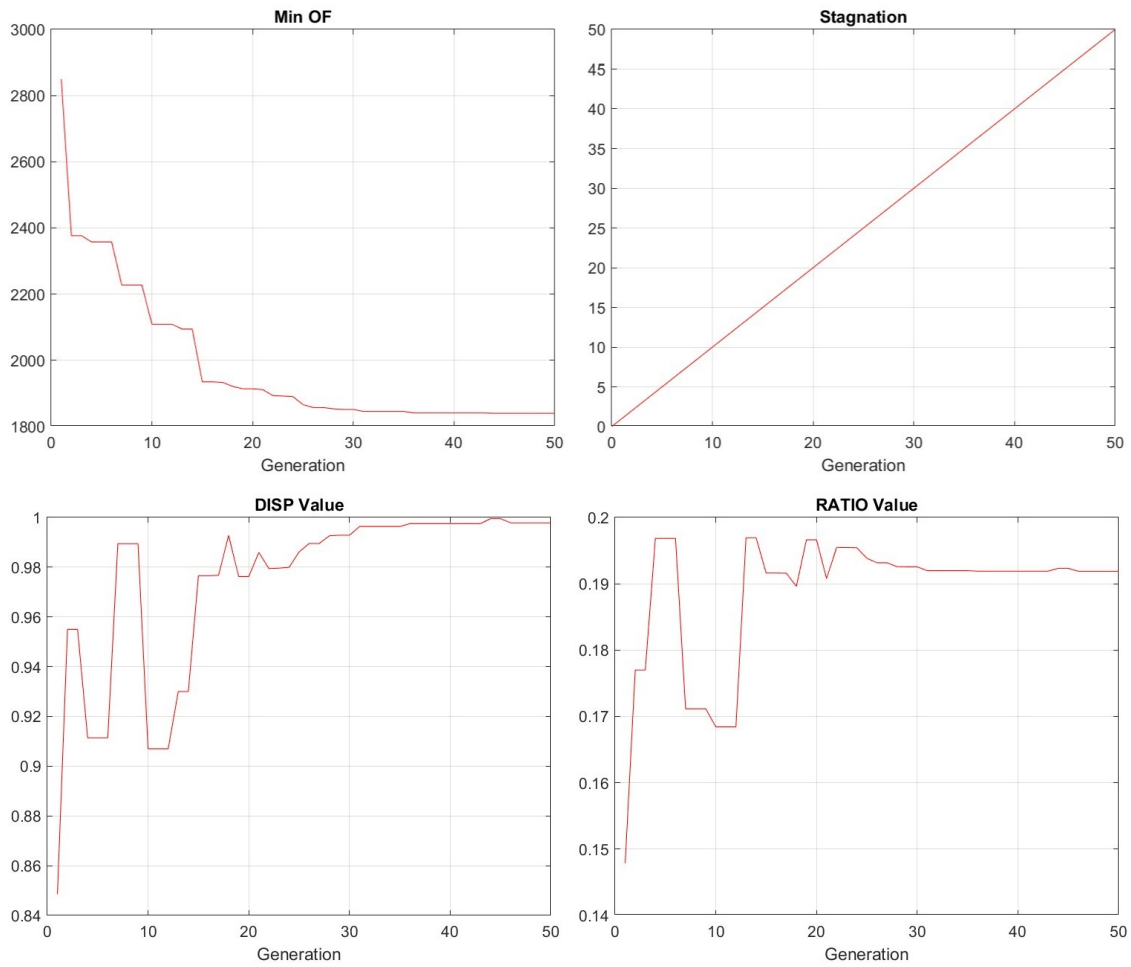


Figure 6.2: Plots of the Optimization (displayed against the iterations):  
 (1) Evolution of the Objective Function (2) Stagnation of the solution (3)  
 Inter-Storey Drift Ratio (4) Demand-Capacity Ratio of the Exoskeletons

In the above graphs, it can be appreciated that the algorithm had a good evolution, the objective function decreases regularly until solutions near to the final one are found, where a refinement of the solution begins, to stagnate in the final solution. The stagnation indicates when the same configuration remains the best one for a certain number of iterations, when this condition is reached, a strategy is implemented to augment the exploration of the algorithm and find, if it exists, a better solution, as explained in 4.1.2. In this case, due to the slight refinements approaching the final iterations, the algorithm never stagnated.

The inter-storey drifts' ratio and the structural verifications' ratio have opposite behaviors, a solution with one of these values closer to 1 has a lower value than the other one, but as the solutions evolve we reach solution in high both values are maximized. It is interesting to notice that the controlling constraint is given by the inter-storey drifts' ratio.

## 6.1.2 Structural Interpretation of the Results

### Final Exoskeleton's Design

From the 16 binary design variables, the final configuration is composed of **eight exoskeletons**, positioned as shown in the images below.

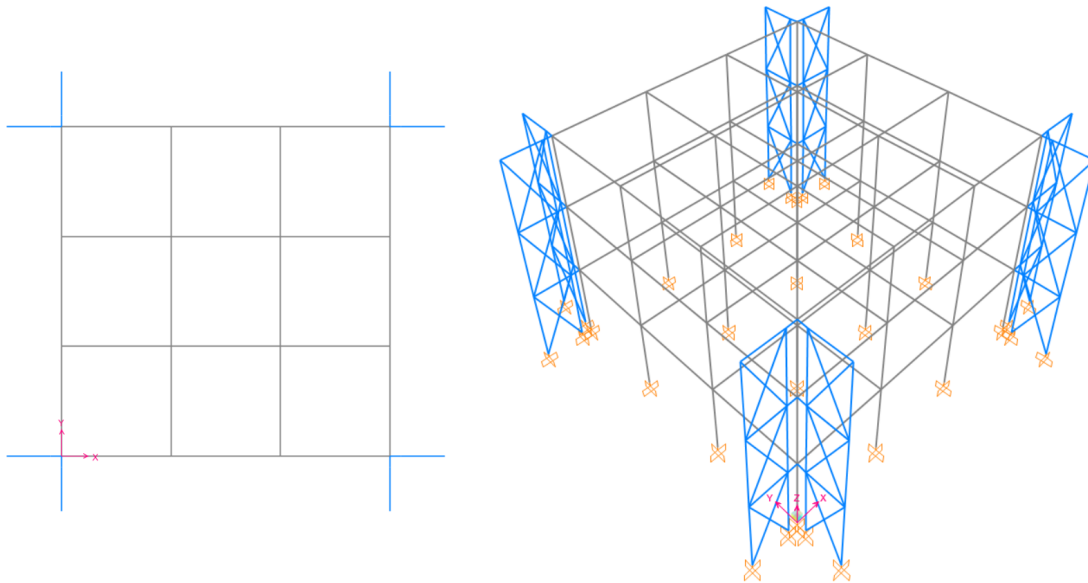


Figure 6.3: Top and axonometric views of the final exoskeleton's configuration

This distribution of exoskeletons was expected, considering that the nodes farthest from the rigidity center of the structure, in this case, coincident with the geometric center, are the ones more susceptible to big displacements. In this way, the arm of the forces provided by the exoskeletons are the grater possible ones.

From the last four design variables, the chosen steel profiles for the elements of the exoskeletons are the following ones.

STEEL SECTIONS			
ELEMENT	DIAMETER [cm]	THICKNESS [cm]	AREA [cm <sup>2</sup> ]
columns	61.00	4.00	716.28
beams	40.64	1.42	174.96
bracings	45.70	3.00	402.44
connection	27.30	1.60	129.18

Table 6.2: Circular Hollow Sections of the exoskeleton's elements

### Main Effects of the Intervention

The main goal of the intervention was defined as the reduction of inter-storey drifts, the effects are shown in the following graph, as a comparison of the drifts of each floor before and after the retrofit. The maximum inter-storey drift decreases from **24.73 mm** to **6.66 mm**.

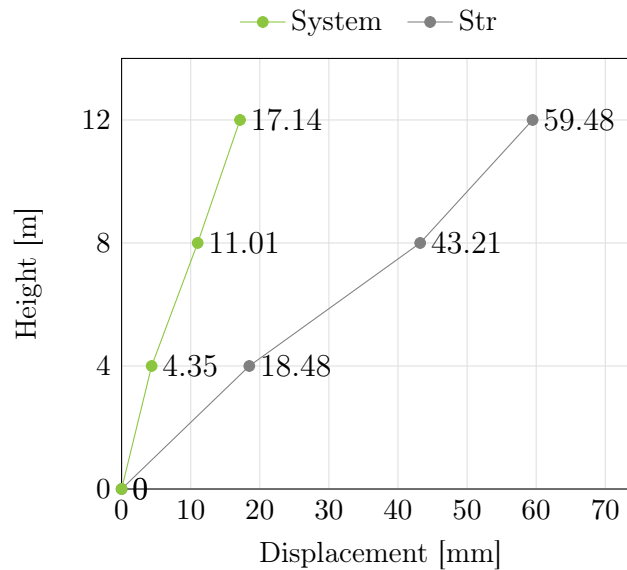


Figure 6.4: Maximum displacement of each storey of the existing building and of the retrofitted system

As another consequence of the introduction of the retrofiting system, the coupled structure (System) takes a greater base shear in comparison to the existing building before the intervention (Str). Nevertheless, in the final configuration, **21%** of

the base shear is taken by the original structure (System - Str) and **79%** by the exoskeletons (System - Exosk). Therefore, the original structure is unloaded by the introduction of the exoskeletons.

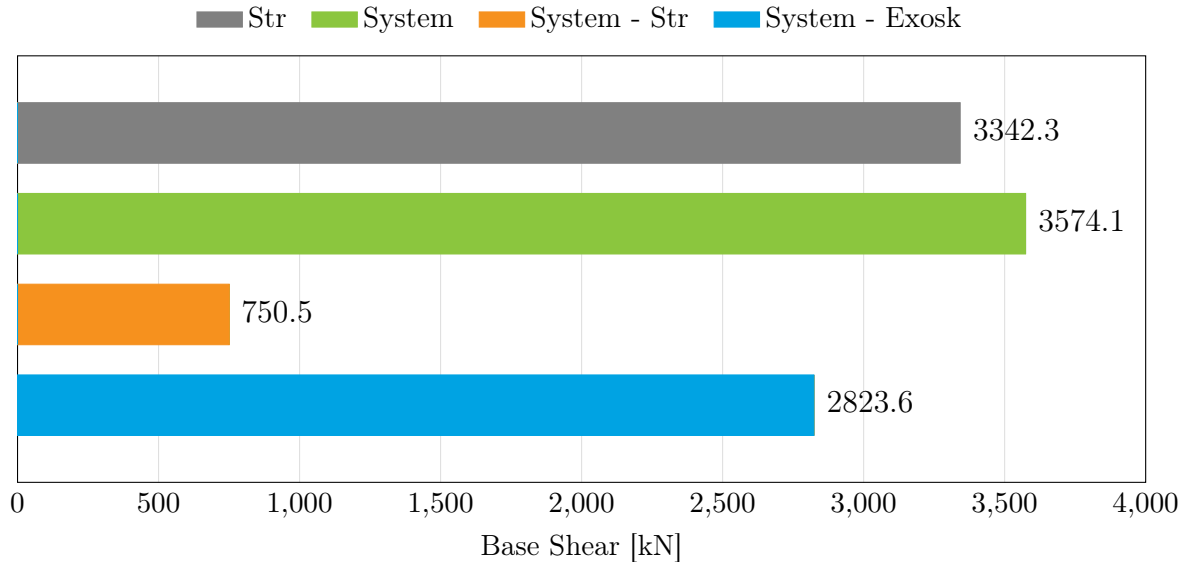


Figure 6.5: Comparison of total base shear of the existing structure before the retrofit (Str), the retrofitted system (System), the building after the retrofit (System-Str), the exoskeletons (System-Exosk)

The repercussions on the vibration modes' periods and participating masses are shown in the tables below. The main remark about these results is that, even though the exoskeletons were introduced, the main modes remain global, being translational in both directions and rotational ones. The periods of the first modes decrease significantly, anyway, they correspond to the same acceleration, in the response spectrum, than the ones of the existing structure, since they are all in the 'plateau' of the spectrum.

Nevertheless, the participating masses are lower than for the unretrofitted building, implying that the rest of the mass will be obtained with the following vibration modes, with even lower periods. These other periods will be located in the ascendant part of the spectrum, having lower accelerations than the showed ones, generating in this way, smaller seismic forces on the system. This situation helps control the increase of base shear after the intervention, given by the mass added by the exoskeletons.

Existing Structure							
MODE	period	U <sub>x</sub>	U <sub>y</sub>	R <sub>z</sub>	$\sum U_x$	$\sum U_y$	$\sum R_z$
	[s]	[%]	[%]	[%]	[%]	[%]	[%]
1	0.5645	84	0.6	0	84	0.6	0
2	0.5645	0.6	84	0	85	85	0
3	0.5122	0	0	85	85	85	85
Retrofitted System							
MODE	period	U <sub>x</sub>	U <sub>y</sub>	R <sub>z</sub>	$\sum U_x$	$\sum U_y$	$\sum R_z$
	[s]	[%]	[%]	[%]	[%]	[%]	[%]
9	0.2986	1	75	0	3.2	77	6.6
10	0.2986	75	1	0	78	78	6.6
19	0.2287	0	0	68	80	80	79

Table 6.3: Summary of fundamental vibration modes' information before and after the retrofit

### 6.1.3 Results in Relation to the Stiffness Ratio

In 3, the current approach proposed by the Italian regulation is explained, in which a comparison of the stiffnesses of the existing building and of the retrofitted system, under horizontal actions, is done. Then, a new approach is proposed, based on the imposition of an inter-storey drift threshold to the existing structure, that must be achieved with the intervention, guaranteeing the satisfaction of the structural verification of the building.

The structural verifications of each element are performed and the results of the existing and retrofitted configurations are shown in the images below. The maximum demand-capacity ratio decreases from **2.708**, for the building as-is, to **0.956**, for the structure after the intervention.

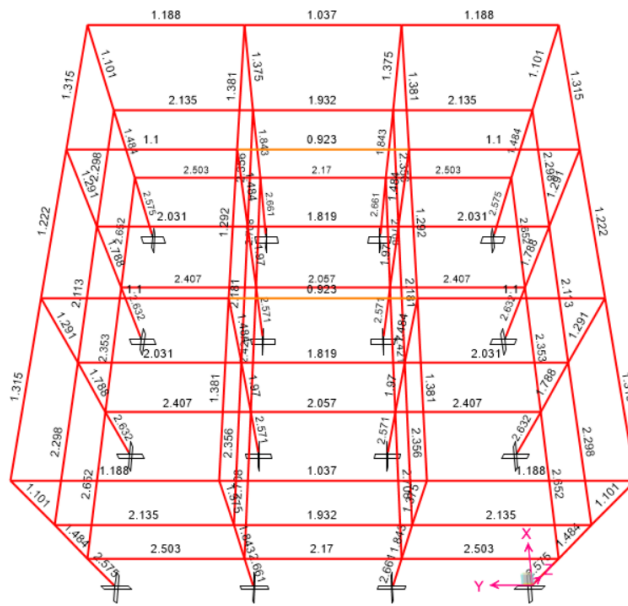


Figure 6.6: Capacity-Demand Ratio check of the unreinforced building

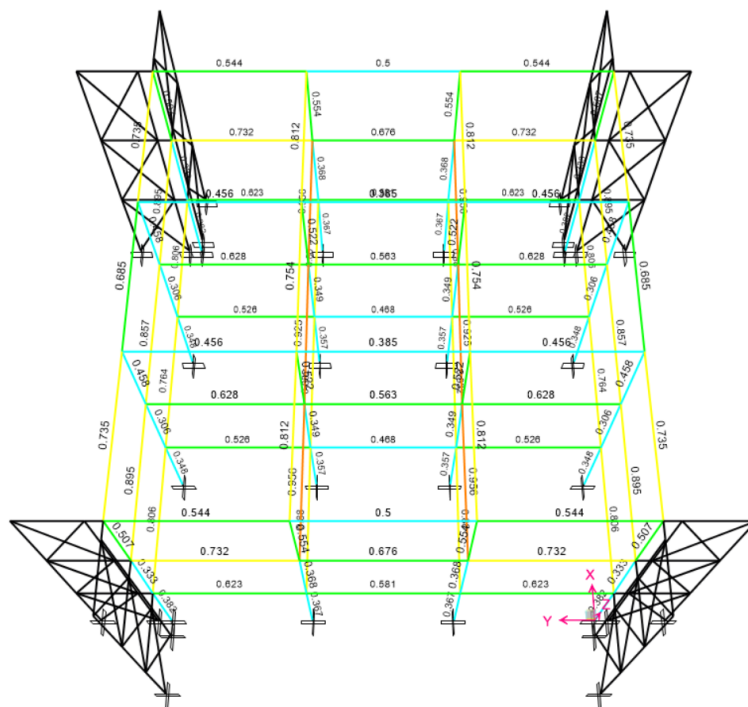


Figure 6.7: Capacity-Demand Ratio check of the retrofitted building

Then, the stiffnesses under horizontal actions of both bare and retrofitted configura-

tions are determined through pushover analyses as explained in 4.2.2, and the ratio is computed.

In this case, as the structure is regular and symmetrical, the stiffnesses in the 'x' and 'y' directions are equal. The results are presented below.

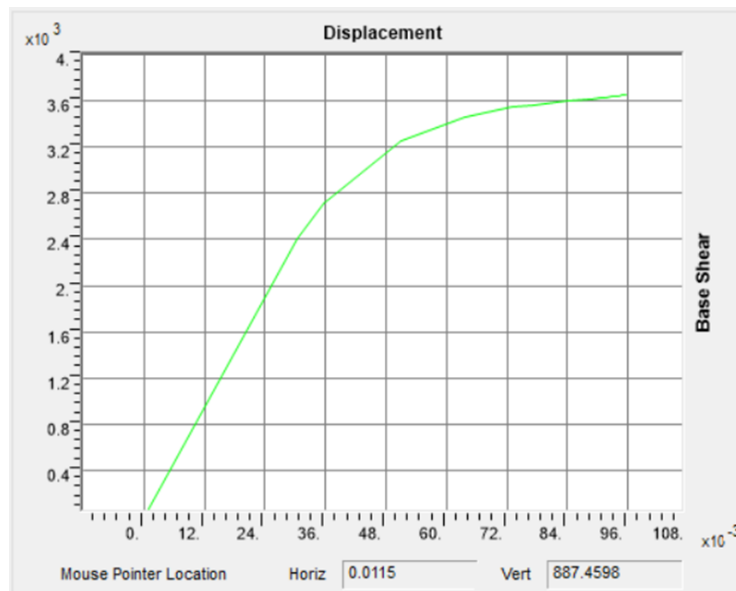


Figure 6.8: Pushover curve of the existing building corresponding to group 1 of static equivalent loads

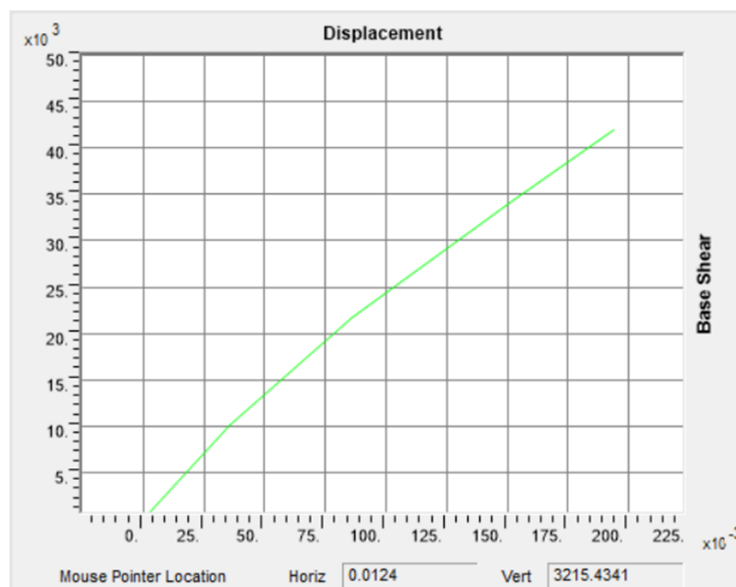


Figure 6.9: Pushover curve of the retrofitted system corresponding to group 1 of static equivalent loads

Existing Structure		Retrofitted System	
top displacement	11.35 mm	top displacement	12.12 mm
F - group 1	887.5 kN	F - group 1	3215.4 kN
F - group 2	1067.5 kN	F - group 2	3858.5 kN
F - average	977.5 kN	F - average	3537.0 kN
$K(\text{str}) = F/d$	86122.6 kN/m	$K(\text{syst}) = F/d$	291829.8 kN/m

Table 6.4: Summary of displacement and forces to determine the stiffness of the existing building ( $K_{str}$ ) and of the coupled system ( $K_{syst}$ )

$$\frac{K_{syst}}{K_{str}} = 3.39$$

In this way, the stiffness ratio obtained following the proposed approach, based on displacement control, is much lower than the one suggested by the regulation, while the existing structure satisfies the structural verifications.

## 6.2 Case Study 2

The first case study is given by the 'Structure 1' retrofitted by Parallel Exoskeletons. In this case study, there are 12 positions where an exoskeleton can be placed, each representing one of the binary design variables. In the following image, a graphic representation of the exoskeleton to which each design variable corresponds is given.

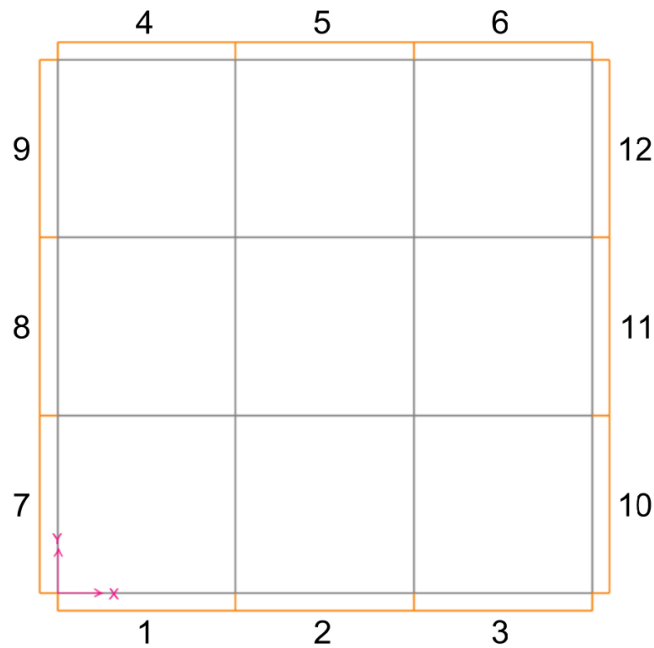


Figure 6.10: Definition of Topology DV as potential exoskeleton's positions

The maximum inter-storey drift imposed as constraint for this case is shown below,  $H$  being the storey height.

$$\frac{H}{600} = 6.67mm$$

### 6.2.1 Results of the Optimization

The main outputs of the algorithm are given by the chromosome, that provides the information of the disposition and amount of exoskeletons, as well as the steel profiles of their composing elements. The parameters that compose the objective function, hence, the weight, inter-storey drift ratio, and stress ratio of the exoskeletons, are shown, along with the chromosome, in the following table.

OUTPUTS	
chromosome	[ 0,1,1   1,1,0   0,1,1   1,1,0   4,1,8,24 ]
weight	311.3 kN
inter-storey drift ratio	0.9925
stress ratio of the exosk.	0.7020
iteration of stagnation	42

Table 6.5: Summary of the main results of the optimization

To give an indication of how the algorithm worked and evolved towards the final configuration, the plots of the Objective Function, Stagnation, Inter-Storey Drift Ratio, and Stress Ratio of the Exoskeletons, against the iterations, are useful.

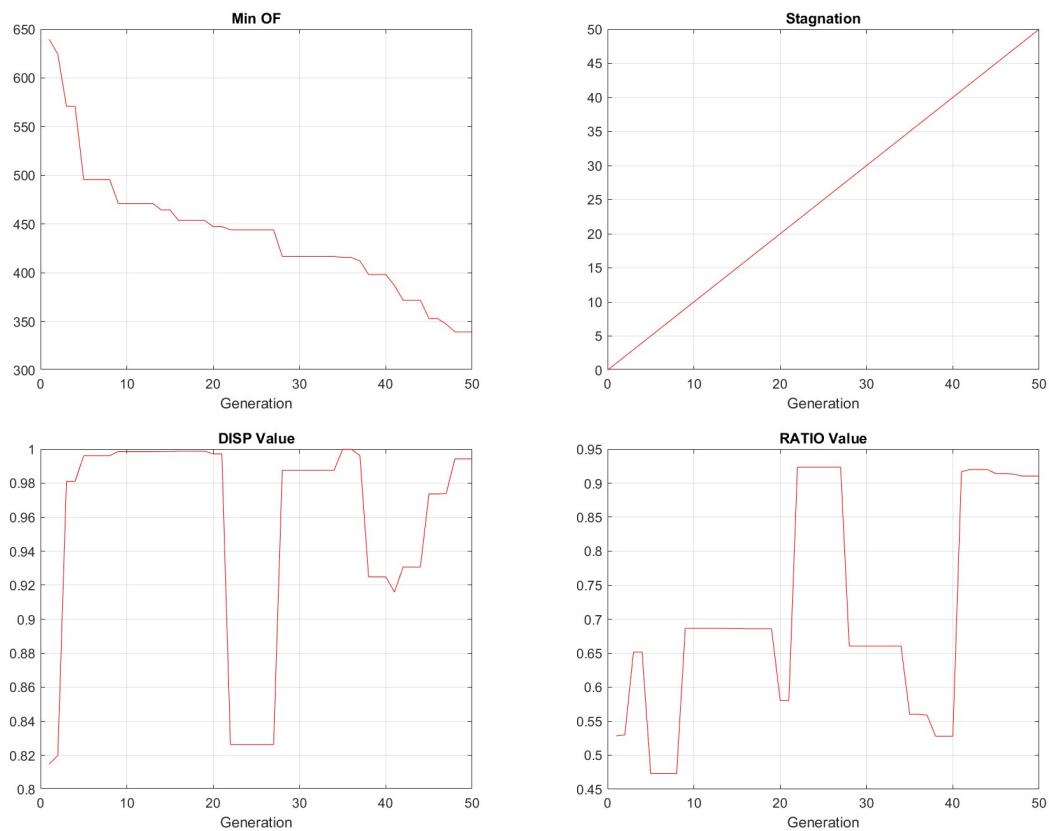


Figure 6.11: Plots of the Optimization (displayed against the iterations):  
 (1) Evolution of the Objective Function (2) Stagnation of the solution (3)  
 Inter-Storey Drift Ratio (4) Demand-Capacity Ratio of the Exoskeletons

In this case study, the Objective Function evolution over the passing of the iterations is solid and regular, and the solutions never stagnated. Since in the final iteration, number 50, the weight reached a value of approximately half of the initial one, we can consider that the results are very satisfactory. About the inter-storey drift and capacity-demand ratio of the exoskeletons, their behavior is, as for case study 1, generally opposite, but for the final solution, both ratios reach near maximum values.

### 6.2.2 Structural Interpretation of the Results

#### Final Exoskeleton's Design

From the 12 binary design variables, the final configuration is composed of **eight exoskeletons**, positioned as shown in the images below.

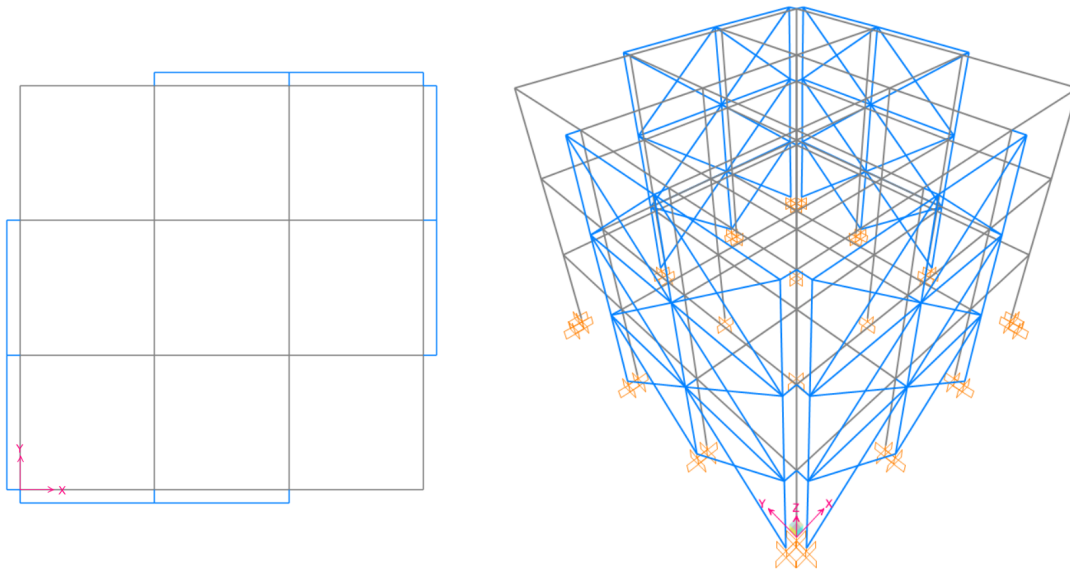


Figure 6.12: Top and axonometric views of the final exoskeleton's configuration

In the final disposition of exoskeletons, it can be noticed that a solution where these are positioned together is preferred. By placing two or more exoskeletons side by side, some columns are sheared, decreasing the weight of the configuration. Additionally, a synergistic behavior is given by the collaboration between exoskeletons in the resistance of horizontal actions.

From the last four design variables, the chosen steel profiles for the elements of the exoskeletons are the following ones.

STEEL SECTIONS			
ELEMENT	DIAMETER [ <i>cm</i> ]	THICKNESS [ <i>cm</i> ]	AREA [ <i>cm</i> <sup>2</sup> ]
columns	16.83	0.80	40.29
beams	10.16	0.50	15.17
bracings	19.37	1.42	80.08
connection	40.64	3.00	354.75

Table 6.6: Circular Hollow Sections of the exoskeleton's elements

As explained in 5.2.2, the links between the existing structure and a set of parallel exoskeletons mainly transfer shear forces, this is the reason why the section of the connection is significantly bigger than the ones of the other elements. It becomes evident that the stress ratio of the exoskeletons reaches a higher value for this type of exoskeletons, mainly because these don't have a warping problem, providing the same effects with smaller sections.

#### Main Effects of the Intervention

The main goal of the intervention was defined as the reduction of inter-storey drifts, the effects are shown in the following graph, as a comparison of the drifts of each floor before and after the retrofit. The maximum inter-storey drift decreases from **24.73 mm** to **6.62 mm**.

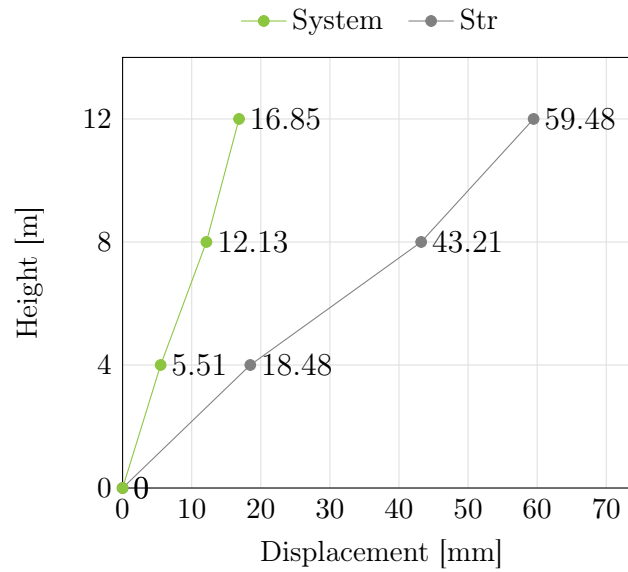
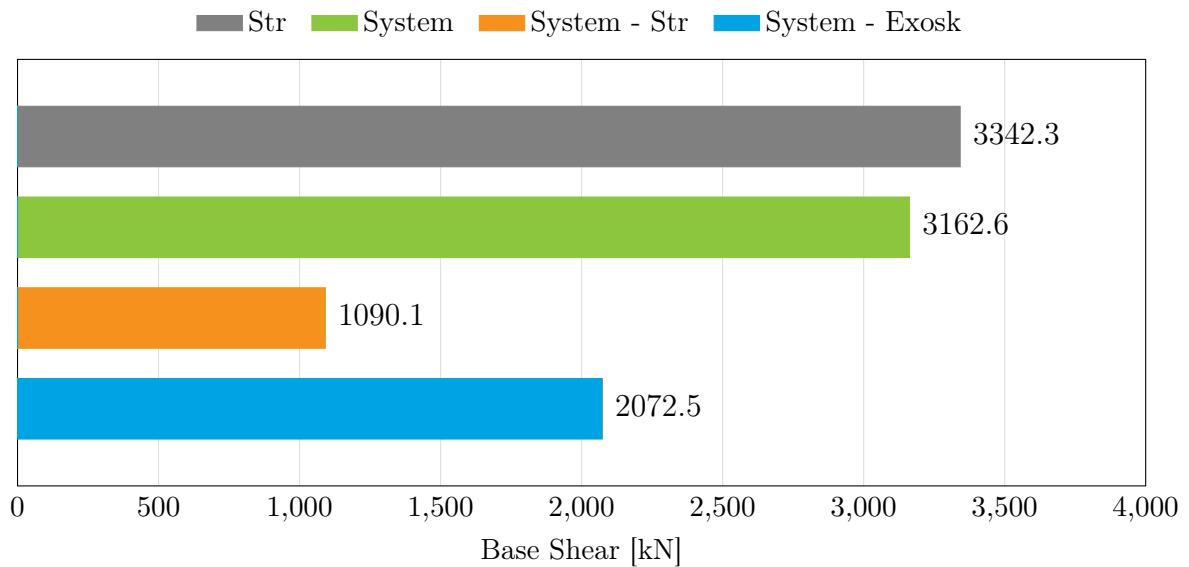


Figure 6.13: Maximum displacement of each storey of the existing building and of the retrofitted system

In the final configuration, **34.5%** of the base shear is taken by the original structure (System - Str) and **65.5%** by the exoskeletons (System - Exosk), as shown in the following chart.



The repercussions on the vibration modes' periods and participating masses are shown in the tables below. The main remark about these results is that, even though

the exoskeletons were introduced, the main modes remain global, being translational in both directions and rotational ones.

Existing Structure							
MODE	period	Ux	Uy	Rz	$\sum$ Ux	$\sum$ Uy	$\sum$ Rz
	[s]	[%]	[%]	[%]	[%]	[%]	[%]
1	0.5645	84	0.6	0	84	0.6	0
2	0.5645	0.6	84	0	85	85	0
3	0.5122	0	0	85	85	85	85
Retrofitted System							
MODE	period	Ux	Uy	Rz	$\sum$ Ux	$\sum$ Uy	$\sum$ Rz
	[s]	[%]	[%]	[%]	[%]	[%]	[%]
1	0.3088	44	44	0	44	44	0
2	0.2845	44	44	0	88	88	0
3	0.1997	0	0	89	88	88	89

Table 6.7: Summary of fundamental vibration modes' information before and after the retrofit

### 6.2.3 Results in Relation to the Stiffness

The structural verifications of each element are performed and the results of the existing and retrofitted configurations are shown in the images below. The maximum demand-capacity ratio decreases from **2.708**, for the building as-is, to **0.788**, for the structure after the intervention.

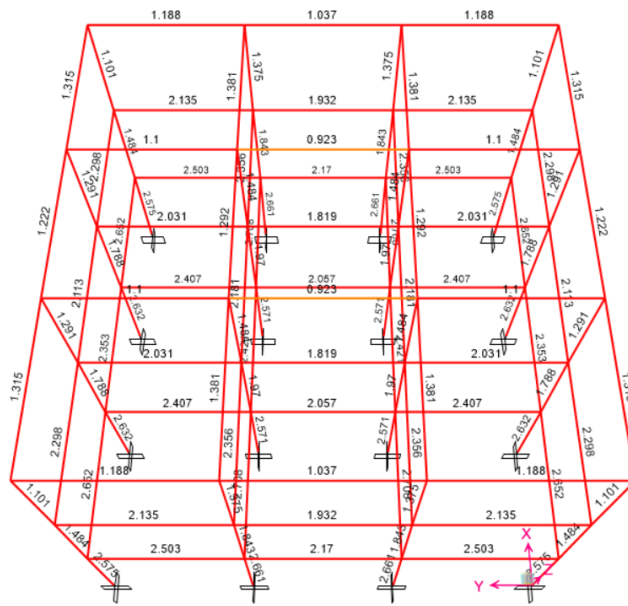


Figure 6.14: Capacity-Demand Ratio check of the unreinforced building

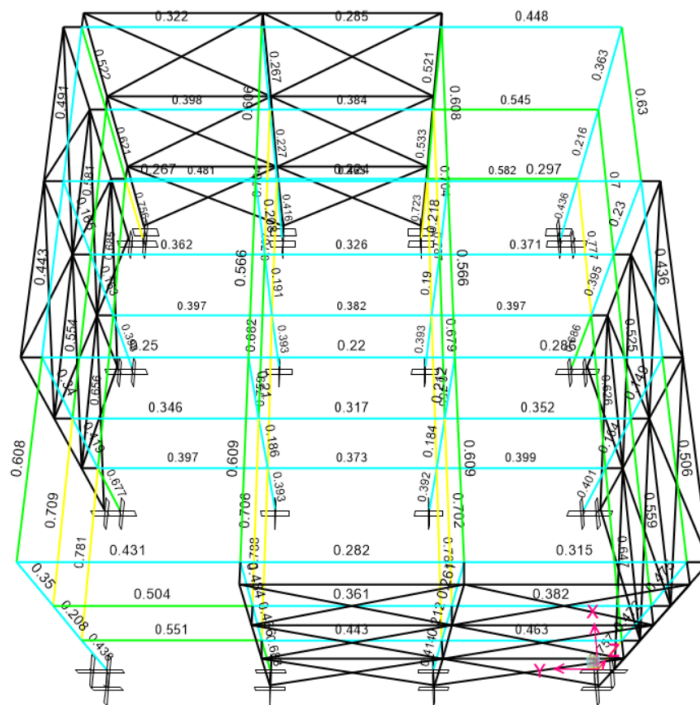


Figure 6.15: Capacity-Demand Ratio check of the retrofitted building

Then, the stiffnesses under horizontal actions of both bare and retrofitted configurations are determined through pushover analyses, the results are presented below.

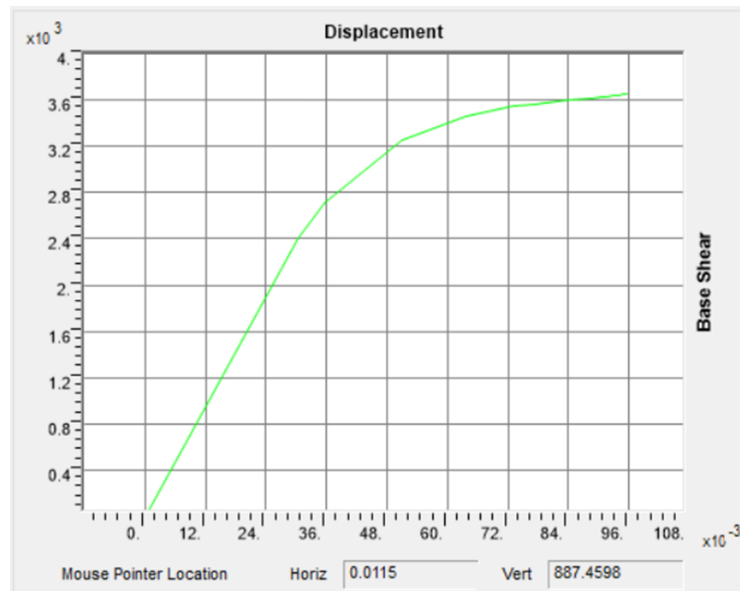


Figure 6.16: Pushover curve of the existing building corresponding to group 1 of static equivalent loads

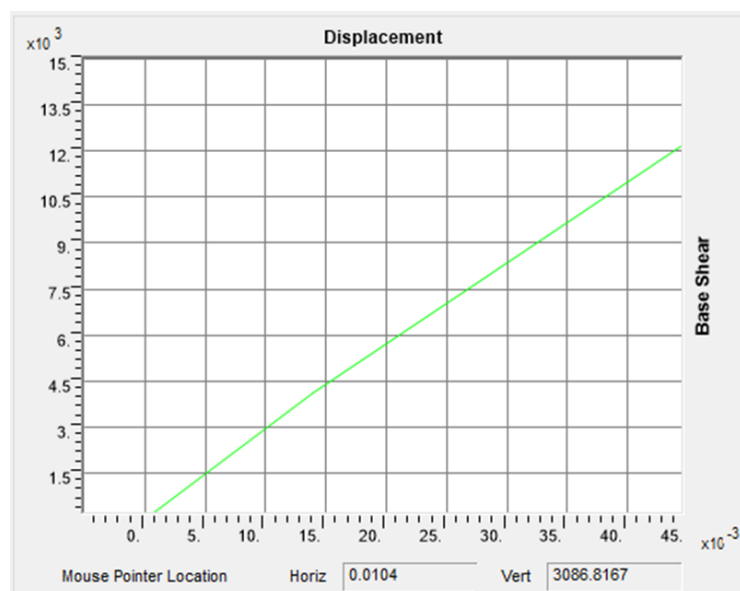


Figure 6.17: Pushover curve of the retrofitted system corresponding to group 1 of static equivalent loads

Existing Structure		Retrofitted System	
top displacement	11.35 mm	top displacement	10.5 mm
F - group 1	887.5 kN	F - group 1	3086.8 kN
F - group 2	1067.5 kN	F - group 2	3713.8 kN
F - average	977.5 kN	F - average	3400.3 kN
$K(\text{str}) = F/d$	86122.6 kN/m	$K(\text{syst}) = F/d$	323840.1 kN/m

Table 6.8: Summary of displacement and forces to determine the stiffness of the existing building ( $K_{str}$ ) and of the coupled system ( $K_{syst}$ )

$$\frac{K_{syst}}{K_{str}} = 3.76$$

In this way, the stiffness ratio obtained following the proposed approach, based on displacement control, is much lower than the one suggested by the regulation, while the existing structure satisfies the structural verifications.

## 6.3 Case Study 3

The first case study is given by the 'Structure 2' retrofitted by Orthogonal Exoskeletons. In this case study, there are 34 positions where an exoskeleton can be placed, each representing one of the binary design variables. In the following image, a graphic representation of the exoskeleton to which each design variable corresponds is given.

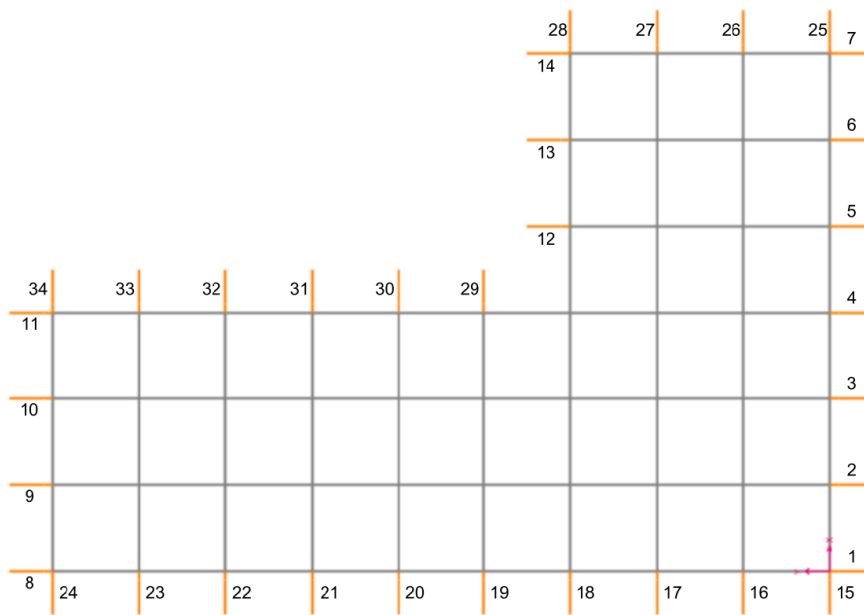


Figure 6.18: Definition of Topology DV as potential exoskeleton's positions

The maximum inter-storey drift imposed as constraint for this case is shown below,  $H$  being the storey height.

$$\frac{H}{600} = 6.67mm$$

### 6.3.1 Results of the Optimization

The main outputs of the algorithm are given by the chromosome, that provides the information of the disposition and amount of exoskeletons, as well as the steel profiles of their composing elements. The parameters that compose the objective function, hence, the weight, inter-storey drift ratio, and stress ratio of the exoskeletons, are shown, along with the chromosome, in the following table.

<b>OUTPUTS</b>	
chromosome	[ 1,1,1,0,1,1,1   1,1,1,0   0,0,0   1,1,1,0,0,0,0,1,0,1     1,1,1,0   0,0,0,1,0,1   35,20,28,18 ]
weight	6208.6 kN
inter-storey drift ratio	0.9995
stress ratio of the exosk.	0.1912
iteration of stagnation	40

Table 6.9: Summary of the main results of the optimization

To give an indication of how the algorithm worked and evolved towards the final configuration, the plots of the Objective Function, Stagnation, Inter-Storey Drift Ratio, and Stress Ratio of the Exoskeletons, against the iterations, are useful.

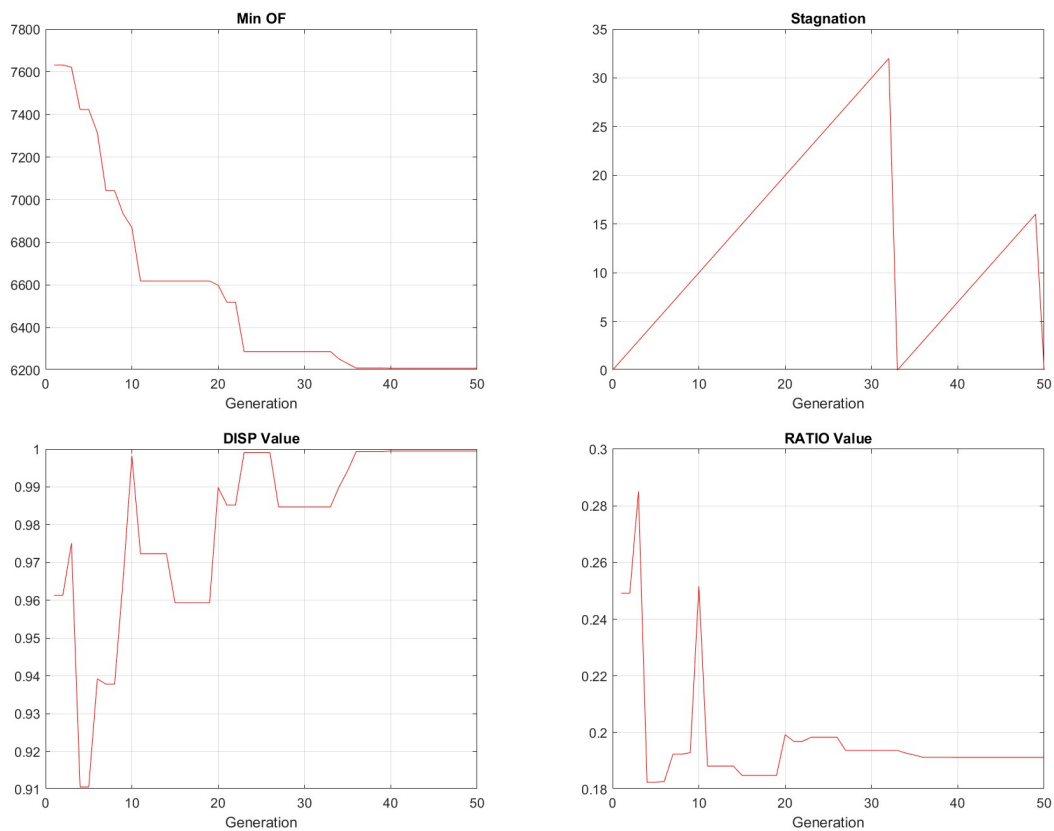


Figure 6.19: Plots of the Optimization (displayed against the iterations):  
 (1) Evolution of the Objective Function (2) Stagnation of the solution (3)  
 Inter-Storey Drift Ratio (4) Demand-Capacity Ratio of the Exoskeletons

In these plots, the evolution of the Objective Function is very satisfactory. Three plateaus can be appreciated in this plot, for the first one, it seems that the algorithm could find a better solution by implementing the internal strategies explained in 4.1.2, such as 'mutation of the repeated individuals'; instead, for the second one, the stagnation condition was reached, which helped the algorithm find an improved solution; finally, the last plateau is where the algorithm found the final solution, stagnating again towards the end.

The inter-storey drift and capacity-demand ratio of the exoskeletons have randomic behaviors, the peaks at the beginning of both plots indicate that some solutions were found that provided a maximization of both ratios. Maximum ratio values indicate that the solution cannot improve significantly through a refinement of the design variables, this kind of situation is appreciated reaching the end of the iterations, because it can happen because the better solution is already found. Instead, in this case, these were probably non-optimal exoskeletons' dispositions, from which the algorithm managed to move away rapidly.

### 6.3.2 Structural Interpretation of the Results

#### Final Exoskeleton's Design

From the 34 binary design variables, the final configuration is composed of **nineteen exoskeletons**, positioned as shown in the images below.

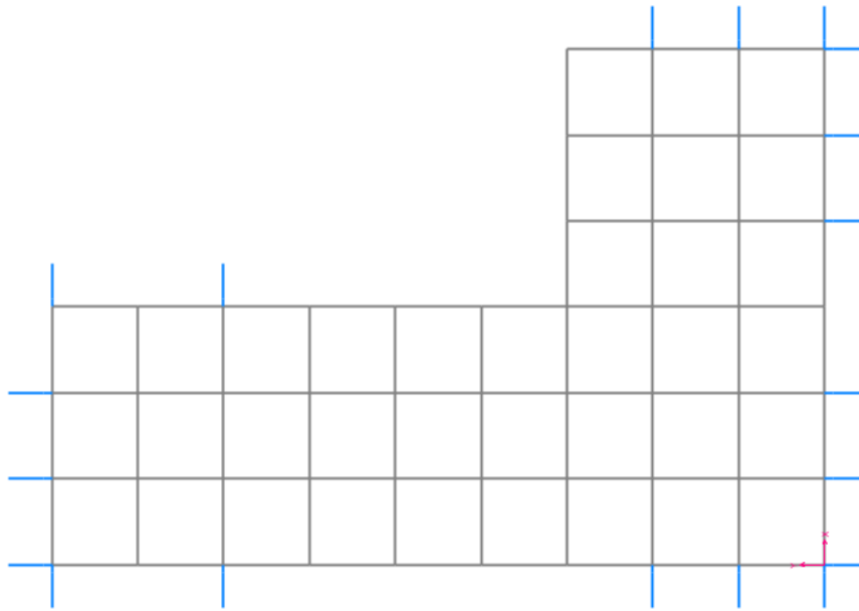


Figure 6.20: Top view of the final exoskeleton's configuration

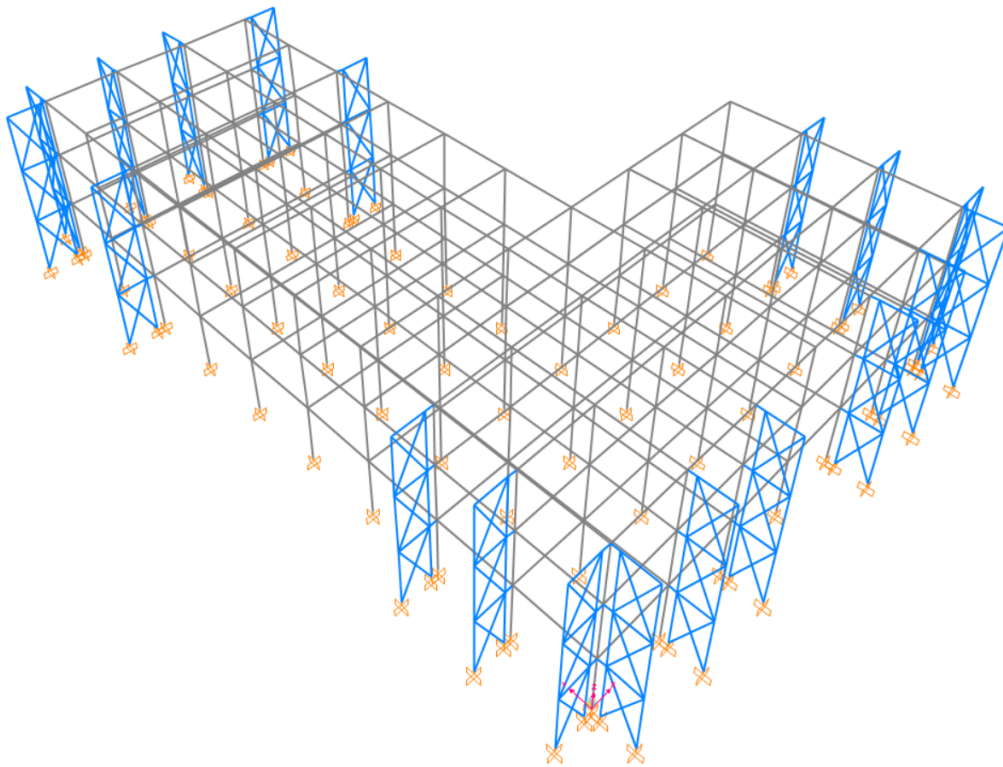


Figure 6.21: Axonometric view of the final exoskeleton's configuration

This distribution of exoskeletons was expected, considering that the nodes farthest from the rigidity center of the structure are the ones more susceptible to big displacements. In this way, the arm of the forces provided by the exoskeletons are the grater possible ones.

From the last four design variables, the chosen steel profiles for the elements of the exoskeletons are the following ones.

STEEL SECTIONS			
ELEMENT	DIAMETER [ <i>cm</i> ]	THICKNESS [ <i>cm</i> ]	AREA [ <i>cm</i> <sup>2</sup> ]
columns	76.20	5.00	1118.41
beams	35.56	2.00	210.86
bracings	45.7	4.00	524.02
connection	32.39	2.00	190.95

Table 6.10: Circular Hollow Sections of the exoskeleton's elements

#### Main Effects of the Intervention

The main goal of the intervention was defined as the reduction of inter-storey drifts, the effects are shown in the following graph, as a comparison of the drifts of each floor before and after the retrofit. The maximum inter-storey drift decreases from **26.33 mm** to **6.67 mm**.

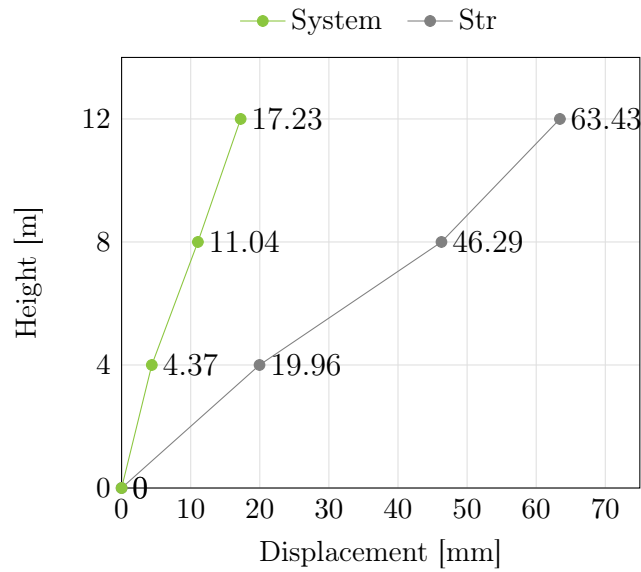
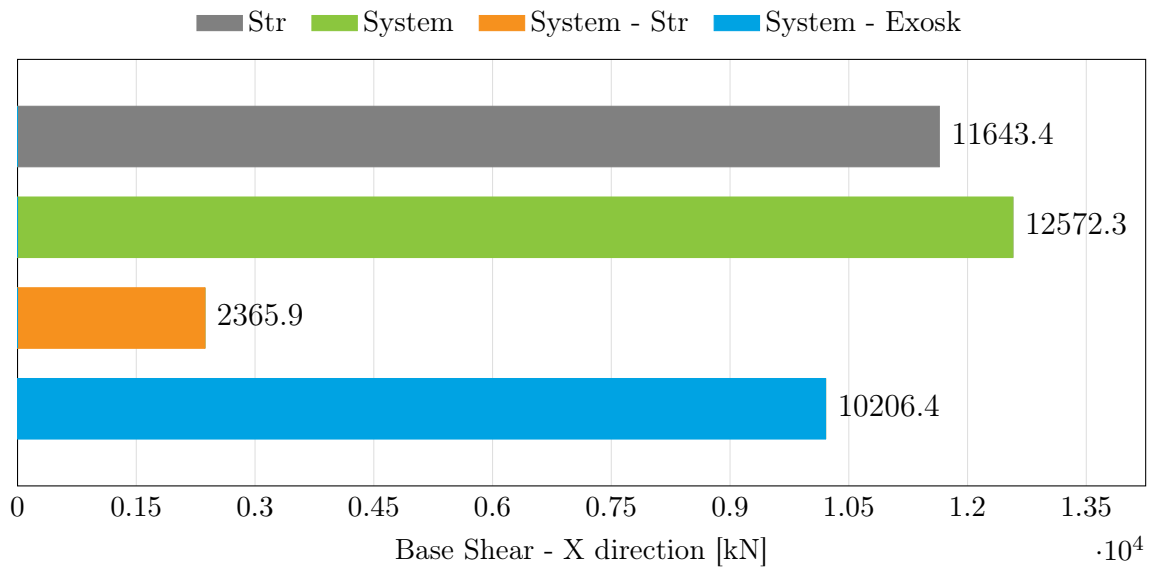


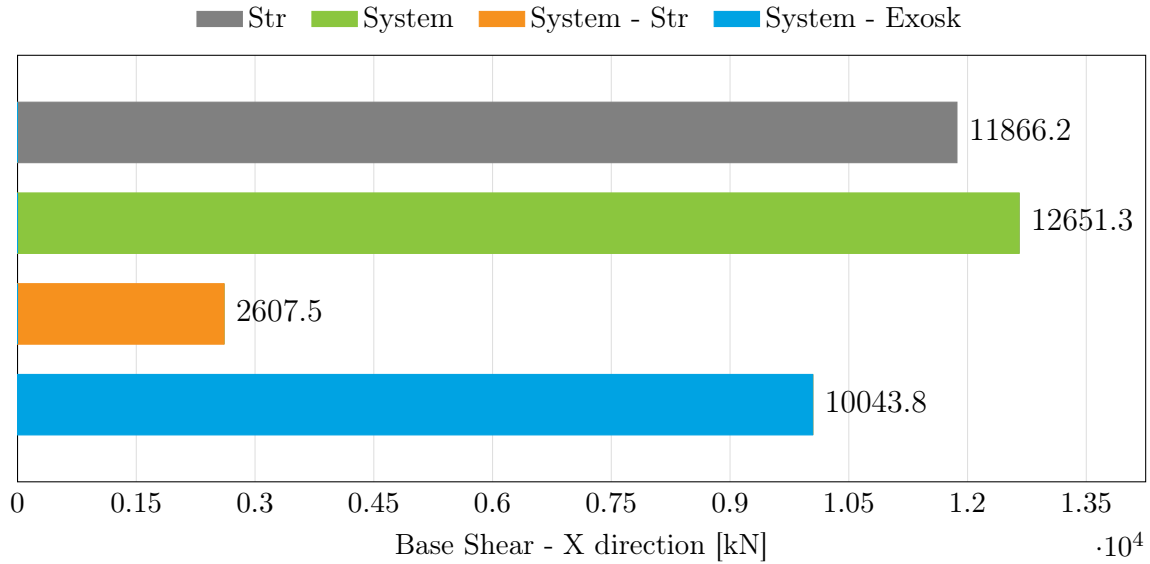
Figure 6.22: Maximum displacement of each storey of the existing building and of the retrofitted system

In the final configuration, **18.8%** of the base shear in X direction is taken by the original structure (System - Str) and **81.2%** by the exoskeletons (System - Exosk), as shown in the following chart.



In the final configuration, **20.6%** of the base shear in Y direction is taken by the original structure (System - Str) and **79.4%** by the exoskeletons (System - Exosk),

as shown in the following chart.



The repercussions on the vibration modes' periods and participating masses are shown in the tables below. The main remark about these results is that, even though the exoskeletons were introduced, the main modes remain global, being translational in both directions and rotational ones.

Existing Structure							
MODE	period	U <sub>x</sub>	U <sub>y</sub>	R <sub>z</sub>	∑ U <sub>x</sub>	∑ U <sub>y</sub>	∑ R <sub>z</sub>
	[s]	[%]	[%]	[%]	[%]	[%]	[%]
1	0.5785	80	0.3	5	80	0.3	5
2	0.5657	1.1	80	3.8	81	81	8.8
3	0.5514	4.3	4.7	76	85	85	85
Retrofitted System							
MODE	period	U <sub>x</sub>	U <sub>y</sub>	R <sub>z</sub>	∑ U <sub>x</sub>	∑ U <sub>y</sub>	∑ R <sub>z</sub>
	[s]	[%]	[%]	[%]	[%]	[%]	[%]
1	0.3014	0	76	0	0	76	0
2	0.2904	76	0	76	76	88	0
21	0.2494	0	0	69	78	78	74

Table 6.11: Summary of fundamental vibration modes' information before and after the retrofit

### 6.3.3 Results in Relation to the Stiffness

The structural verifications of each element are performed and the results of the existing and retrofitted configurations are shown in the images below. The maximum demand-capacity ratio decreases from **3.437**, for the building as-is, to **0.994**, for the structure after the intervention.

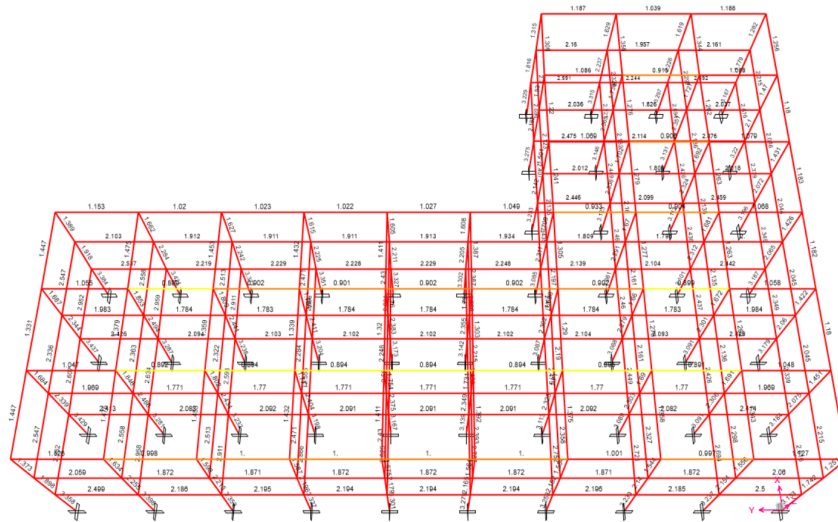


Figure 6.23: Capacity-Demand Ratio check of the unretrofitted building

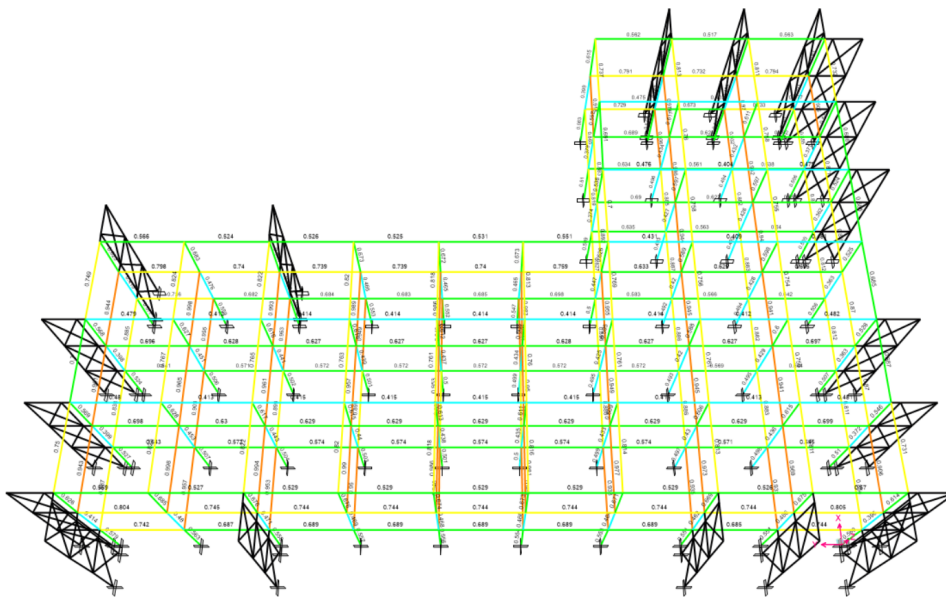


Figure 6.24: Capacity-Demand Ratio check of the retrofitted building

X direction

Then, the stiffnesses under horizontal actions of both bare and retrofitted configurations are determined through pushover analyses, the results are presented below.

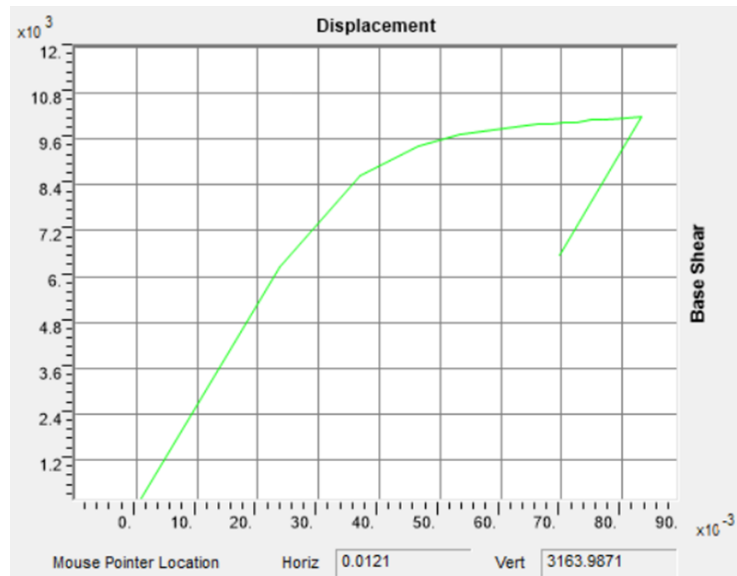


Figure 6.25: Pushover curve of the existing building in X direction corresponding to group 1 of static equivalent loads

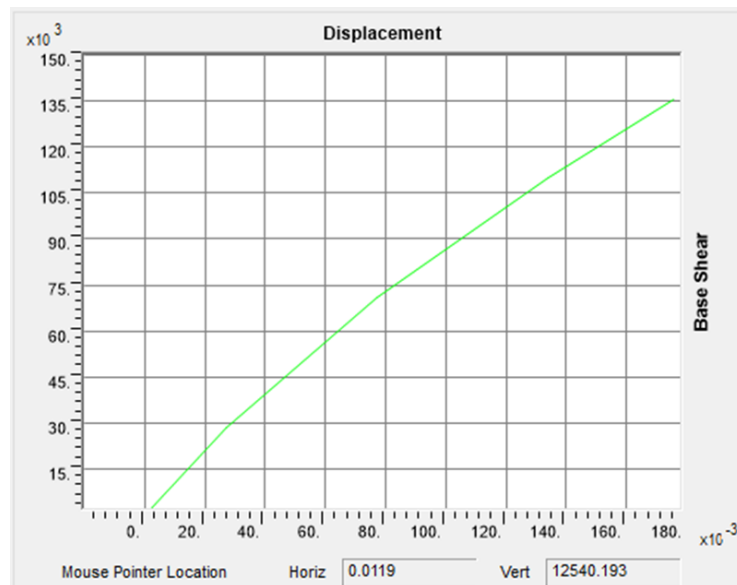


Figure 6.26: Pushover curve of the retrofitted system in X direction corresponding to group 1 of static equivalent loads

Existing Structure		Retrofitted System	
top displacement	12.02 mm	top displacement	11.77 mm
F - group 1	3164.0 kN	F - group 1	12540.2 kN
F - group 2	3742.8 kN	F - group 2	14791.0 kN
F - average	3453.4 kN	F - average	13665.6 kN
$K(str) = F/d$	287302.5 kN/m	$K(syst) = F/d$	1161053 kN/m

Table 6.12: Summary of displacement and forces to determine the stiffness of the existing building ( $K_{str}$ ) and of the coupled system ( $K_{syst}$ ) in X dir.

$$\frac{K_{syst}}{K_{str}} = 4.04$$

#### Y direction

Analogously, the analyses are performed in Y direction.

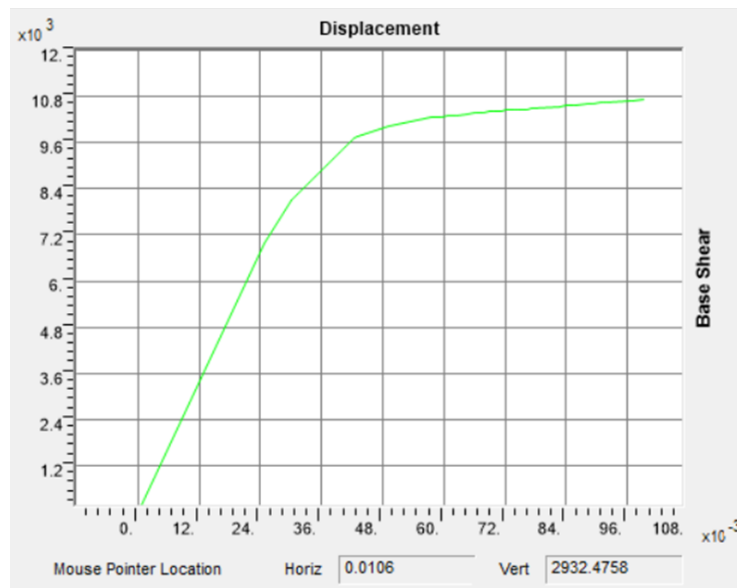


Figure 6.27: Pushover curve of the existing building in Y direction corresponding to group 1 of static equivalent loads

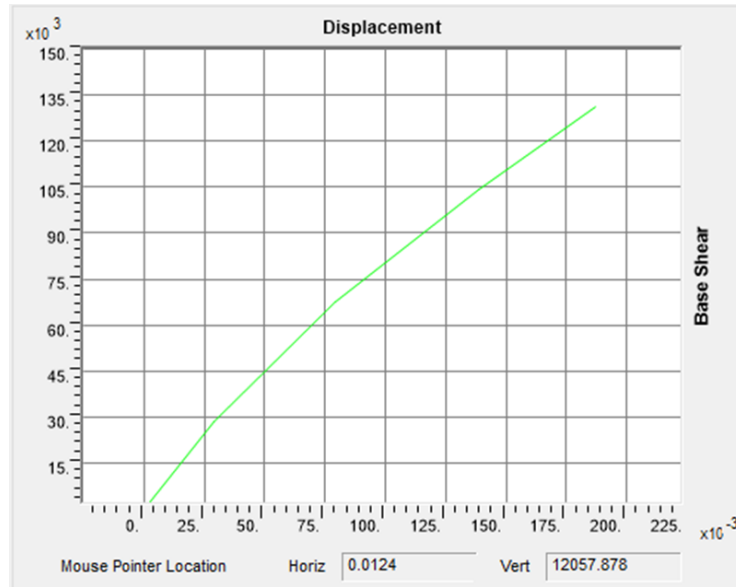


Figure 6.28: Pushover curve of the retrofitted system in Y direction corresponding to group 1 of static equivalent loads

Existing Structure		Retrofitted System	
top displacement	10.66 mm	top displacement	12.44 mm
F - group 1	2932.5 kN	F - group 1	12057.9 kN
F - group 2	3511.3 kN	F - group 2	14791.0 kN
F - average	3221.9 kN	F - average	13424.4 kN
$K(\text{str}) = F/d$	302238.7 kN/m	$K(\text{syst}) = F/d$	1079134.8 kN/m

Table 6.13: Summary of displacement and forces to determine the stiffness of the existing building ( $K_{str}$ ) and of the coupled system ( $K_{syst}$ ) in Y dir.

$$\frac{K_{syst}}{K_{str}} = 3.57$$

In this way, the stiffness ratios obtained following the proposed approach, based on displacement control, is much lower than the one suggested by the regulation, while the existing structure satisfies the structural verifications.

## 6.4 Case Study 4

The first case study is given by the 'Structure 2' retrofitted by Parallel Exoskeletons. In this case study, there are 30 positions where an exoskeleton can be placed, each representing one of the binary design variables. In the following image, a graphic representation of the exoskeleton to which each design variable corresponds is given.

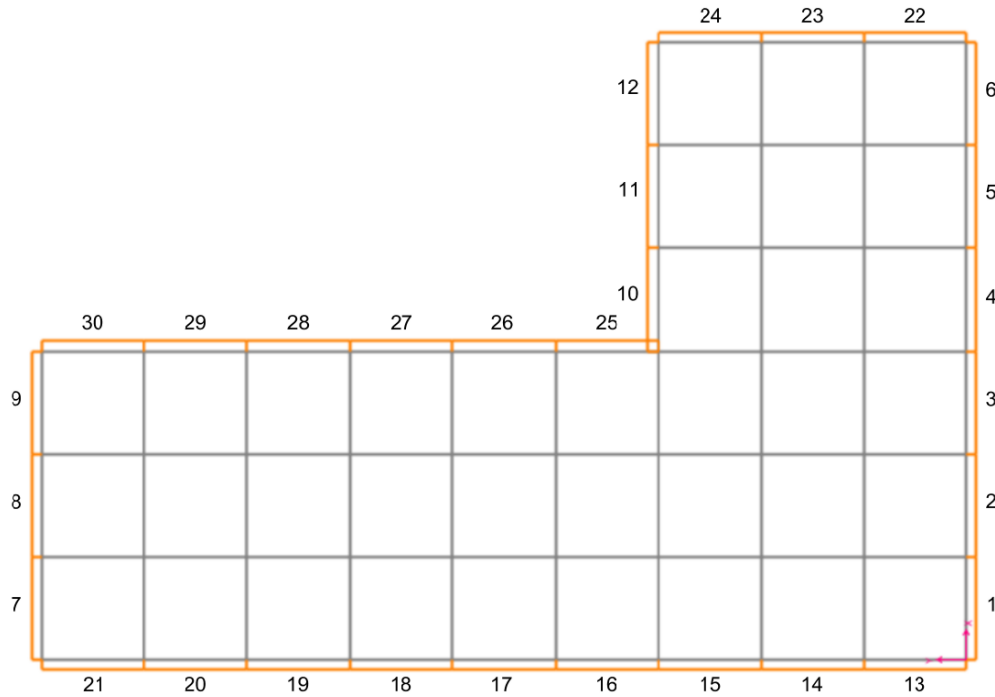


Figure 6.29: Definition of Topology DV as potential exoskeleton's positions

The maximum inter-storey drift imposed as constraint for this case is shown below,  $H$  being the storey height.

$$\frac{H}{750} = 5.33mm$$

### 6.4.1 Results of the Optimization

The main outputs of the algorithm are given by the chromosome, that provides the information of the disposition and amount of exoskeletons, as well as the steel profiles of their composing elements. The parameters that compose the objective function, hence, the weight, inter-storey drift ratio, and stress ratio of the exoskeletons, are shown, along with the chromosome, in the following table.

<b>OUTPUTS</b>	
chromosome	[ 1,1,1,1,0,0   1,1,1   0,0,0   1,1,1,0,0,0,0,0,0     1,1,1   0,0,0,0,0,0   6,1,22,29 ]
weight	1239.5 kN
inter-storey drift ratio	0.9916
stress ratio of the exosk.	0.7407
iteration of stagnation	75

Table 6.14: Summary of the main results of the optimization

To give an indication of how the algorithm worked and evolved towards the final configuration, the plots of the Objective Function, Stagnation, Inter-Storey Drift Ratio, and Stress Ratio of the Exoskeletons, against the iterations, are useful.

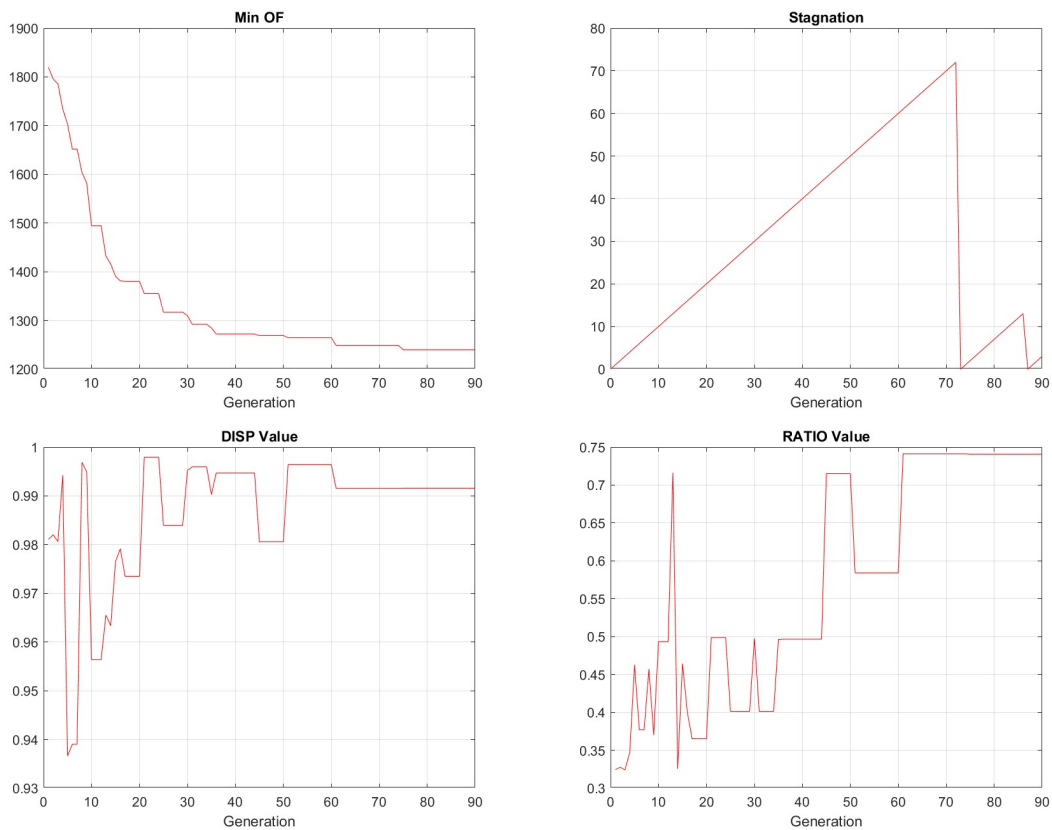


Figure 6.30: Plots of the Optimization (displayed against the iterations):  
 (1) Evolution of the Objective Function (2) Stagnation of the solution (3)  
 Inter-Storey Drift Ratio (4) Demand-Capacity Ratio of the Exoskeletons

The evolution of the Objective Function shown in the plot demonstrates that the algorithm performed in an efficient manner in this case study. During the beginning of the optimization, the Objective Function experiences big decreases, reaching rapidly the outline of the solution; then, as the optimization moves forward, the progress of the solution is more related to the refinement of the configuration, with a slighter pendent towards the end. Reaching the end, the condition of stagnation was reached twice, but the Objective Function did not experience significant changes due to it. These are indicators that the chosen solution is not a local optima.

Additionally, even though the inter-storey drift and capacity-demand ratio of the exoskeletons begin with a more randomic behavior, they tend to stabilize and maximize their values with the refinement.

## 6.4.2 Structural Interpretation of the Results

### Final Exoskeleton's Design

From the 30 binary design variables, the final configuration is composed of **thirteen exoskeletons**, positioned as shown in the images below.

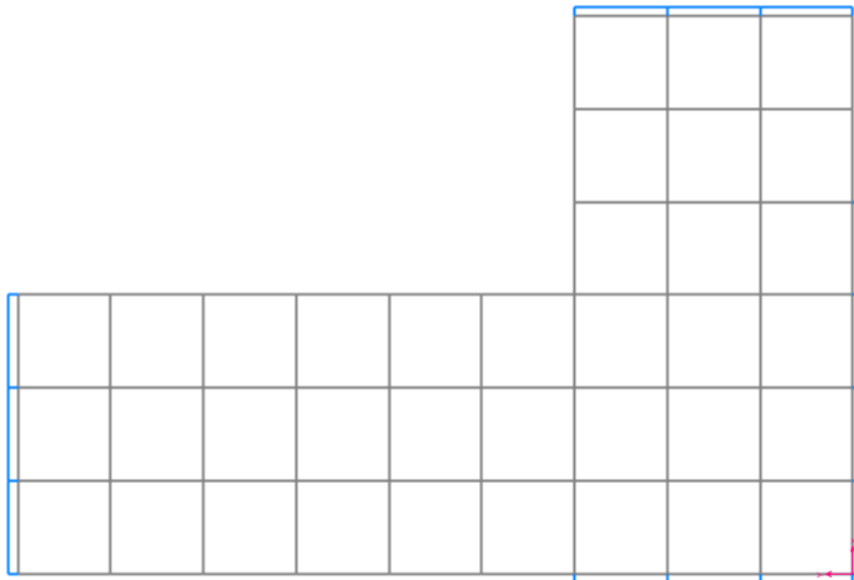


Figure 6.31: Top view of the final exoskeleton's configuration

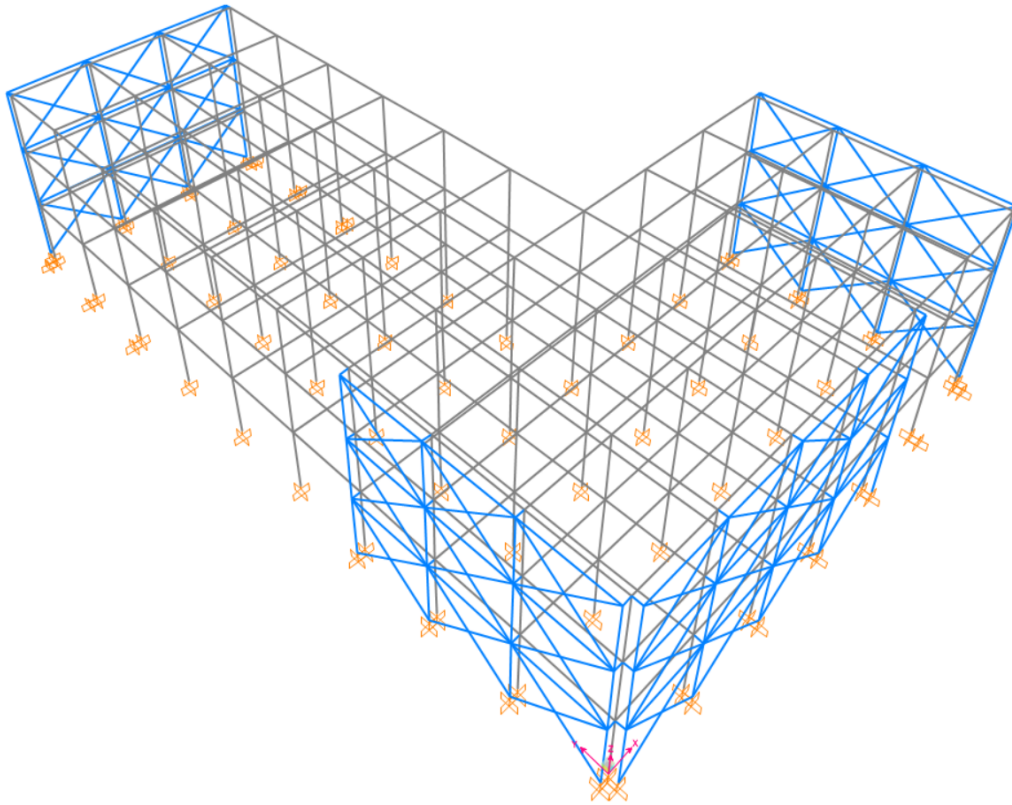


Figure 6.32: Axonometric view of the final exoskeleton's configuration

This distribution of exoskeletons was expected, considering that the nodes farthest from the rigidity center of the structure are the ones more susceptible to big displacements. In this way, the arm of the forces provided by the exoskeletons are the greater possible ones. Furthermore, it can be noticed that a solution where they are positioned together is preferred. By placing two or more exoskeletons side by side, some columns are sheared, decreasing the weight of the configuration. Additionally, a synergistic behavior is given by the collaboration between exoskeletons in the resistance of horizontal actions.

From the last four design variables, the chosen steel profiles for the elements of the exoskeletons are the following ones.

STEEL SECTIONS			
ELEMENT	DIAMETER [cm]	THICKNESS [cm]	AREA [cm <sup>2</sup> ]
columns	21.91	1.00	65.69
beams	10.16	0.50	15.17
bracings	35.56	2.50	259.65
connection	50.8	4.00	588.11

Table 6.15: Circular Hollow Sections of the exoskeleton's elements

### Main Effects of the Intervention

The main goal of the intervention was defined as the reduction of inter-storey drifts, the effects are shown in the following graph, as a comparison of the drifts of each floor before and after the retrofit. The maximum inter-storey drift decreases from **26.33 mm** to **5.29 mm**.

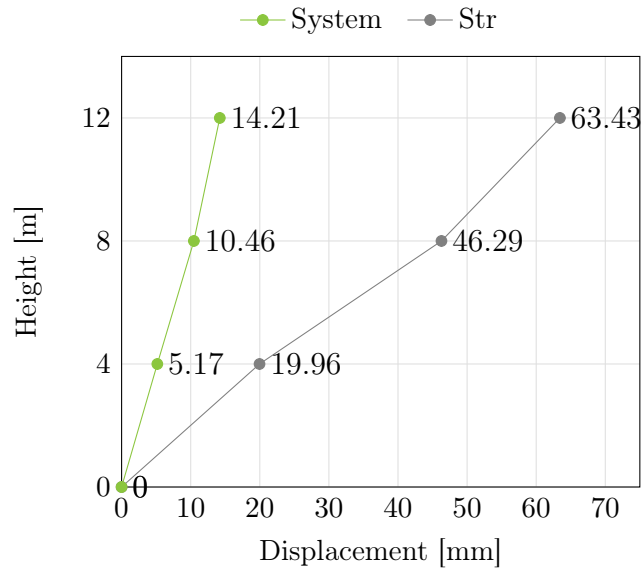
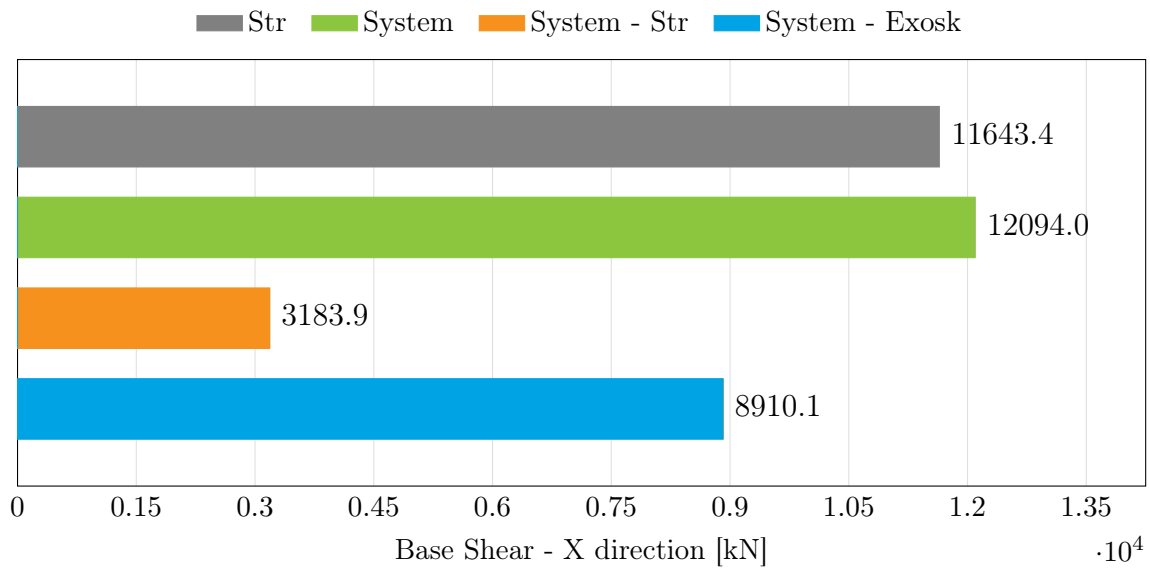
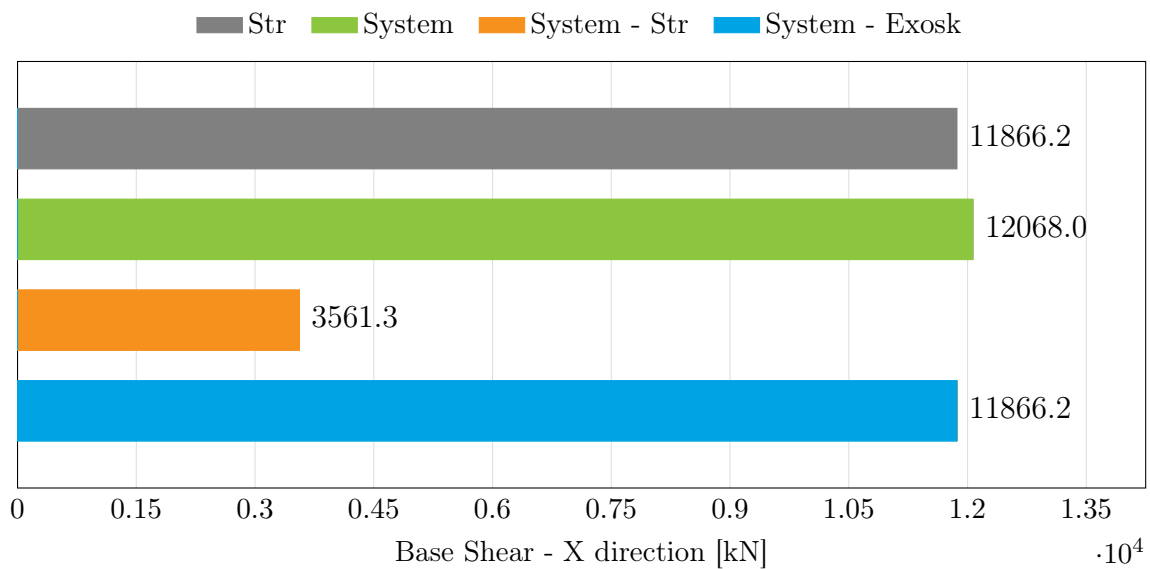


Figure 6.33: Maximum displacement of each storey of the existing building and of the retrofitted system

In the final configuration, **26.3%** of the base shear in X direction is taken by the original structure (System - Str) and **73.7%** by the exoskeletons (System - Exosk), as shown in the following chart.



In the final configuration, **29.5%** of the base shear in Y direction is taken by the original structure (System - Str) and **70.5%** by the exoskeletons (System - Exosk), as shown in the following chart.



The repercussions on the vibration modes' periods and participating masses are shown in the tables below. The main remark about these results is that, even though the exoskeletons were introduced, the main modes remain global, being translational in both directions and rotational ones.

Existing Structure							
MODE	period	U <sub>x</sub>	U <sub>y</sub>	R <sub>z</sub>	$\sum$ U <sub>x</sub>	$\sum$ U <sub>y</sub>	$\sum$ R <sub>z</sub>
	[s]	[%]	[%]	[%]	[%]	[%]	[%]
1	0.5785	80	0.3	5	80	0.3	5
2	0.5657	1.1	80	3.8	81	81	8.8
3	0.5514	4.3	4.7	76	85	85	85
Retrofitted System							
MODE	period	U <sub>x</sub>	U <sub>y</sub>	R <sub>z</sub>	$\sum$ U <sub>x</sub>	$\sum$ U <sub>y</sub>	$\sum$ R <sub>z</sub>
	[s]	[%]	[%]	[%]	[%]	[%]	[%]
1	0.2808	8.8	77.9	0.2	8.8	77.9	0.2
2	0.2658	78.2	9	0	87	87	0.2
21	0.1693	0	0	87.4	87	87	87.6

Table 6.16: Summary of fundamental vibration modes' information before and after the retrofit

### 6.4.3 Results in Relation to the Stiffness

The structural verifications of each element are performed and the results of the existing and retrofitted configurations are shown in the images below. The maximum demand-capacity ratio decreases from **3.437**, for the building as-is, to **0.997**, for the structure after the intervention.

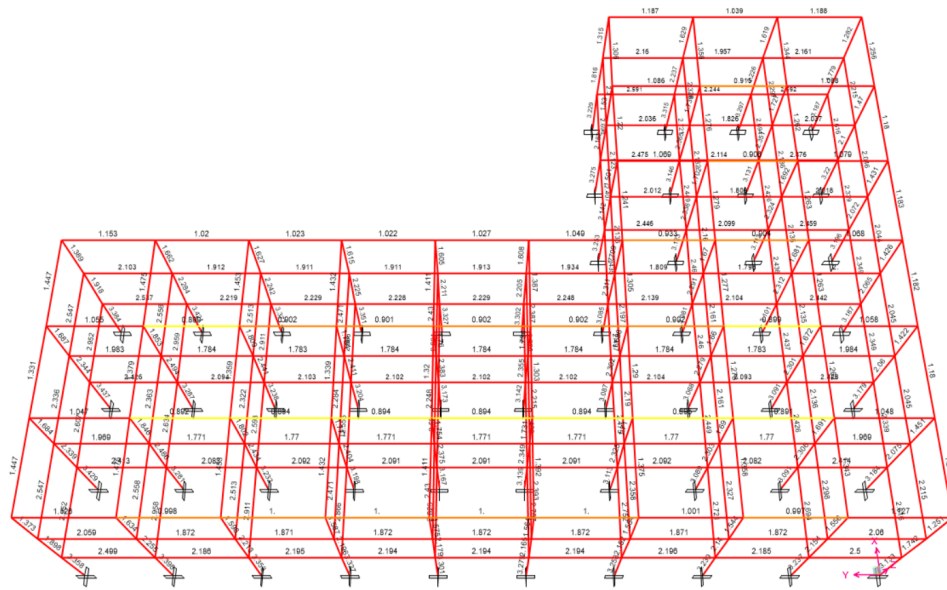


Figure 6.34: Capacity-Demand Ratio check of the unretrofitted building

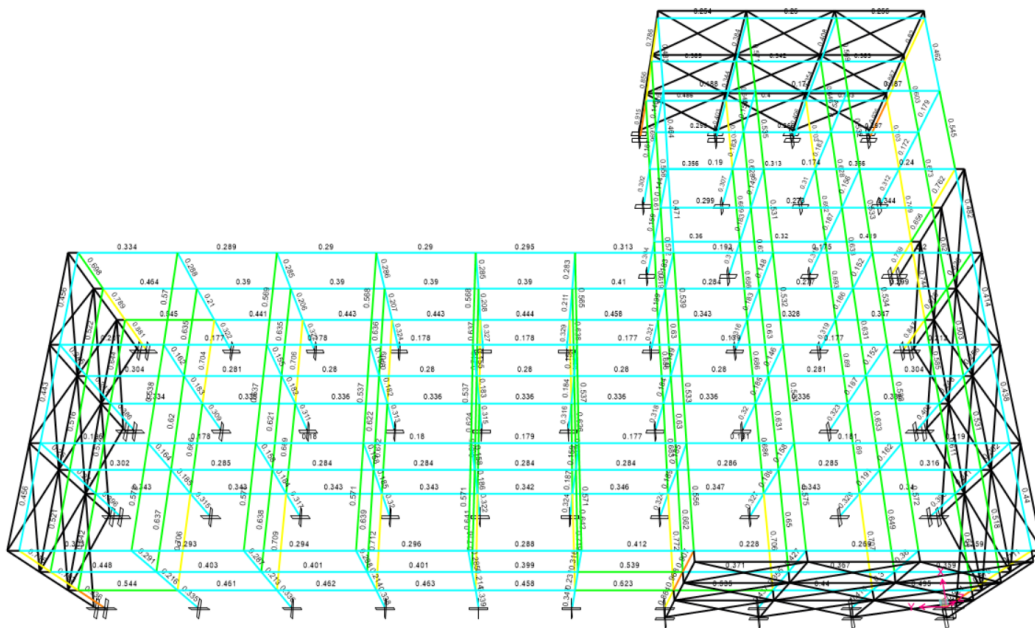


Figure 6.35: Capacity-Demand Ratio check of the retrofitted building

X direction

Then, the stiffnesses under horizontal actions of both bare and retrofitted configurations are determined through pushover analyses, the results are presented below.

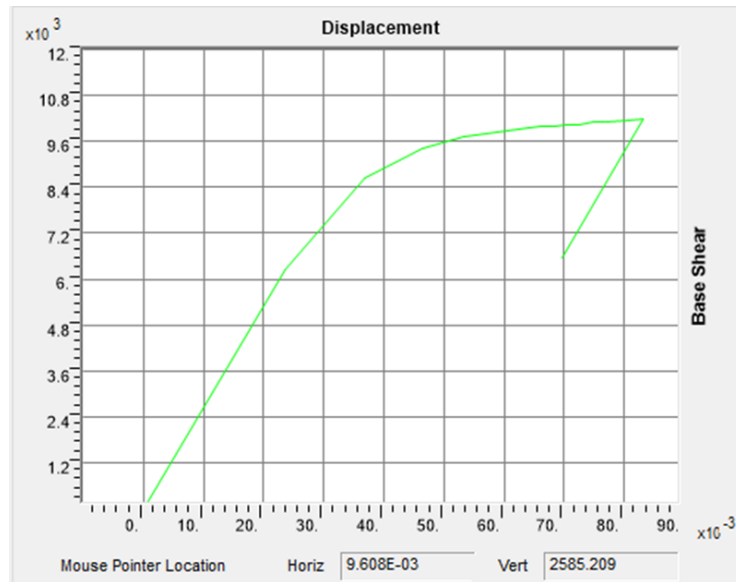


Figure 6.36: Pushover curve of the existing building in X direction corresponding to group 1 of static equivalent loads

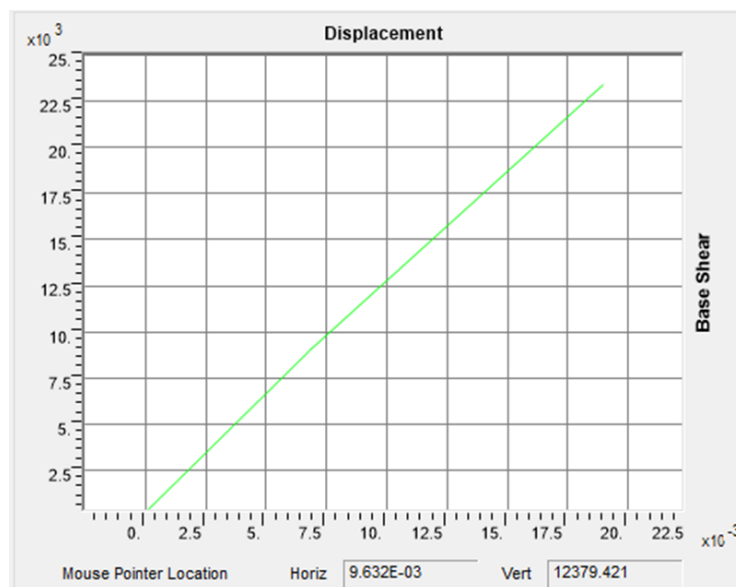


Figure 6.37: Pushover curve of the retrofitted system in X direction corresponding to group 1 of static equivalent loads

Existing Structure		Retrofitted System	
top displacement	9.61 mm	top displacement	9.66 mm
F - group 1	2585.2 kN	F - group 1	12379.4 kN
F - group 2	3009.6 kN	F - group 2	14758.8 kN
F - average	2797.4 kN	F - average	13569.1 kN
$K(\text{str}) = F/d$	291050.1 kN/m	$K(\text{syst}) = F/d$	1404201.1 kN/m

Table 6.17: Summary of displacement and forces to determine the stiffness of the existing building ( $K_{str}$ ) and of the coupled system ( $K_{syst}$ ) in X dir.

$$\frac{K_{syst}}{K_{str}} = 4.82$$

#### Y direction

Analogously, the analyses are performed in Y direction.

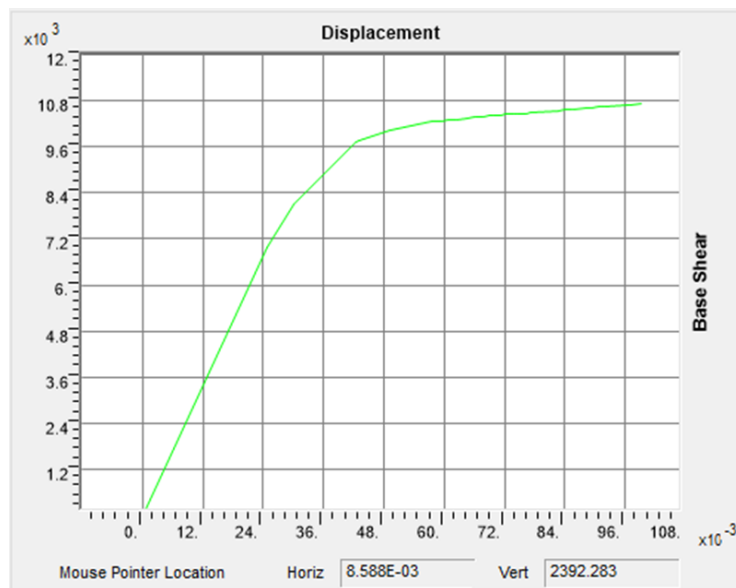


Figure 6.38: Pushover curve of the existing building in Y direction corresponding to group 1 of static equivalent loads

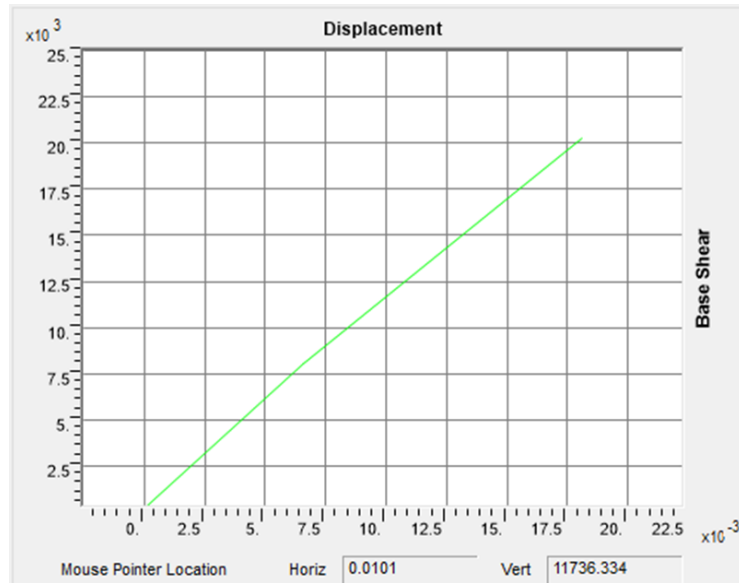


Figure 6.39: Pushover curve of the retrofitted system in Y direction corresponding to group 1 of static equivalent loads

Existing Structure		Retrofitted System	
top displacement	8.53 mm	top displacement	10.13 mm
F - group 1	2392.3 kN	F - group 1	11736.3 kN
F - group 2	2855.3 kN	F - group 2	14067.5 kN
F - average	2623.8 kN	F - average	12901.9 kN
$K(\text{str}) = F/d$	307617.7 kN/m	$K(\text{syst}) = F/d$	1274327.5 kN/m

Table 6.18: Summary of displacement and forces to determine the stiffness of the existing building ( $K_{str}$ ) and of the coupled system ( $K_{syst}$ ) in Y dir.

$$\frac{K_{syst}}{K_{str}} = 4.14$$

In this way, the stiffness ratios obtained following the proposed approach, based on displacement control, is much lower than the one suggested by the regulation, while the existing structure satisfies the structural verifications.

## 6.5 Case Study 5

The first case study is given by the 'Structure 3' retrofitted by Orthogonal Exoskeletons. In this case study, there are 52 positions where an exoskeleton can be placed, each representing one of the binary design variables. In the following image, a graphic representation of the exoskeleton to which each design variable corresponds is given.

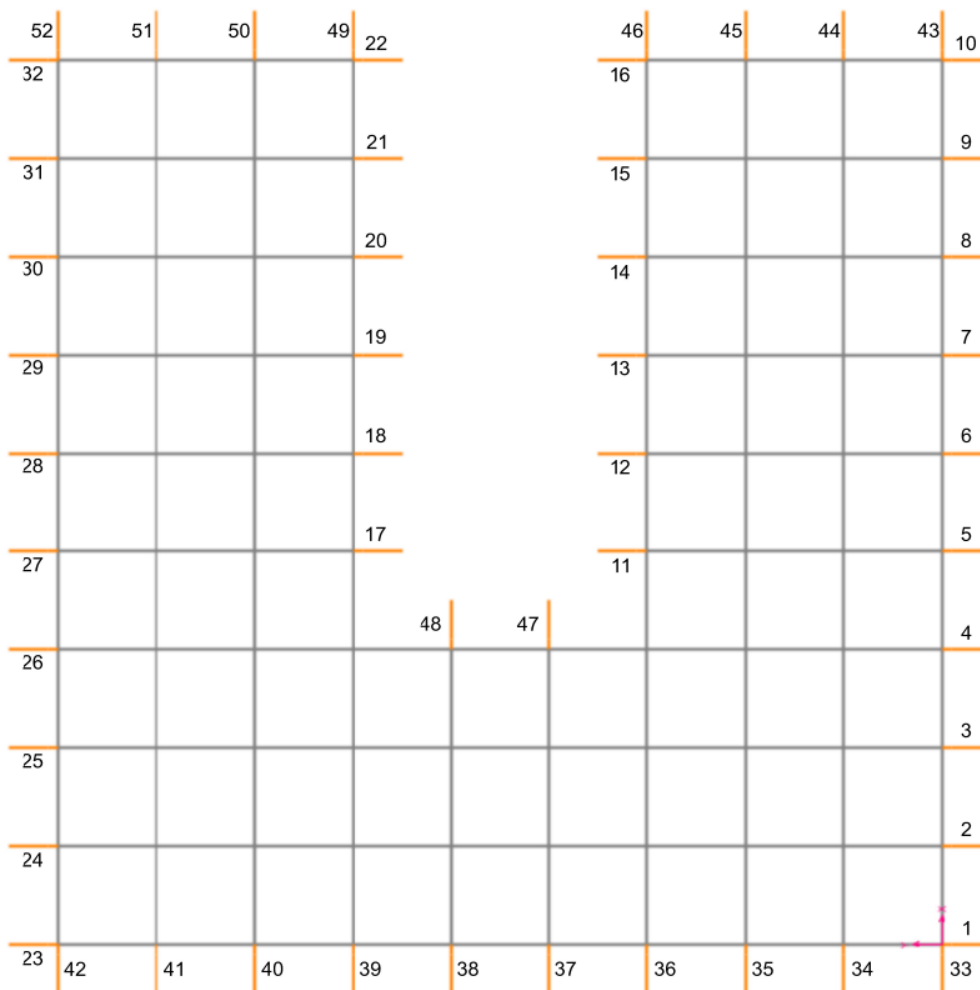


Figure 6.40: Definition of Topology DV as potential exoskeleton's positions

The maximum inter-storey drift imposed as constraint for this case is shown below,  $H$  being the storey height.

$$\frac{H}{550} = 7.27mm$$

### 6.5.1 Results of the Optimization

The main outputs of the algorithm are given by the chromosome, that provides the information of the disposition and amount of exoskeletons, as well as the steel profiles of their composing elements. The parameters that compose the objective function, hence, the weight, inter-storey drift ratio, and stress ratio of the exoskeletons, are shown, along with the chromosome, in the following table.

<b>OUTPUTS</b>	
chromosome	[ 1,1,0,0,0,0,1,0,0,0   0,1,1,1,0,0     0,1,1,1,0,0   1,1,0,0,0,1,1,0,0,0   1,1,1,0,0,0,0,1,1,1     1,1,1,1   0,0   1,1,1,1   35,24,29,22 ]
weight	9381.0 kN
inter-storey drift ratio	0.9965
stress ratio of the exosk.	0.2203
iteration of stagnation	96

Table 6.19: Summary of the main results of the optimization

To give an indication of how the algorithm worked and evolved towards the final configuration, the plots of the Objective Function, Stagnation, Inter-Storey Drift Ratio, and Stress Ratio of the Exoskeletons, against the iterations, are useful.

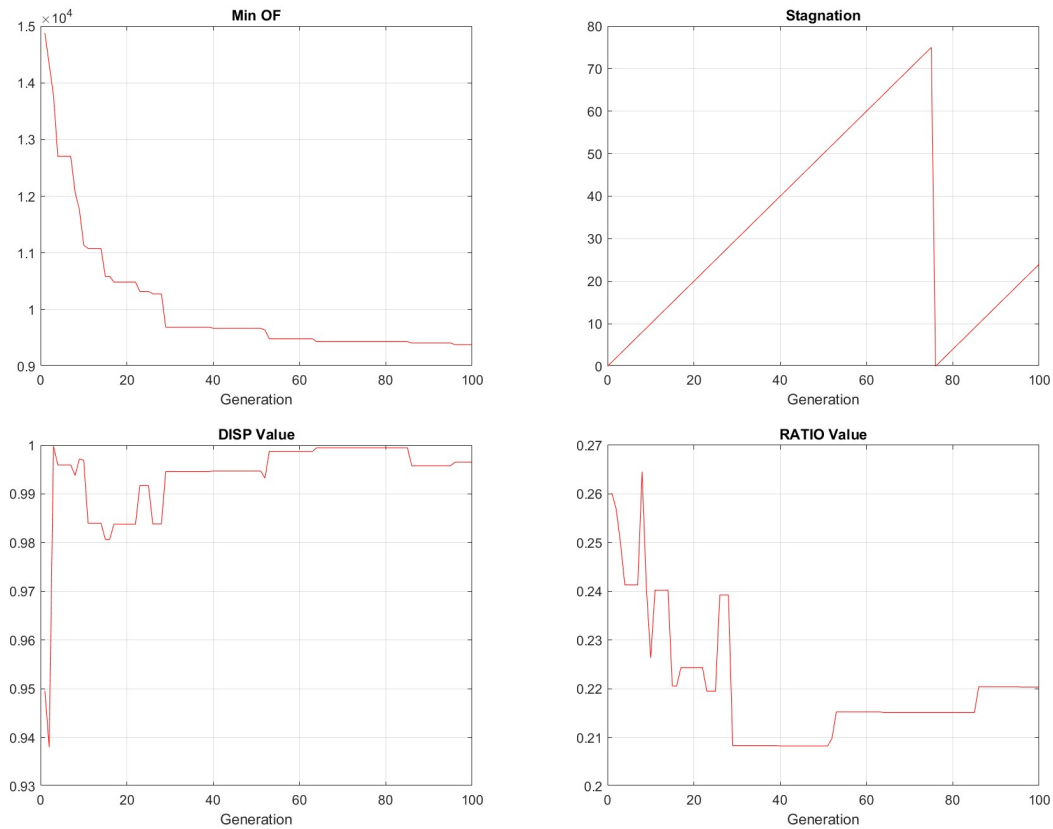


Figure 6.41: Plots of the Optimization (displayed against the iterations):  
 (1) Evolution of the Objective Function (2) Stagnation of the solution (3)  
 Inter-Storey Drift Ratio (4) Demand-Capacity Ratio of the Exoskeletons

In the same way as for the Case Study 4, the evolution of the Objective Function is marked by significant decreases in the beginning, reaching a refinement stage around iteration 30. Accompanied by the reaching of the stagnation condition only approaching the end, and the stabilization and increase of the inter-storey drift and capacity-demand ratios, it can be presumed that the final solution is not a local optima.

## 6.5.2 Structural Interpretation of the Results

### Final Exoskeleton's Design

From the 52 binary design variables, the final configuration is composed of **twenty-seven exoskeletons**, positioned as shown in the images below.



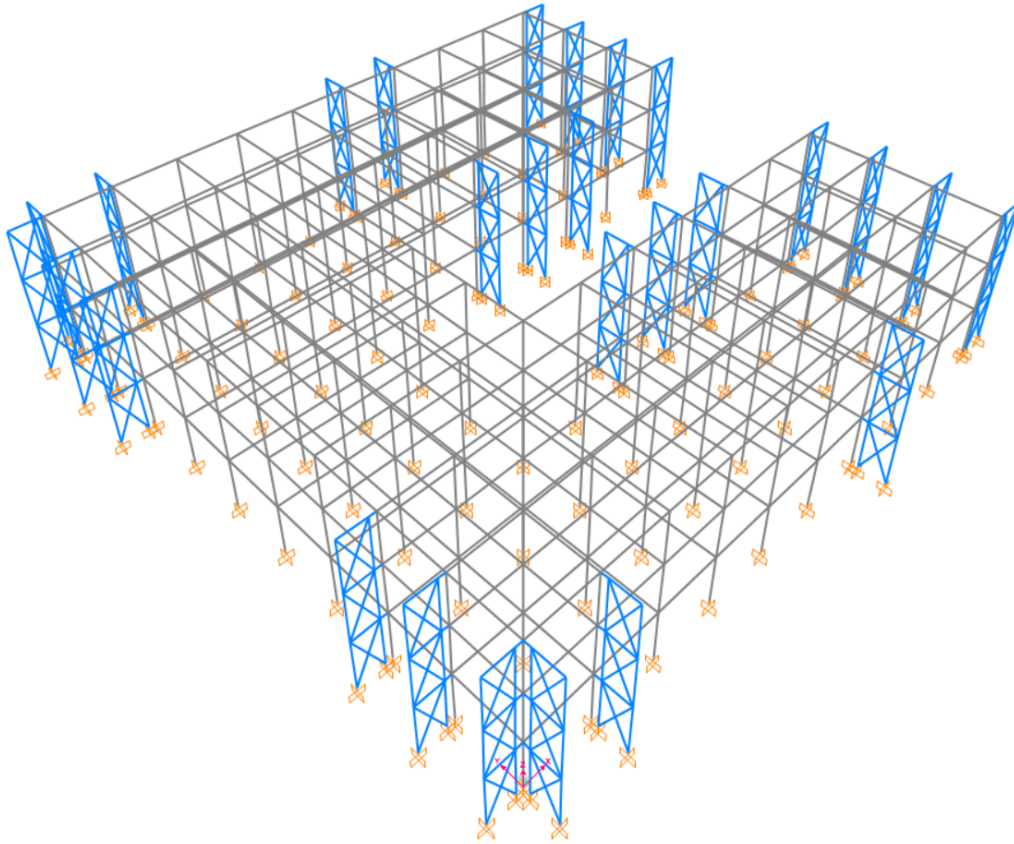


Figure 6.43: Axonometric view of the final exoskeleton's configuration

This distribution of exoskeletons was expected, considering that the nodes farthest from the rigidity center of the structure are the ones more susceptible to big displacements. In this way, the arm of the forces provided by the exoskeletons are the greater possible ones.

From the last four design variables, the chosen steel profiles for the elements of the exoskeletons are the following ones.

STEEL SECTIONS			
ELEMENT	DIAMETER [cm]	THICKNESS [cm]	AREA [cm <sup>2</sup> ]
columns	76.20	5.00	1118.41
beams	40.64	3.00	354.75
bracings	50.8	4.00	588.11
connection	35.56	2.50	259.65

Table 6.20: Circular Hollow Sections of the exoskeleton's elements

### Main Effects of the Intervention

The main goal of the intervention was defined as the reduction of inter-storey drifts, the effects are shown in the following graph, as a comparison of the drifts of each floor before and after the retrofit. The maximum inter-storey drift decreases from **25.74 mm** to **7.24 mm**.

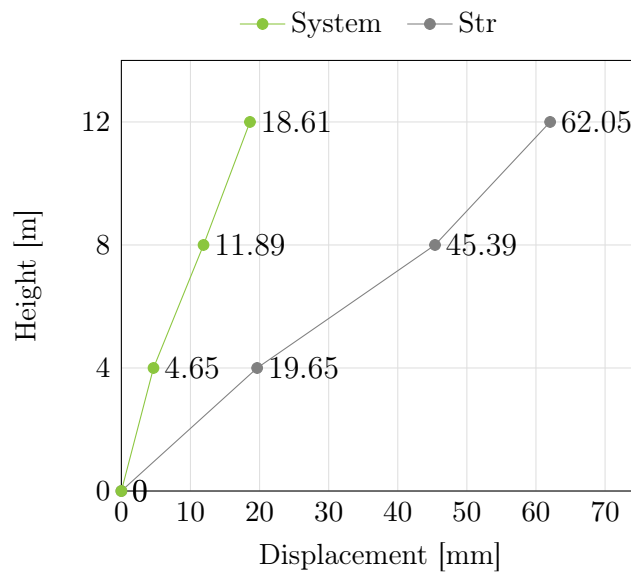
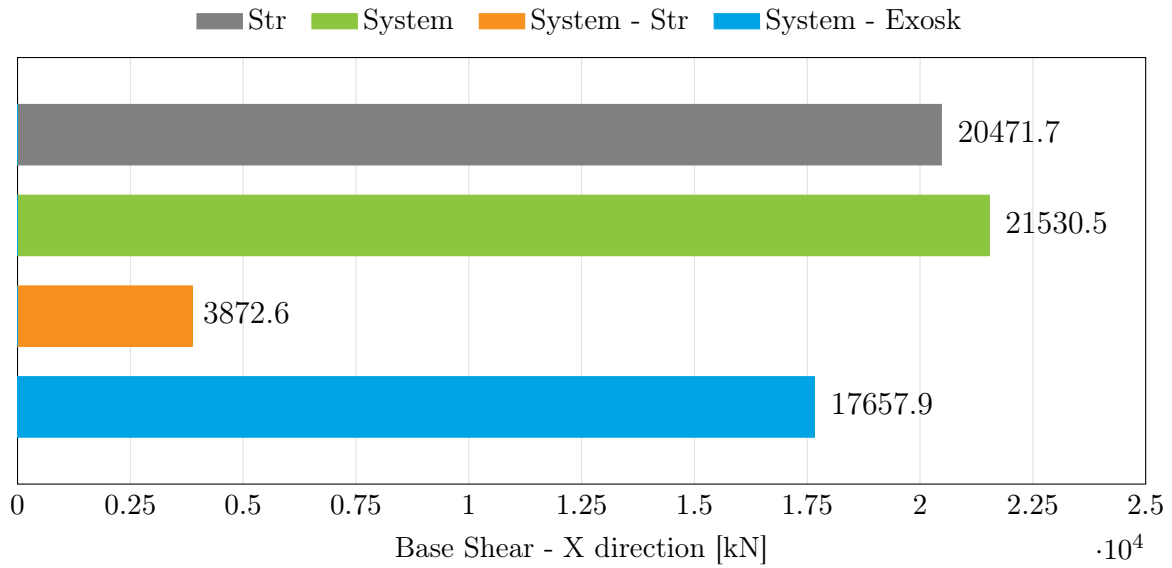
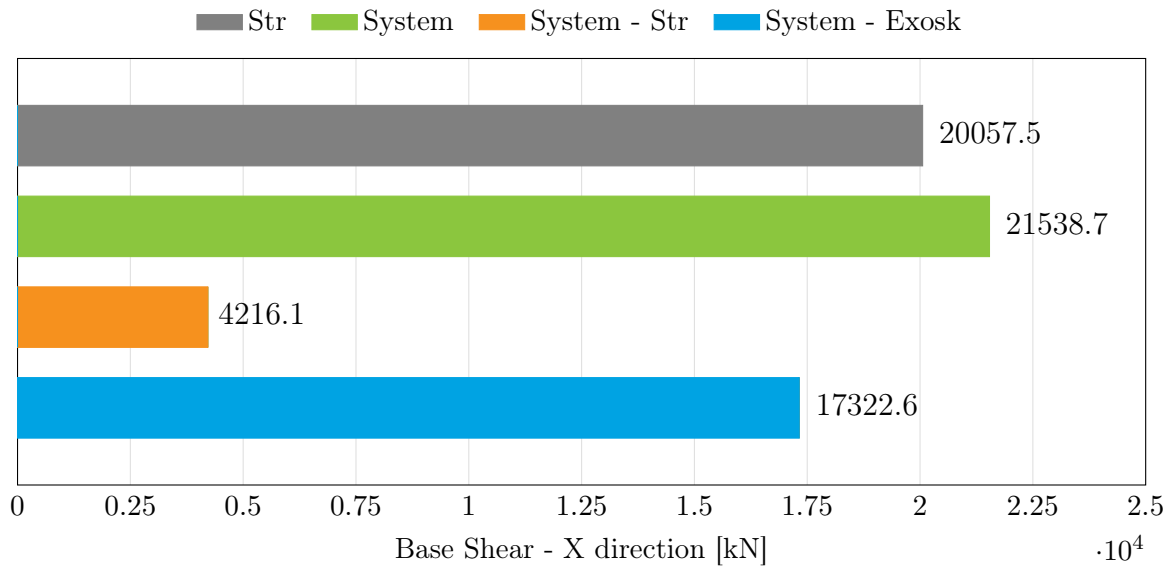


Figure 6.44: Maximum displacement of each storey of the existing building and of the retrofitted system

In the final configuration, **18.0%** of the base shear in X direction is taken by the original structure (System - Str) and **82.0%** by the exoskeletons (System - Exosk), as shown in the following chart.



(Y-dir) In the final configuration, **19.6%** of the base shear in Y direction is taken by the original structure (System - Str) and **80.4%** by the exoskeletons (System - Exosk), as shown in the following chart.



The repercussions on the vibration modes' periods and participating masses are shown in the tables below. The main remark about these results is that, even though the exoskeletons were introduced, the main modes remain global, being translational in both directions and rotational ones.

Existing Structure							
MODE	period	U <sub>x</sub>	U <sub>y</sub>	R <sub>z</sub>	$\sum$ U <sub>x</sub>	$\sum$ U <sub>y</sub>	$\sum$ R <sub>z</sub>
	[s]	[%]	[%]	[%]	[%]	[%]	[%]
1	0.5797	0	83	2.2	0	83	2.2
2	0.5650	86	0	0	86	83	2.2
3	0.5529	0	2.3	83	86	85	85
Retrofitted System							
MODE	period	U <sub>x</sub>	U <sub>y</sub>	R <sub>z</sub>	$\sum$ U <sub>x</sub>	$\sum$ U <sub>y</sub>	$\sum$ R <sub>z</sub>
	[s]	[%]	[%]	[%]	[%]	[%]	[%]
1	0.3149	0	75.8	0.4	0	75.8	0.4
2	0.3048	76.4	0	0	76.4	75.8	0.4
3	0.2991	0	0.2	71.5	76.4	76	71.8

Table 6.21: Summary of fundamental vibration modes' information before and after the retrofit

### 6.5.3 Results in Relation to the Stiffness

The structural verifications of each element are performed and the results of the existing and retrofitted configurations are shown in the images below. The maximum demand-capacity ratio decreases from **3.420**, for the building as-is, to **0.963**, for the structure after the intervention.

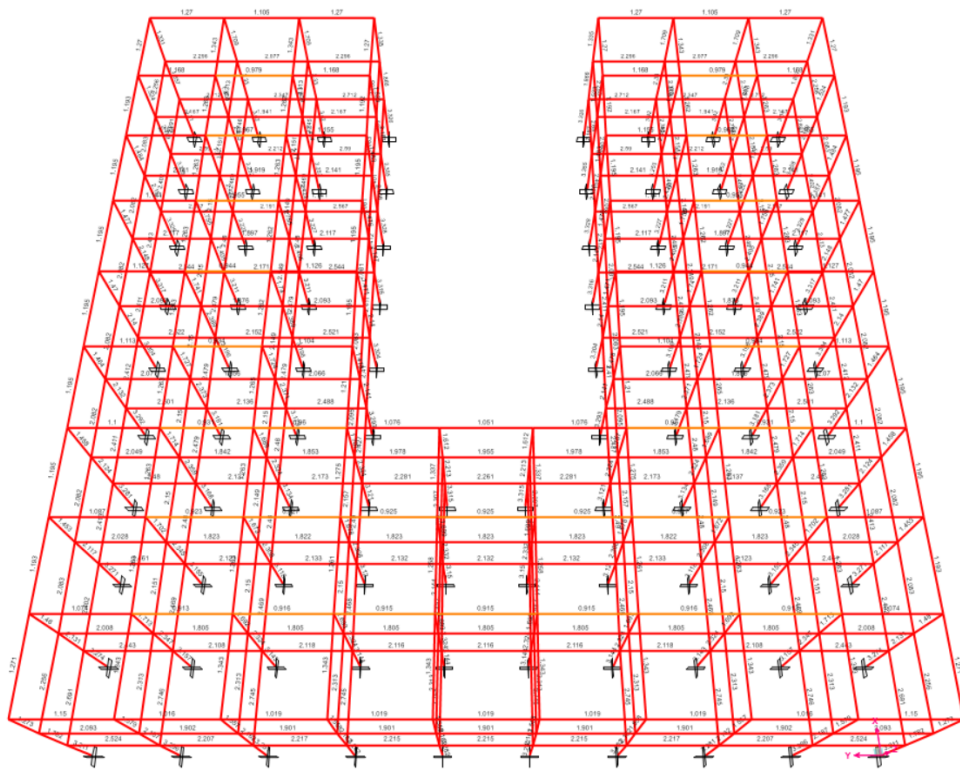


Figure 6.45: Capacity-Demand Ratio check of the unretrofitted building

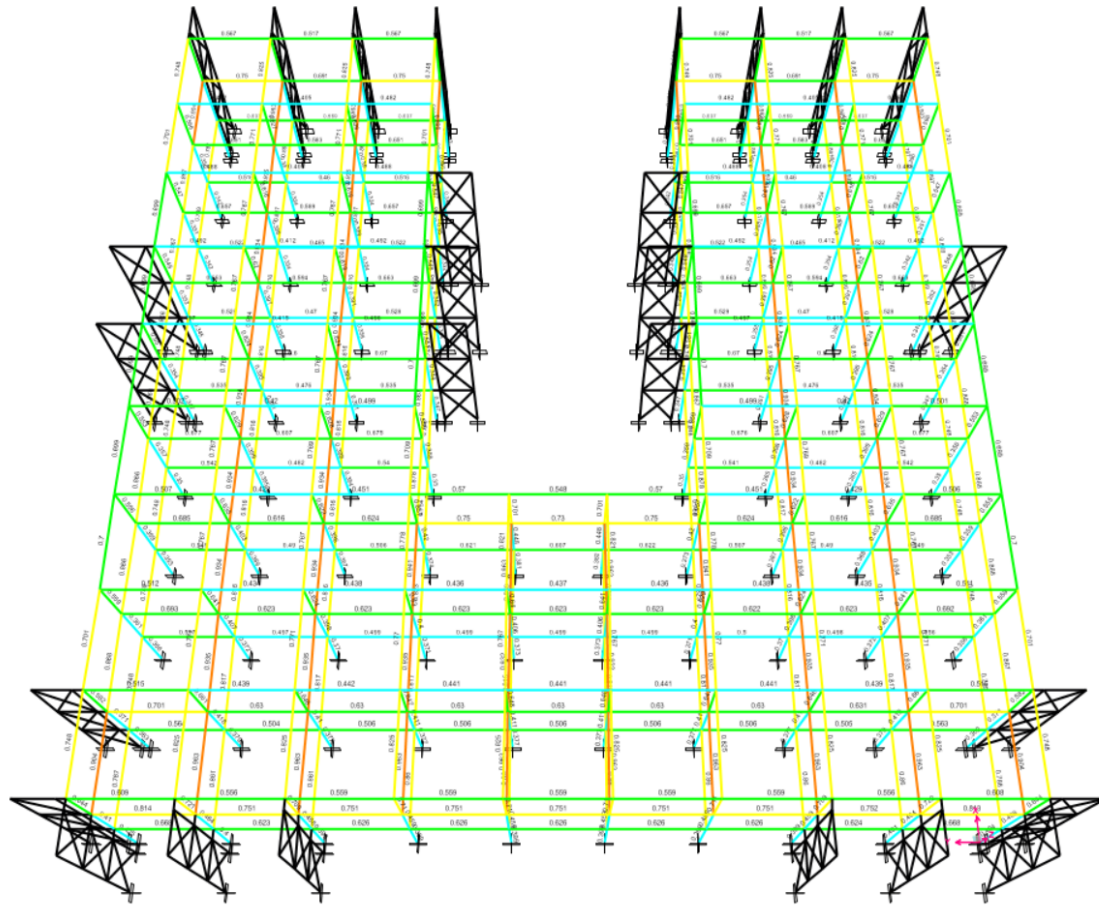


Figure 6.46: Capacity-Demand Ratio check of the retrofitted building

X direction

Then, the stiffnesses under horizontal actions of both bare and retrofitted configurations are determined through pushover analyses, the results are presented below.

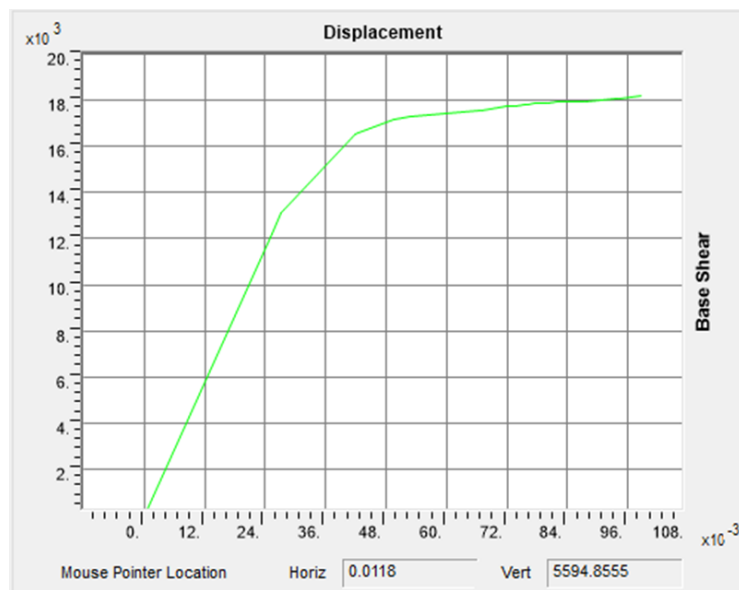


Figure 6.47: Pushover curve of the existing building in X direction corresponding to group 1 of static equivalent loads

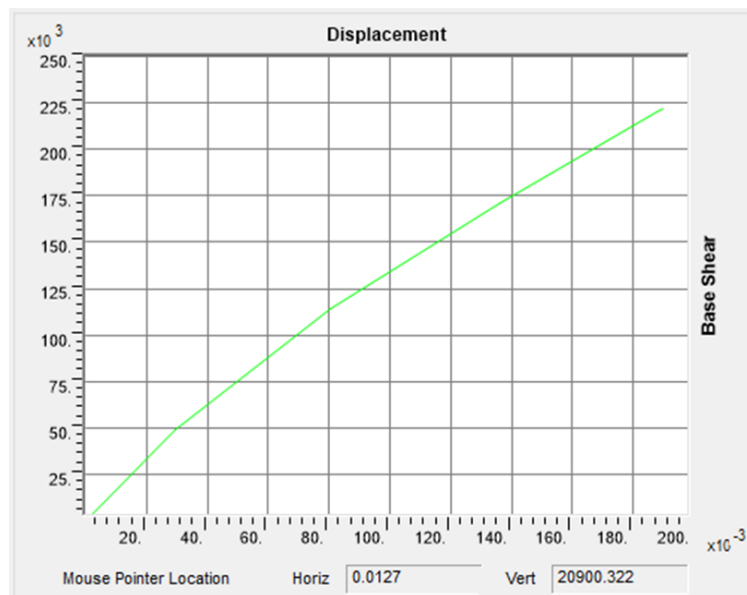


Figure 6.48: Pushover curve of the retrofitted system in X direction corresponding to group 1 of static equivalent loads

Existing Structure		Retrofitted System	
top displacement	11.86 mm	top displacement	12.63 mm
F - group 1	5594.9 kN	F - group 1	20900.3 kN
F - group 2	6816.7 kN	F - group 2	25080.4 kN
F - average	6205.8 kN	F - average	22990.4 kN
$K(\text{str}) = F/d$	523174.2 kN/m	$K(\text{syst}) = F/d$	1820773.0 kN/m

Table 6.22: Summary of displacement and forces to determine the stiffness of the existing building ( $K_{str}$ ) and of the coupled system ( $K_{syst}$ ) in X dir.

$$\frac{K_{syst}}{K_{str}} = 3.48$$

### Y direction

Analogously, the analyses are performed in Y direction.

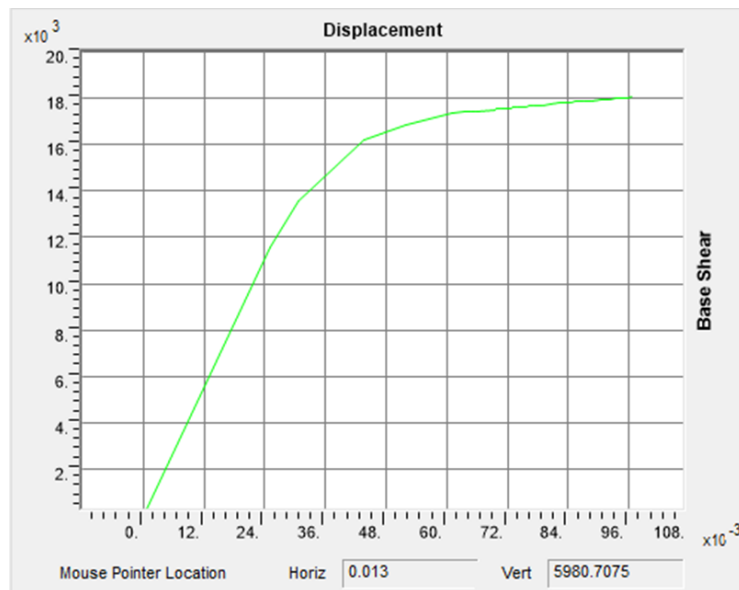


Figure 6.49: Pushover curve of the existing building in Y direction corresponding to group 1 of static equivalent loads

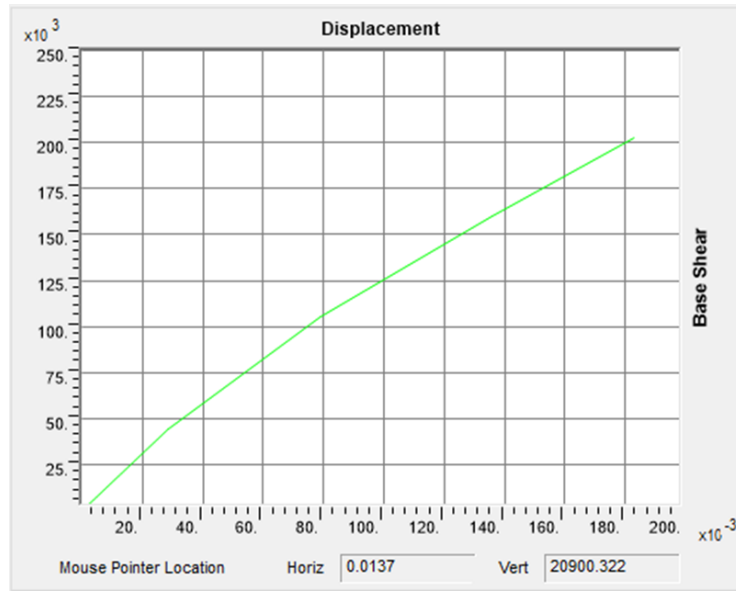


Figure 6.50: Pushover curve of the retrofitted system in Y direction corresponding to group 1 of static equivalent loads

Existing Structure		Retrofitted System	
top displacement	12.90 mm	top displacement	13.67 mm
F - group 1	5980.7 kN	F - group 1	20900.3 kN
F - group 2	7202.6 kN	F - group 2	27009.6 kN
F - average	6591.6 kN	F - average	23955.0 kN
$K(str) = F/d$	510932.3 kN/m	$K(syst) = F/d$	1752449.4 kN/m

Table 6.23: Summary of displacement and forces to determine the stiffness of the existing building ( $K_{str}$ ) and of the coupled system ( $K_{syst}$ ) in Y dir.

$$\frac{K_{syst}}{K_{str}} = 3.43$$

In this way, the stiffness ratios obtained following the proposed approach, based on displacement control, is much lower than the one suggested by the regulation, while the existing structure satisfies the structural verifications.

## 6.6 Case Study 6

The first case study is given by the 'Structure 3' retrofitted by Parallel Exoskeletons. In this case study, there are 48 positions where an exoskeleton can be placed, each representing one of the binary design variables. In the following image, a graphic representation of the exoskeleton to which each design variable corresponds is given.

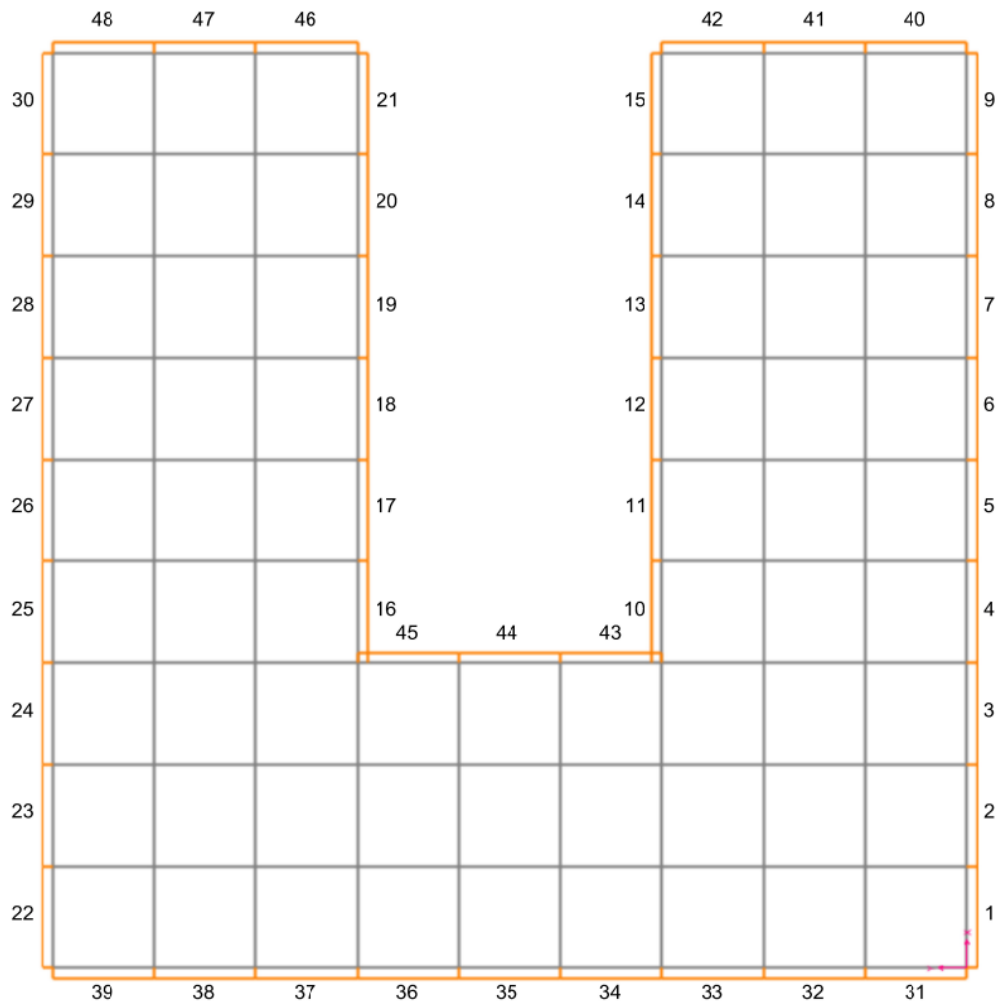


Figure 6.51: Definition of Topology DV as potential exoskeleton's positions

The maximum inter-storey drift imposed as constraint for this case is shown below,  $H$  being the storey height.

$$\frac{H}{750} = 5.33mm$$

### 6.6.1 Results of the Optimization

The main outputs of the algorithm are given by the chromosome, that provides the information of the disposition and amount of exoskeletons, as well as the steel profiles of their composing elements. The parameters that compose the objective function, hence, the weight, inter-storey drift ratio, and stress ratio of the exoskeletons, are shown, along with the chromosome, in the following table.

<b>OUTPUTS</b>	
chromosome	[ 1,1,0,0,0,0,0,1,1   0,0,0,0,0,0   0,0,0,0,0,0   1,1,0,0,0,0,1,1,1     1,1,0,0,0,0,0,1,1   1,1,1   0,0,0   0,0,0   11,1,25,33 ]
weight	2446.3 kN
inter-storey drift ratio	0.9999
stress ratio of the exosk.	0.6169
iteration of stagnation	98

Table 6.24: Summary of the main results of the optimization

To give an indication of how the algorithm worked and evolved towards the final configuration, the plots of the Objective Function, Stagnation, Inter-Storey Drift Ratio, and Stress Ratio of the Exoskeletons, against the iterations, are useful.

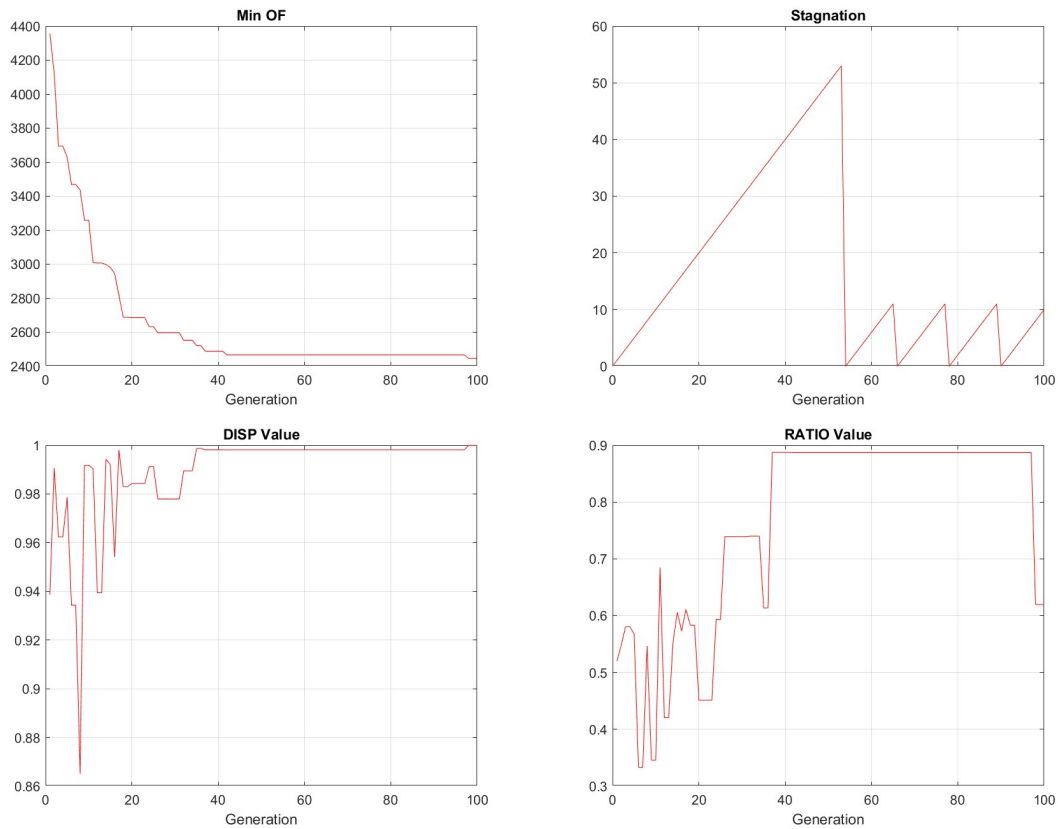


Figure 6.52: Plots of the Optimization (displayed against the iterations):  
 (1) Evolution of the Objective Function (2) Stagnation of the solution (3)  
 Inter-Storey Drift Ratio (4) Demand-Capacity Ratio of the Exoskeletons

In the same way as for the Case Study 4 and 5, the evolution of the Objective Function is marked by significant decreases in the beginning, reaching a refinement stage around iteration 30. Accompanied by the fact that, even if it reached of the stagnation condition several times from the iteration 40 until the end, the Objective Function maintained, suggests that the solution is a global optimal or near-optimal solution. Additionally, the stabilization and increase of the inter-storey drift and capacity-demand ratios are good indicators.

## 6.6.2 Structural Interpretation of the Results

### Final Exoskeleton's Design

From the 48 binary design variables, the final configuration is composed of **sixteen exoskeletons**, positioned as shown in the images below.

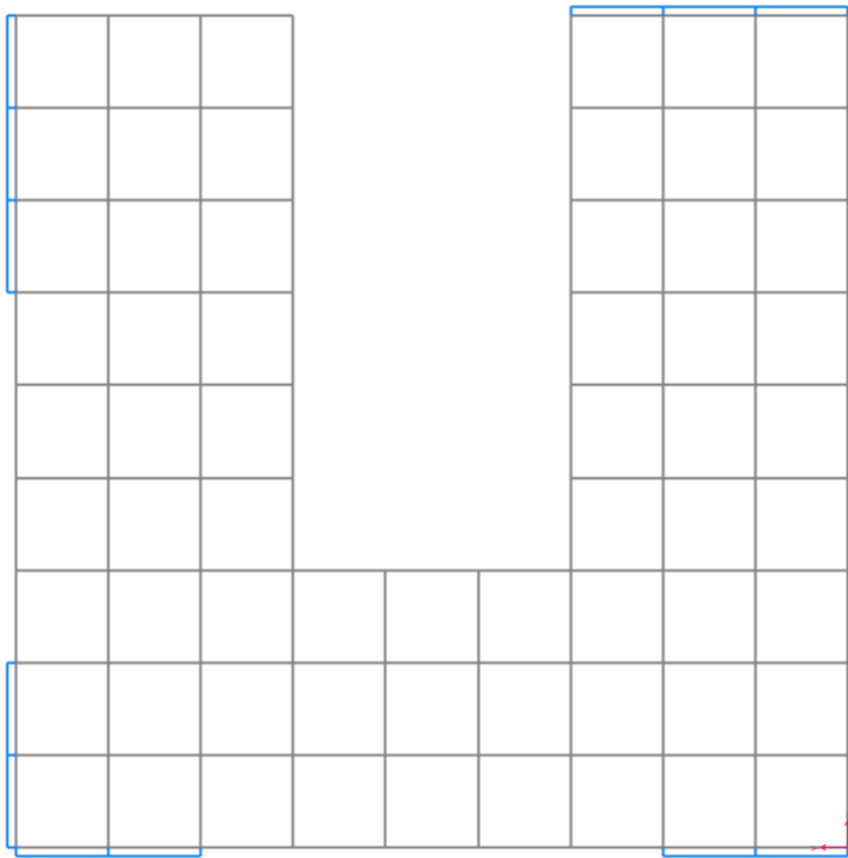


Figure 6.53: Top view of the final exoskeleton's configuration

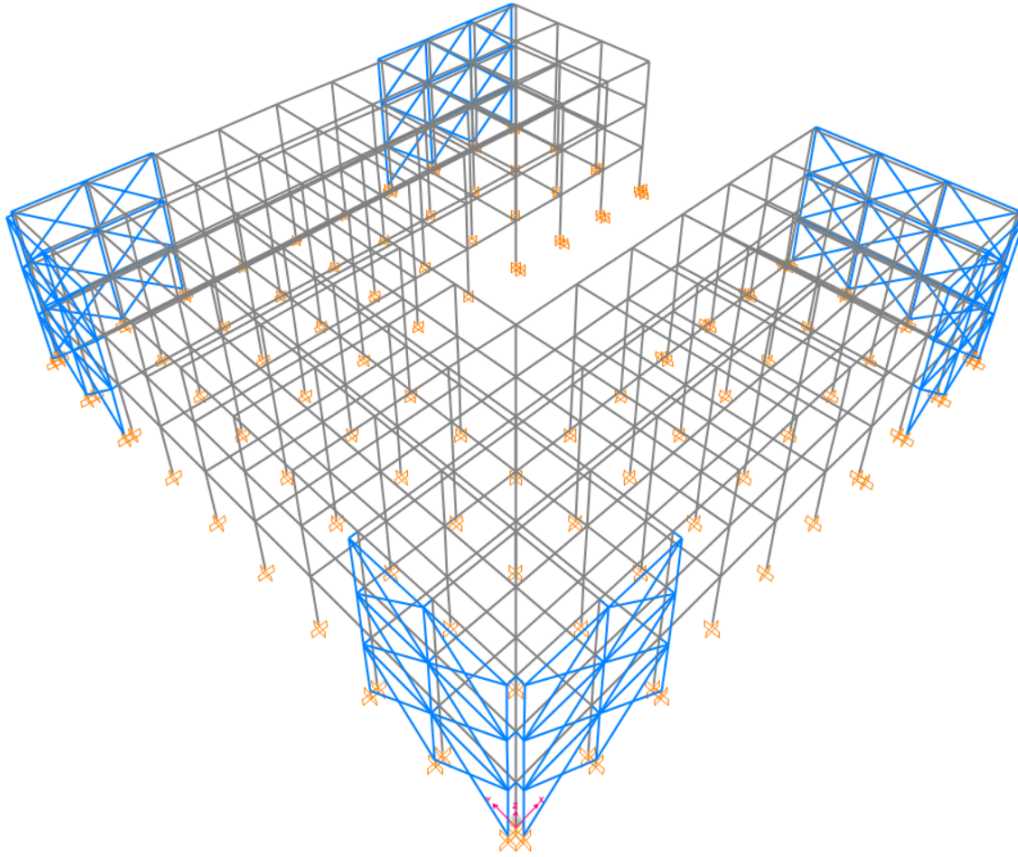


Figure 6.54: Axonometric view of the final exoskeleton's configuration

This distribution of exoskeletons was expected, considering that the nodes farthest from the rigidity center of the structure are the ones more susceptible to big displacements. In this way, the arm of the forces provided by the exoskeletons are the greater possible ones. Furthermore, it can be noticed that a solution where they are positioned together is preferred. By placing two or more exoskeletons side by side, some columns are sheared, decreasing the weight of the configuration. Additionally, a synergistic behavior is given by the collaboration between exoskeletons in the resistance of horizontal actions.

From the last four design variables, the chosen steel profiles for the elements of the exoskeletons are the following ones.

STEEL SECTIONS			
ELEMENT	DIAMETER [cm]	THICKNESS [cm]	AREA [cm <sup>2</sup> ]
columns	27.30	1.42	115.45
beams	10.16	0.50	15.17
bracings	45.70	3.00	402.44
connection	76.20	4.00	907.29

Table 6.25: Circular Hollow Sections of the exoskeleton's elements

### Main Effects of the Intervention

The main goal of the intervention was defined as the reduction of inter-storey drifts, the effects are shown in the following graph, as a comparison of the drifts of each floor before and after the retrofit. The maximum inter-storey drift decreases from **25.74 mm** to **5.33 mm**.

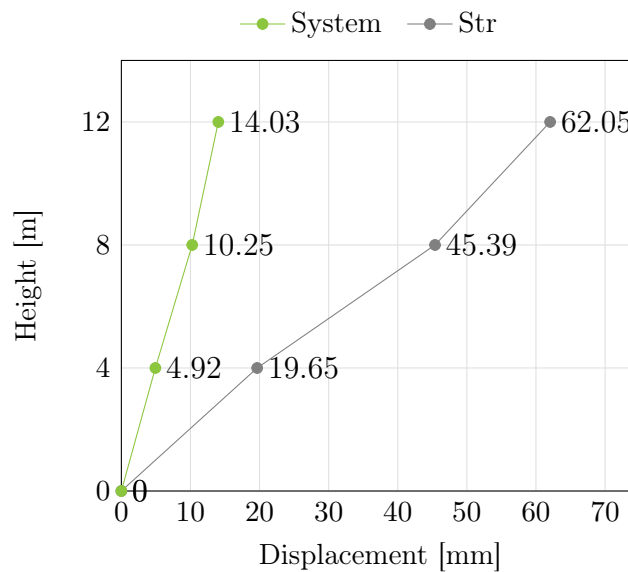
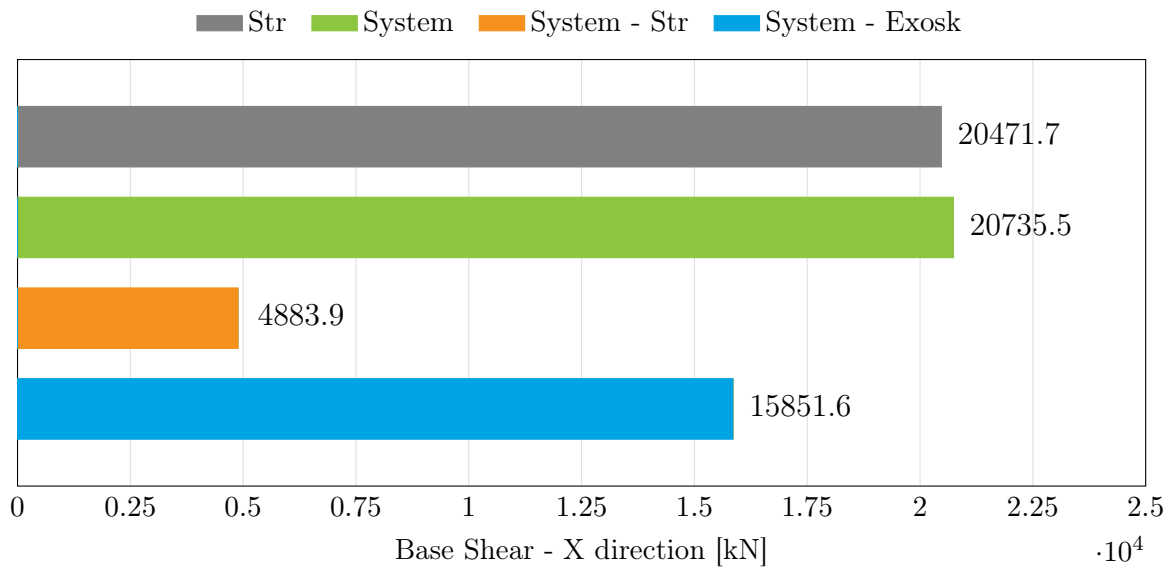
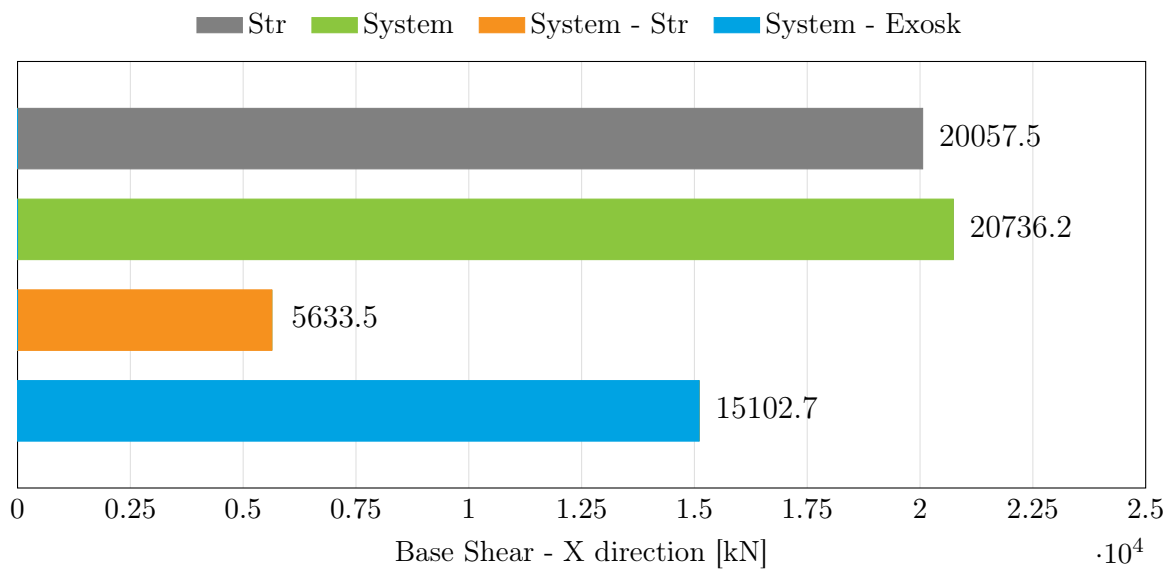


Figure 6.55: Maximum displacement of each storey of the existing building and of the retrofitted system

(X-dir) In the final configuration, **23.6%** of the base shear in X direction is taken by the original structure (System - Str) and **76.4%** by the exoskeletons (System - Exosk), as shown in the following chart.



(Y-dir) In the final configuration, **27.2%** of the base shear in Y direction is taken by the original structure (System - Str) and **72.8%** by the exoskeletons (System - Exosk), as shown in the following chart.



The repercussions on the vibration modes' periods and participating masses are shown in the tables below. The main remark about these results is that, even though the exoskeletons were introduced, the main modes remain global, being translational in both directions and rotational ones.

Existing Structure							
MODE	period	U <sub>x</sub>	U <sub>y</sub>	R <sub>z</sub>	$\sum$ U <sub>x</sub>	$\sum$ U <sub>y</sub>	$\sum$ R <sub>z</sub>
	[s]	[%]	[%]	[%]	[%]	[%]	[%]
1	0.5797	0	83	2.2	0	83	2.2
2	0.5650	86	0	0	86	83	2.2
3	0.5529	0	2.3	83	86	85	85
Retrofitted System							
MODE	period	U <sub>x</sub>	U <sub>y</sub>	R <sub>z</sub>	$\sum$ U <sub>x</sub>	$\sum$ U <sub>y</sub>	$\sum$ R <sub>z</sub>
	[s]	[%]	[%]	[%]	[%]	[%]	[%]
1	0.2825	3.4	82.9	0.1	3.4	82.9	0.1
2	0.2565	82.9	3.4	0.2	86.3	86.3	0.3
3	0.1701	0.1	0.1	87.3	86.4	86.4	87.6

Table 6.26: Summary of fundamental vibration modes' information before and after the retrofit

### 6.6.3 Results in Relation to the Stiffness

The structural verifications of each element are performed and the results of the existing and retrofitted configurations are shown in the images below. The maximum demand-capacity ratio decreases from **3.420**, for the building as-is, to **0.913**, for the structure after the intervention.

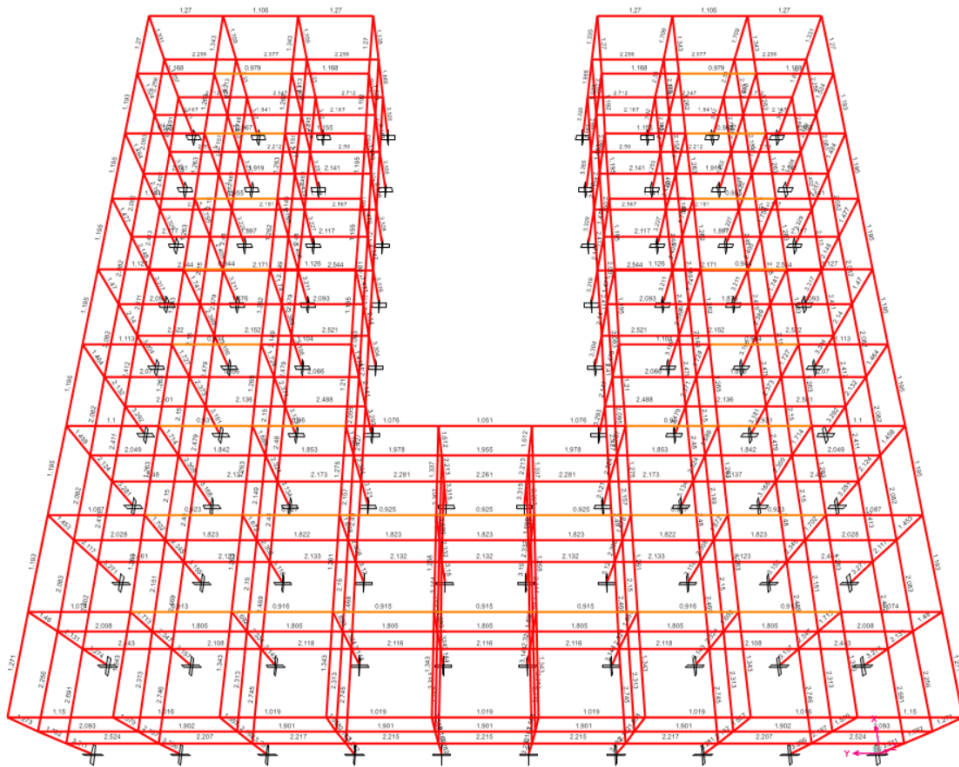


Figure 6.56: Capacity-Demand Ratio check of the unretrofitted building

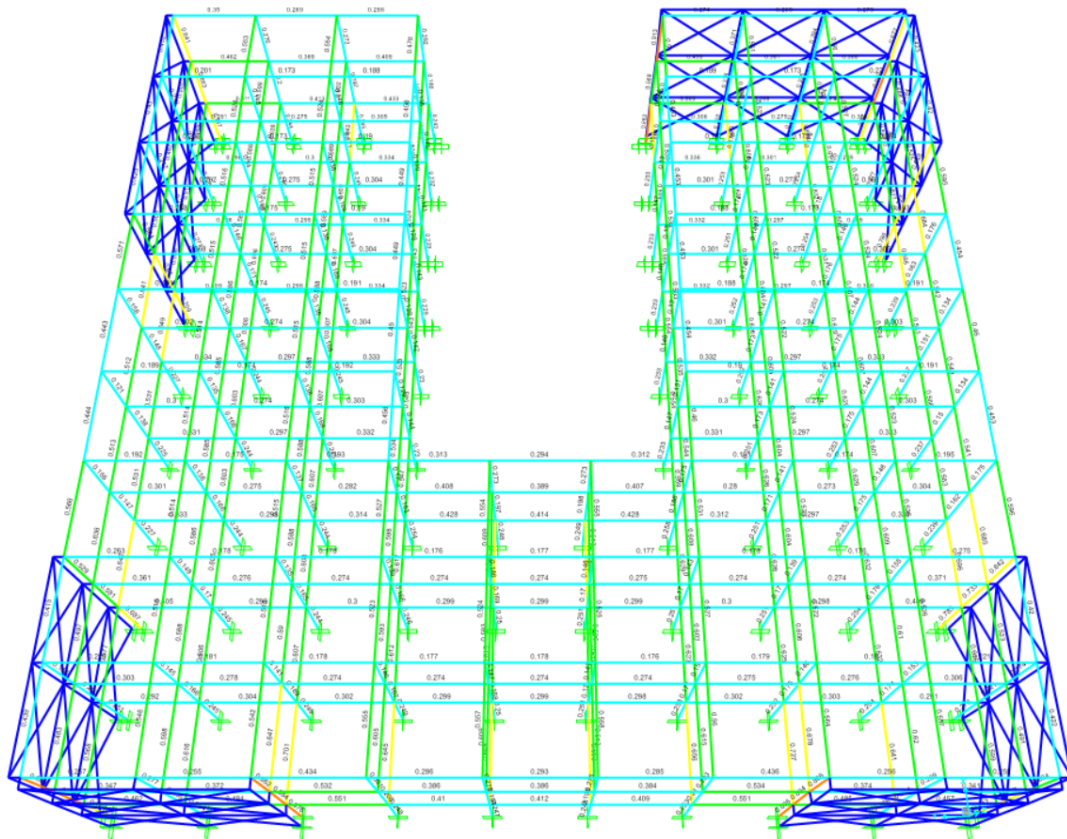


Figure 6.57: Capacity-Demand Ratio check of the retrofitted building

### X direction

Then, the stiffnesses under horizontal actions of both bare and retrofitted configurations are determined through pushover analyses, the results are presented below.

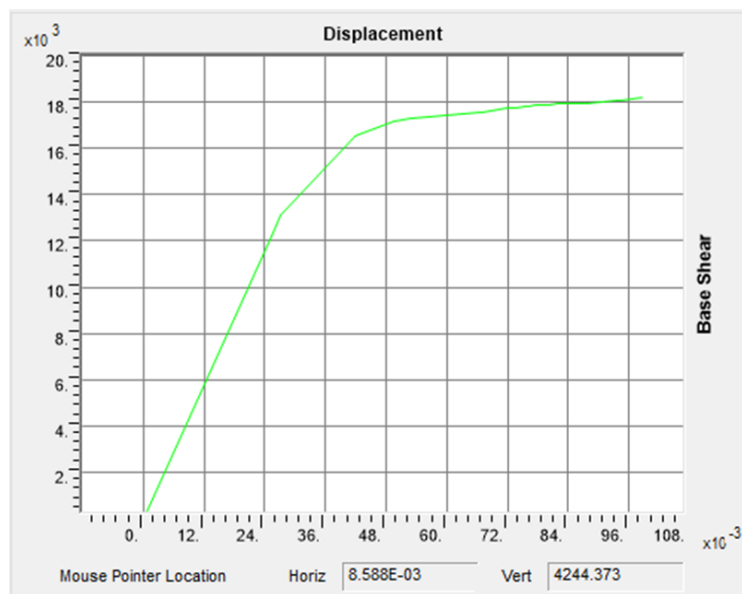


Figure 6.58: Pushover curve of the existing building in X direction corresponding to group 1 of static equivalent loads

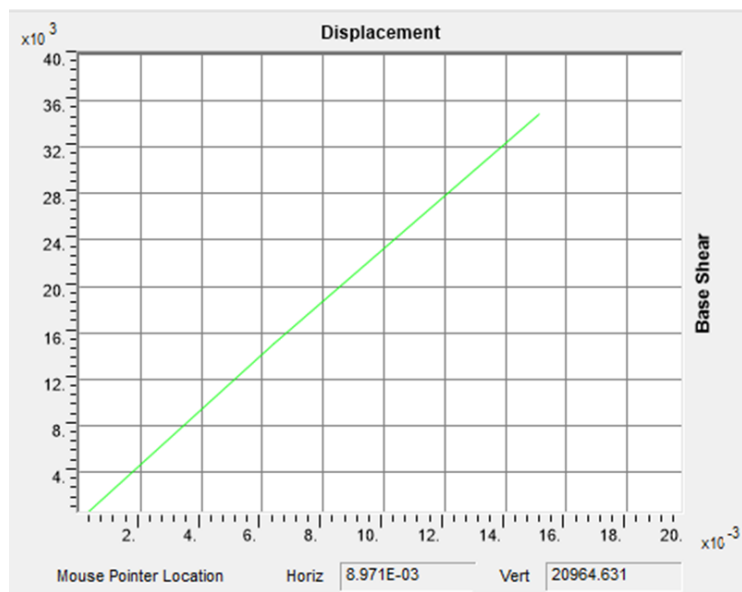


Figure 6.59: Pushover curve of the retrofitted system in X direction corresponding to group 1 of static equivalent loads

Existing Structure		Retrofitted System	
top displacement	8.70 mm	top displacement	8.98 mm
F - group 1	4244.4 kN	F - group 1	20964.6 kN
F - group 2	5016.1 kN	F - group 2	25080.4 kN
F - average	4630.2 kN	F - average	23022.5 kN
$K(\text{str}) = F/d$	532375.0 kN/m	$K(\text{syst}) = F/d$	2562412.7 kN/m

Table 6.27: Summary of displacement and forces to determine the stiffness of the existing building ( $K_{str}$ ) and of the coupled system ( $K_{syst}$ ) in X dir.

$$\frac{K_{syst}}{K_{str}} = 4.81$$

Y direction

Analogously, the analyses are performed in Y direction.

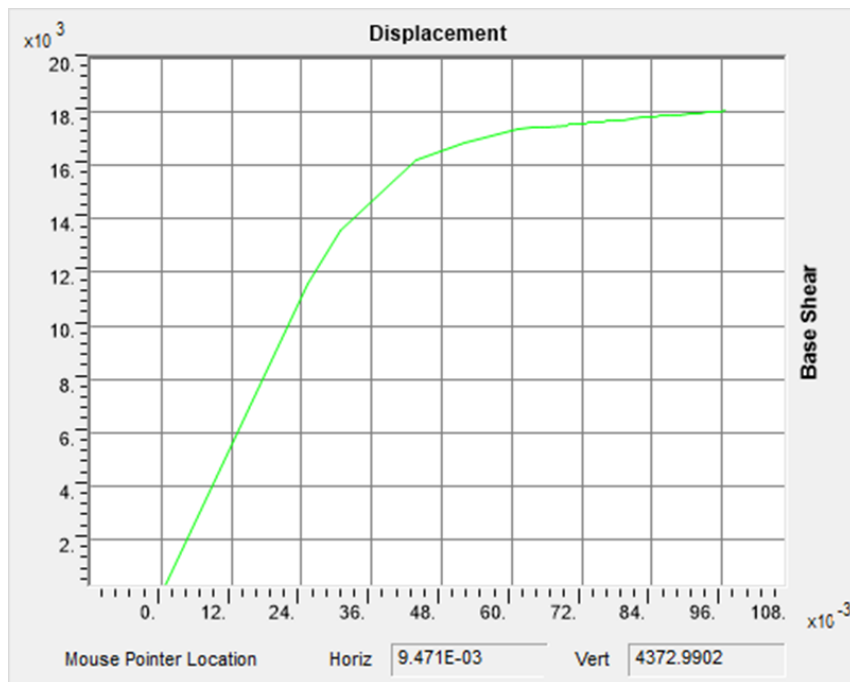


Figure 6.60: Pushover curve of the existing building in Y direction corresponding to group 1 of static equivalent loads

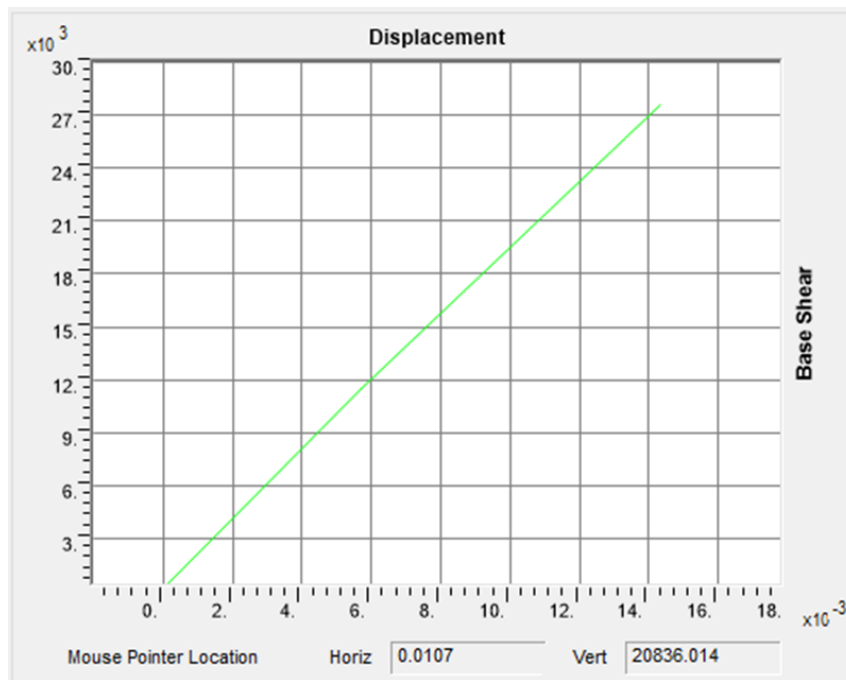


Figure 6.61: Pushover curve of the retrofitted system in Y direction corresponding to group 1 of static equivalent loads

Existing Structure		Retrofitted System	
top displacement	9.46 mm	top displacement	10.67 mm
F - group 1	4373.0 kN	F - group 1	20836.0 kN
F - group 2	5144.7 kN	F - group 2	24951.8 kN
F - average	4758.8 kN	F - average	22896.9 kN
$K(\text{str}) = F/d$	503160.6 kN/m	$K(\text{syst}) = F/d$	2145551.3 kN/m

Table 6.28: Summary of displacement and forces to determine the stiffness of the existing building ( $K_{str}$ ) and of the coupled system ( $K_{syst}$ ) in Y dir.

$$\frac{K_{syst}}{K_{str}} = 4.26$$

In this way, the stiffness ratios obtained following the proposed approach, based on displacement control, is much lower than the one suggested by the regulation, while the existing structure satisfies the structural verifications.

## Chapter 7

# Conclusions and Future Developments

In this thesis, an exhaustive study of exoskeletons, as a retrofitting technique for existing buildings, was done. The literature review enlightened the importance of this innovative solution for the many advantages it presents, such as the reduction in construction times and costs and the possibility of avoiding the interruption of the activities inside the building to be intervened. Additionally, this solution is suitable for a holistic design approach, addressing the structural, energetic, and architectural needs of the building stock, respecting the Life Cycle Thinking principles.

Nevertheless, even though an intervention with exoskeletons can overcome many of the primary limits and barriers associated with retrofitting nowadays, there still are limitations to their design that require further investigation. The main gap found in the literature is the lack of strategies for the topological design of the solution, regarding the amount and spatial placing of exoskeletons, as the size of their constituent elements.

To address this situation, an optimization procedure based on Genetic Programming was performed in this thesis. The aim is the reduction of the weight, reducing in this way the overall cost of the intervention, while satisfying specific constraints. The first imposed constraint guarantees that the existing building remains in the elastic

range, considering the maximum inter-storey drift after which the non-structural elements and infills suffer any damage. The second constraint is related to the capacity-demand ratio of the exoskeleton's elements, assuring their correct behavior by maintaining the ratios below 1. The third constraint aims to consider a constructive aspect related to architectonic barriers and free space around the buildings, preferring solutions with fewer exoskeletons.

To evaluate the behavior of the structure and determine the fitness of each solution in the optimization, linear dynamic analyses were performed in SAP2000. Using MatLab to control SAP2000 OAPI, an automatic routine for the generation, modification, and analysis of the models is conducted.

Six case studies were considered, each of them constituted by one existing structure, that can be squared-shaped, L-shaped, or U-shaped. These structures are being retrofitted by one of the exoskeleton typologies studied, being orthogonal or parallel to the façade of the building. All the case studies are located in Foggia, Italy, and their seismic behavior is analyzed for the earthquake that corresponds to the Life State Limit State.

Analyzing the results presented in 6, the first observation to make is that, in general, exoskeletons tend to be positioned in the points that are farthest from the rigidity center, because these areas are the most susceptible to important displacements.

The table 7.1, presented at the end of this chapter, allows a comparison of the main results for each case study. In terms of inter-storey drift, exoskeletons managed to control greatly this parameter, then, significant reductions are obtained, between 70% and 80% for all the case studies.

Regarding the seismic forces, it can be appreciated from the percentages of base shear taken by the building and by the exoskeletons, that all the retrofitting configurations manage to unload significantly the structure. Even though the building cannot be considered 'secondary' according to the standard regulation, from the capacity-demand ratios of the system it is noticeable that all the elements comply with the structural verifications.

The total base shear of the coupled system, of building and exoskeleton, augmented

---

with respect to the one of the unretrofitted structure. Nevertheless, most of it is taken by the exoskeletons, while the base structure is unloaded in comparison to the initial configuration.

Confronting the results of the different exoskeleton typologies analyzed, orthogonal and parallel to the façade, for each case study, an interesting comparison can be made. In the first place, the interventions with parallel exoskeletons reach the same order of results of orthogonal exoskeletons, with a weight of about 20%. Additionally, the maximum capacity-demand ratios of the elements of orthogonal exoskeletons are in the order of 0.2, while for parallel exoskeletons they reach values of 0.7.

This poor behavior of orthogonal exoskeletons, in comparison to parallel ones, is due to the warping effect that their external column suffers when subjected to out-of-plane forces. This could be prevented by, for example, connecting the exoskeletons' outer points between them. On the other hand, parallel exoskeletons take a smaller portion of the base shear than the orthogonal ones, unloading less the structure.

On the other hand, a study of the Italian regulation NTC18 was done. The section 7.2.3 suggests that, to perform a retrofit with exoskeletons, the retrofitted coupled system should have a contribution of stiffness to horizontal actions of 6.67 times the analog one of the unretrofitted existing building. This consideration leads to oversized and expensive interventions.

In the present work, a different approach is proposed, basing the design of the exoskeleton system on the inter-storey drift control. By maintaining this parameter in an elastic range, where the structural infills of the building do not suffer damage, it has been proved that the entire existing structure is verified. The capacity demand ratios of the building before and after the retrofit, that demonstrate this statement, are reported in [7.1](#).

The interest is given by the fact that, while satisfying the structural verifications of the existing building, all the stiffness ratios are maintained below the threshold suggested by the regulation, 6.67. The values of  $\frac{K_{sys}}{K_{str}}$  obtained for each case study, in the 'x' and 'y' directions, are reported in the following charts.

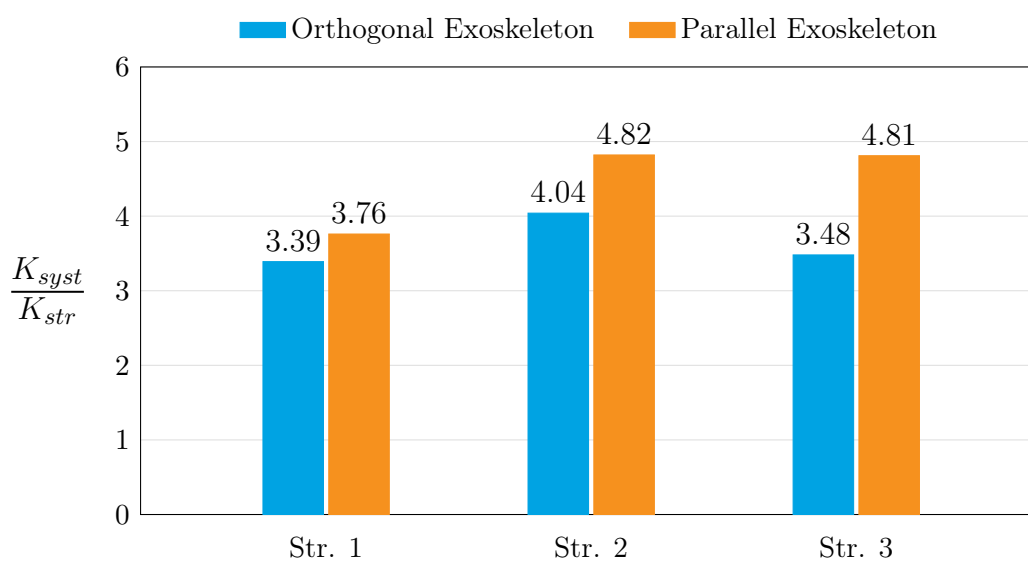


Figure 7.1: Ratios between the stiffness to horizontal actions of the retrofitted coupled system and the one of the unretrofitted building, for the different existing structures considered, in X direction

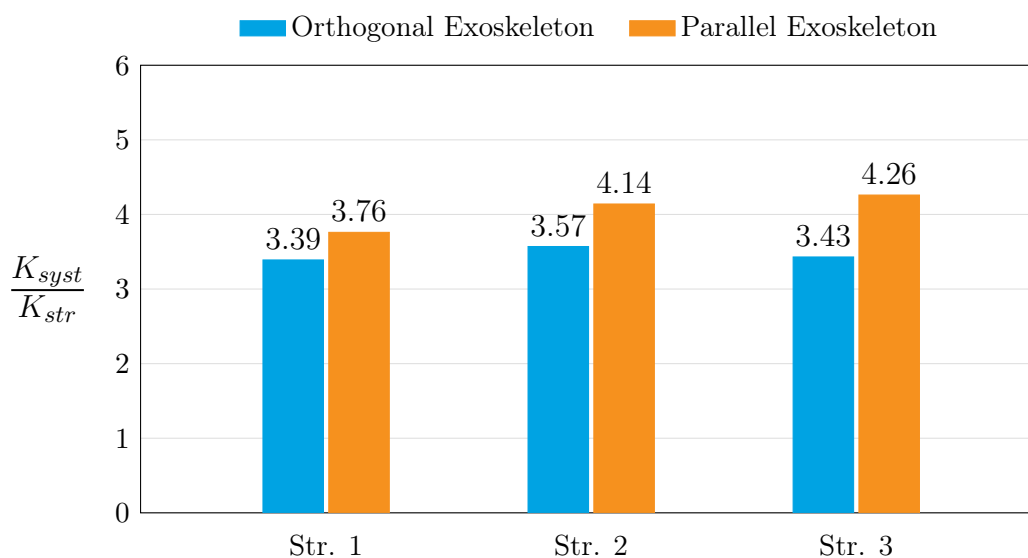


Figure 7.2: Ratios between the stiffness to horizontal actions of the retrofitted coupled system and the one of the unretrofitted building, for the different existing structures considered, in Y direction

Interesting insights into the susceptibility of the stiffness ratios to the different typologies of exoskeletons, and existing structures in consideration, derive from the presented results. The main point to remark is that all the stiffness ratios are below

6.67, which is the value proposed by the NTC2018.

Furthermore, comparing the capacity-demand ratios of the unretrofitted building, from table 7.1, we can see that the most critical structure is the L-shaped, number 2, followed by the U-shaped, number 3. The stiffness ratios tend to be higher with the augment in the building's complexity and irregularity, since a bigger added stiffness is needed to accomplish comparable results. Finally, the stiffness ratios for orthogonal exoskeletons are lower than for parallel exoskeletons in every case study, even though their weight is significantly higher, due to the efficient behavior of the parallel solutions.

Consequently, it can be affirmed that imposing a maximum inter-storey drift to the existing structure, at least for the considered case studies, guarantees the structural safety of the entire existing structure. However, it is interesting to notice that the imposed threshold is not the same for every case study considered, as it depends on the typology of the exoskeleton used for the retrofit and on the criticality of the existing structure. Consequently, this is a design parameter that should be carefully evaluated for each case.

In conclusion, the proposed displacement-based approach ensures the structural verification of the existing building and maintains the structure's infills undamaged, while achieving lower stiffness ratios than the suggested by the standard regulation. This approach leads to lighter, cost-effective solutions.

	case study 1	case study 2	case study 3	case study 4	case study 5	case study 6
structure	1	1	2	2	3	3
exoskeleton	orthogonal	parallel	orthogonal	parallel	orthogonal	parallel
inter-storey drift syst. [mm]	6.66	6.62	6.67	5.29	7.24	5.33
inter-storey drift str. [mm]	24.73	24.73	26.33	26.33	25.74	25.74
inter-storey drift reduction [%]	73.07	73.23	74.68	79.91	71.87	79.29
weight [kN]	1800	311.3	6208.6	1239.5	9381.0	2446.3
C-D ratio exosk.	0.1919	0.7020	0.1912	0.7407	0.2203	0.6169
base shear exosk. X-dir [%]	79.0	65.5	81.2	73.7	82.0	76.4
base shear str. X-dir [%]	21.0	34.5	18.8	26.3	18.0	23.6
base shear exosk. Y-dir [%]	79.0	65.5	79.4	70.5	80.4	72.8
base shear str. Y-dir [%]	21.0	34.5	20.6	29.5	19.6	27.2
C-D ratio str.	2.708	2.708	3.437	3.437	3.420	3.420
C-D ratio system	0.956	0.788	0.994	0.997	0.963	0.913

Table 7.1: Summary of the main results for each case study, in terms of maximum inter-storey drift of the building before and after the retrofit, and the percentual reduction it represents; the weight of the exoskeleton system; maximum capacity-demand ratio among the exoskeleton's elements; percentage of total base shear taken by the building and by the exoskeletons in the coupled system, in X and Y directions; maximum capacity-demand ratio among the building's elements before and after the retrofit

# Chapter 8

## Bibliography

- [1] Statistiche Istat. Censimento popolazione abtiazioni.
- [2] Isi ingegneria sismica italiana.
- [3] Housing statistics.
- [4] Andrea Belleri and Alessandra Marini. Does seismic risk affect the environmental impact of existing buildings? *Energy and Buildings*, 110:149–158, 2016.
- [5] Sebastiano D’Urso and Bruno Cicero. From the efficiency of nature to parametric design. a holistic approach for sustainable building renovation in seismic regions. *Sustainability*, 11(5):1227, 2019.
- [6] Chiara Passoni, Jack Guo, Constantin Christopoulos, Alessandra Marini, and Paolo Riva. Design of dissipative and elastic high-strength exoskeleton solutions for sustainable seismic upgrades of existing rc buildings. *Engineering Structures*, 221:111057, 2020.
- [7] Chiara Passoni, Alessandra Marini, Andrea Belleri, and Costantino Menna. A multi-step design framework based on life cycle thinking for the holistic renovation of the existing buildings stock. In *IOP Conference Series: Earth and Environmental Science*, volume 290, page 012134. IOP Publishing, 2019.
- [8] Building Performance Institute Europe (BPIE). *Europe’s buildings under the microscope: A country-by-country review of the energy performance of the buildings*. Brussels, 2011.

- 
- [9] Paolo Foraboschi, Esther Giani, et al. Esoscheletri: prerogative architettoniche e strutturali: seconda parte. *Structural*, 214:1–23, 2017.
- [10] Christopher Mora, Omar Garza, and Ricardo Hernandez. Seismic retrofit of a steel moment frame california hospital building using exterior viscous damped frames. In *Structures Congress 2012*, pages 1620–1636, 2012.
- [11] Janine M Benyus. *Biomimicry: Innovation inspired by nature*. Morrow New York, 1997.
- [12] Göran Pohl and Werner Nachtigall. *Biomimetics for Architecture & Design: Nature-Analogies-Technology*. Springer, 2015.
- [13] Gianmaria Di Lorenzo, Eleonora Colacurcio, Agustina Di Filippo, Antonio Formisano, Alfredo Massimilla, and Raffaele Landolfo. State-of-the-art on steel exoskeletons for seismic retrofit of existing rc buildings. *International Journal*, 37(1-2020), 2020.
- [14] A Caverzan, M Lamperti Tornaghi, and PA Negro. Roadmap for the improvement of earthquake resistance and eco-efficiency of existing buildings and cities. In *Proceedings of SAFESUST Workshop; JRC, JRC Science Hub: Ispra, Italy*, pages 1–136, 2015.
- [15] American Society of Civil Engineers. Minimum design loads for buildings and other structures. American Society of Civil Engineers, 2013.
- [16] Anna Reggio, Rita Greco, Giuseppe Carlo Marano, and Giuseppe Andrea Ferro. Stochastic multi-objective optimisation of exoskeleton structures. *Journal of Optimization Theory and Applications*, 187:822–841, 2020.
- [17] Federal Emergency Management Agency (FEMA). Techniques for the seismic rehabilitation of existing buildings. Technical Report FEMA 547/2006, 2006.
- [18] Anna Reggio, Luciana Restuccia, Lucrezia Martelli, and Giuseppe Andrea Ferro. Seismic performance of exoskeleton structures. *Engineering Structures*, 198:109459, 2019.
- [19] Francesca Feroldi, Alessandra Marini, Andrea Belleri, Chiara Passoni, Paolo Riva, Marco Preti, Ezio Giuriani, and Giovanni Plizzari. Miglioramento e

- adeguamento sismico di edifici contemporanei mediante approccio integrato energetico, architettonico e strutturale con soluzioni a doppio involucro a minimo impatto ambientale. *Progettazione sismica*, (2), 2014.
- [20] Alessandra Marini, Chiara Passoni, Paolo Riva, Paolo Negro, Elvira Romano, Fabio Taucer, et al. Technology options for earthquake resistant, eco-efficient buildings in europe: Research needs. *European Commission, Joint Research Centre Scientific and Policy Reports*, 2014.
- [21] F Feroldi. Sustainable renewal of the post wwii building stock through engineered double skin, allowing for structural retrofit, energy efficiency upgrade, architectural restyling and urban regeneration. *University of Brescia*, 2014.
- [22] Alessandra Marini, A Belleri, F Feroldi, Chiara Passoni, Marco Preti, P Riva, E Giuriani, and Giovanni Plizzari. Coupling energy refurbishment with structural strengthening in retrofit interventions. In *SAFESUST Workshop*, pages 26–27. SAFESUST Ispra, Italy, 2015.
- [23] C Passoni. *Holistic renovation of existing RC buildings: a framework for possible integrated structural interventions*. PhD thesis, Ph. D. thesis, University of Brescia, 2016.
- [24] A Marini, A Belleri, C Passoni, F Feroldi, M Preti, G Metelli, E Giuriani, P Riva, and G Plizzari. Integrated architectural, energy and seismic renovation of the reinforced concrete building stock targeting sustainability and resilience. *Submitted to Journal of Civil and Environmental Engineering*, 2016.
- [25] Paolo Foraboschi, Esther Giani, et al. Esoscheletri: miglioramento sismico e rigenerazione architettonica: seconda parte. *Structural*, 215(gennaio-febbraio):1–19, 2018.
- [26] Gianmaria DI LORENZO, Colacurcio Eleonora, Agustina Di Filippo, Antonio Formisano, Alfredo Massimilla, Raffaele Landolfo, et al. Stato dell’arte sugli esoscheletri in acciaio per il retrofit sismico di costruzioni esistenti in calcestruzzo armato. In *Atti del XXVII Congresso CTA*, volume 1, pages 179–186, 2019.
- [27] A Caverzan, M Lamperti Tornaghi, and P Negro. Taxonomy of the redevelopment methods for non-listed architecture: from façade refurbishment to the

- 
- exoskeleton system. In *JRC, Conference and workshop Reports, Proceedings of Safesust Workshop, Ispra, November*, pages 26–27, 2016.
- [28] Gianmaria Di Lorenzo, Roberto Tartaglia, Alessandro Prota, and Raffaele Landolfo. Design procedure for orthogonal steel exoskeleton structures for seismic strengthening. *Engineering Structures*, 275:115252, 2023.
- [29] Simone Labò, Chiara Passoni, Alessandra Marini, and Andrea Belleri. Design of diagrid exoskeletons for the retrofit of existing rc buildings. *Engineering Structures*, 220:110899, 2020.
- [30] Japan Building Disaster Prevention Association (JBDPA). Standards for evaluation of seismic capacity and guidelines for seismic rehabilitation of existing reinforced concrete buildings. Technical report, 1990. Revised 1990 (in Japanese).
- [31] Fabio Mazza. Dissipative steel exoskeletons for the seismic control of reinforced concrete framed buildings. *Structural Control and Health Monitoring*, 28(3):e2683, 2021.
- [32] Terri Meyer Boake. *Diagrid structures: systems, connections, details*. Walter de Gruyter, 2014.
- [33] Valentina Tomei, Maura Imbimbo, and Elena Mele. Optimization of structural patterns for tall buildings: The case of diagrid. *Engineering Structures*, 171:280–297, 2018.
- [34] Simone Labò, Chiara Passoni, Alessandra Marini, Andrea Belleri, Guido Camata, Paolo Riva, Enrico Spacone, et al. Prefabricated responsive diagrids for holistic renovation of existing mid-rise rc buildings. *Proceedings of the COMP-DYN*, 2017.
- [35] Simone Labò, Chiara Passoni, Alessandra Marini, Andrea Belleri, Guido Camata, Paolo Riva, Enrico Spacone, et al. Diagrid solutions for a sustainable seismic, energy, and architectural upgrade of european rc buildings. In *Proceedings of the XII International Conference on Structural Repair and Rehabilitation, Porto, Portugal*, pages 26–29, 2016.
- [36] C Christopoulos and A Filiatrault. *Principles of passive supplemental damping and seismic*. IUSS Press, Pavia, Italy, 2006.

- 
- [37] Mohamed Nouredin, Shabir Ahmed Memon, Masom Gharagoz, and Jinkoo Kim. Performance-based seismic retrofit of rc structures using concentric braced frames equipped with friction dampers and disc springs. *Engineering Structures*, 243:112555, 2021.
- [38] Stefano Sorace, Gloria Terenzi, and Anna Frangipane. Incorporation of dissipative connections for seismic retrofit of reinforced concrete prefab structures. 2019.
- [39] MG Ireland, Stefano Pampanin, and DK Bull. Concept and implementation of a selective weakening approach for the seismic retrofit of rc buildings. 2006.
- [40] M Mohammadi, V Akrami, and R Mohammadi-Ghazi. Methods to improve infilled frame ductility. *Journal of Structural Engineering*, 137(6):646–653, 2011.
- [41] Marco Preti and Valentino Bolis. Masonry infill construction and retrofit technique for the infill-frame interaction mitigation: test results. *Engineering Structures*, 132:597–608, 2017.
- [42] Alessandra Marini, Chiara Passoni, and Andrea Belleri. Life cycle perspective in rc building integrated renovation. *Procedia Structural Integrity*, 11:28–35, 2018.
- [43] Marco Lamperti Tornaghi, Arian Loli, and Paolo Negro. Balanced evaluation of structural and environmental performances in building design. *Buildings*, 8(4):52, 2018.
- [44] Catarina Thormark. The effect of material choice on the total energy need and recycling potential of a building. *Building and environment*, 41(8):1019–1026, 2006.
- [45] Chiara Passoni, Alessandra Marini, Andrea Belleri, and Costantino Menna. Redefining the concept of sustainable renovation of buildings: State of the art and an lct-based design framework. *Sustainable Cities and Society*, 64:102519, 2021.
- [46] Paolo La Greca and Giuseppe Margani. Seismic and energy renovation measures for sustainable cities: A critical analysis of the italian scenario. *Sustainability*, 10(1):254, 2018.

- 
- [47] B Angi, editor. *Eutopia Urbana. Eutopia Urbanscape. The combined redevelopment of social housing*. 2018.
- [48] Toru Takeuchi, Koichi Yasuda, and Mamoru Iwata. Seismic retrofitting using energy dissipation façades. In *Improving the Seismic Performance of Existing Buildings and Other Structures*, pages 1000–1009. 2010.
- [49] L Martelli, L Restuccia, and GA Ferro. The exoskeleton: a solution for seismic retrofitting of existing buildings. *Procedia Structural Integrity*, 25:294–304, 2020.
- [50] Alessandra Marini, Chiara Passoni, Andrea Belleri, Francesca Feroldi, Marco Preti, Giovanni Metelli, Paolo Riva, Ezio Giuriani, and Giovanni Plizzari. Combining seismic retrofit with energy refurbishment for the sustainable renovation of rc buildings: A proof of concept. *European Journal of Environmental and Civil Engineering*, 26(7):2475–2495, 2022.
- [51] European Committee for Standardization (CEN). *Design of structures for earthquake resistance*. Brussels, Belgium, 2005.
- [52] V Ciampi, M De Angelis, and F Paolacci. Design of yielding or friction-based dissipative bracings for seismic protection of buildings. *Engineering Structures*, 17(5):381–391, 1995.
- [53] Anna Reggio, Luciana Restuccia, and Giuseppe Andrea Ferro. Feasibility and effectiveness of exoskeleton structures for seismic protection. *Procedia Structural Integrity*, 9:303–310, 2018.
- [54] Rafael Mart, Panos M Pardalos, and Mauricio GC Resende. *Handbook of heuristics*. Springer Publishing Company, Incorporated, 2018.